HOST PROTEIN MANIPULATION AS A MECHANISM IN VIRAL CARDIOMYOPATHY

by

Tse Yuan Wong

B.Sc., Simon Fraser University, 2004

A THESIS SUBMITTED IN PARTIAL FULFILLMENT OF

THE REQUIREMENTS FOR THE DEGREE OF

DOCTOR OF PHILOSOPHY

in

The Faculty of Graduate Studies

(Pathology and Laboratory Medicine)

THE UNIVERSITY OF BRITISH COLUMBIA

(Vancouver)

December 2012

Abstract

Viral myocarditis, the inflammation of myocardium initiated by viral infection, is an important cause of mortality in neonates and children. In addition, it is a precursor to dilated cardiomyopathy (DCM). To date, no effective therapy is available for viral myocarditis/DCM. Coxsackievirus B3 (CVB3) is an important human pathogen of viral myocarditis. Extensive research efforts on CVB3 have broadened our understanding of the virus-host protein interactions. However, the pathogenesis of coxsackievirus-induced myocarditis is not fully understood. The **objective** of this dissertation is to explore the role of host protein manipulation in coxsackieviral replication and pathogenicity. My **hypotheses** are that **(1)** coxsackievirus hijacks host's cellular autophagy mechanism to facilitate its own replication; and **(2)** the serum response factor (SRF) is cleaved by viral protease 2A during coxsackievirus infection and contributes to impaired myocardial function and progression to DCM. **For project 1**, I demonstrated that CVB3 manipulates the host autophagy pathway to supplement viral replication. Autophagy is an evolutionary conserved homeostatic mechanism in eukaryotes that degrades and recycles long-lived cytoplasmic proteins, as well as damaged organelles. The hallmark of autophagy is the formation of double-membrane vesicles known as autophagosomes. I provided the initial evidence that CVB3 infection induces the formation of autophagosomes. Up-regulation of autophagosome formation enhances CVB3 replication, whereas downregulation of autophagy pathway reduces CVB3 replication. My results help clarify the nature of the intracellular membranes previously shown to be required for viral replication. **For project 2**, I demonstrated that CVB3 manipulates SRF expression via protein cleavage. SRF is a transcription factor vital for the expression of cardiac contractile/regulator genes, as well as gene silencing microRNAs. Cardiac-specific knockout of SRF in adult transgenic mice results in disruption of cardiac gene expression and development of severe DCM. I showed that SRF is cleaved in CVB3-infected mouse hearts and cardiomyocytes. Further studies revealed that SRF is cleaved at the 327 amino acids position by CVB3-encoded protease 2A. I demonstrated that SRF cleavage contributes to DCM by abolishing the transactivation property of SRF and generating dominant-negative SRF-truncates. Taken together, these novel viral strategies bridged existing knowledge and may serve as therapeutic targets for viral myocarditis/DCM.

Preface

The portion of following dissertation includes chapters which are based on two manuscripts, in that **Chapter 3** is based on an article published in the *Journal of Virology* [**Wong J**, Zhang J, Si X, Gao G, Mao I, McManus BM, and Luo H (2008). Autophagosome supports coxsackievirus B3 replication in host cells. *J Virol.,* 82(18):9143-9153], and **Chapter 4** is based on another article published in *Cell Research* [**Wong J**, Zhang J, Yanagawa B, Luo Z, Yang X, Chang J, McManus B, and Luo H (2012). Cleavage of serum response factor mediated by enteroviral protease 2A contributes to impaired cardiac function. *Cell Res.,* 22:360-371]. Specifically, I contributed to all experiments and analysis in **Chapter 3** and **Chapter 4**, except *in vivo* coxsackievirus infection and heart function measurement, as well as cardiac gene expression measurement by microarray and subsequent validation by quantitative real-time PCR. In addition, parts of the contents from my review article published in *Cardiovascular Research* [Luo H, **Wong J**, and Wong B (2010). Protein degradation systems in viral myocarditis leading to dilated cardiomyopathy. *Cardiovasc Res.* 85(2):347-356] and book chapter published in Myocarditis [**Wong J** and Luo H (2011). Impaired cardiac function in viral myocarditis, Myocarditis, Cihakova D (Ed.), ISBN: 978-953-307-289-0, InTech, Rijeka, Croatia] are also used in this dissertation.

During my PhD studies, I also conducted additional projects that resulted in two other first-author manuscripts: **Wong J**, Zhang J, Si X, Gao G, Luo H (2007). Inhibition of the extracellular signal-regulated kinase signaling pathway is correlated with proteasome inhibitor suppression of coxsackievirus replication. *Biochem Biophys Res Commun.*, 358(3):903-907., and **Wong J**, Si X, Zhang J, Angeles A, Luo H (2012). Degradation of adenosine-uridine binding factor 1: a strategy for coxsackieviral replication. Manuscript in preparation. In addition, I was involved in a number of related projects that resulted in eight co-author peer reviewed articles.

This study was carried out in strict accordance with the recommendations in the Guide for the Care and Use of Laboratory Animals of the Canadian Council on Animal Care. The protocol was approved by the Committee on Animal Care of the University of British Columbia (A03-0233).

Table of contents

List of tables

List of figures

List of abbreviations

3-MA – 3-methyl adenine

Ambra1 – Activating molecule in beclin-1-regulated autophagy

ANP – Atrial natriuretic factor

ATG – Autophagy related gene

BSA – Bovine serum albumin

CAR – Coxsackievirus and adenovirus Receptor

CREB – cAMP responsive element binding protein

CPE – cytopathic effect

CVA – Coxsackievirus A

CVB – Coxsackievirus B

DAF – Decay accelerating factor

DAPI – 4',6-diamidino-2-phenylindole

DCM – Dilated cardiomyopathy

DMEM - Dulbecco's modified eagle medium

eIF2α - Eukaryotic initiation factor 2α

eIF4G – Eukaryotic initiation factor 4G

ER – Endoplasmic reticulum

EMB – Endomyocardial biopsy

EMSA – Electrophoretic mobility shift assay

FIP2000 – Focal adhesion kinase family interacting protein of 200 kD

FMK – Fluoromethyl ketone

GFP – Green fluorescent protein

HEV – Human enterovirus

IFN-γ – Interferon-γ

IL – Interleukin

IRES – Internal ribosome entry site

LC3-PE – Microtubule-associated protein light-chain 3-phosphatidylethanolamine

LVPW – Left ventricular posterior wall

MADS – MCM1, Agamous, Deficiens, SRF

MEF2 – Myocyte enhancer factor-2

MHC – Myosin heavy chain

miRNA - MicroRNA

MLC – Myosin light chain

MOI – Multiplicity of infection

mTOR – Mammalian target of rapamycin

NFAT – Nuclear factor of activated T-cells

NLS – Nuclear localization signal

NK cells – Natural killer cells

OCT-1 – Octamer-binding transcription factor

ORF – Open reading frame

PABP – Poly-A binding protein

PBS – Phosphate buffered saline

PCR – Polymerase chain reaction

PERK – Protein kinase RNA-like endoplasmic reticulum kinase

PFU – Plaque forming unit

PI3K – Phosphoinositide-3 kinase

PI3P – Phosphatidylinositol 3-phosphate

PKR – Protein kinase R

RT-PCR – Reverse-transcriptional PCR

SERCA – Sarcoplasmic reticulum Ca^{2+}-ATPase

SCID – Severe combined immunodeficiency

SRE – Serum response element

SRF – Serum response factor

siRNA – Small interfering RNA

ssRNA – Single-stranded RNA

TBP – TATA-binding protein

TBS – Tris-buffered saline

TBST – TBS containing 0.1% Tween-20

TNF-α – Tumor necrosis factor-α

ULK1/2 – Uncoordinated 51-like kinase 1/2

UTRs – Untranslated regions

VP1 – Viral capsid protein-1

VPg-pU-pU – Uridylylated VPg

Vps34 – Vacuolar protein sorting-34

Acknowledgements

I dedicate this thesis to my dear parents, Frank and Serena, who selflessly put my career success at their top priority. I cannot thank them enough for their love and care, and most importantly for their guidance in life.

I would like to thank my long-time girlfriend and now my wife Cecilia for her loving, sharing, support, and understanding. She believes strongly in me and thinks highly of my ideas. She cooks me fish head soup to help me through "failed experiments" days. Cecilia is my muse. I attribute my fundamentalist thinking to her seemingly-random purchase of self-help books and her holistic nutrition schooling.

I am enormously thankful for my supervisor Dr. Honglin Luo. She provided a harmonious environment for my post-undergraduate journey. Her excellence in supervision and mentorship inspires me to want the same for my trainees. She balances research guidance with encouraging independent thinking. I thank her trust in me and gave me freedom and resources to explore my research. I also thank her in giving me opportunities to take part in various projects and to interview and supervise undergraduate students. I also like to thank my co-supervisor Dr. Bruce McManus for his vision, leadership, and steadfast encouragement.

I would also like to acknowledge my colleagues at the James Hogg Research Centre. Our humble technician Jingchun Zhang not only gave me great help in completing my projects but also shared his knowledge of traditional Chinese medicine and history with me. Post-doctoral fellow Dr. Xiaoning Si showed me the excitement and possibility of scientific experiments. I would like to thank Dr. Mary Zhang for her scientific guidance. My lab buddies David Lin, Guang Gao, Junyan Shi, Gabrial Fung, Tak Poon, Archie Angeles, Chris Hwang, Jayant Shravah, Allen Xiao, and Ivy Mao that make Luo lab the fun place to hang out. Special thanks to Dr. David Walker and Fanny Chu for guiding me through my electron microscopy work.

I would like to thank all my committee chairs (Drs. Colin Fyfe and Haydn Pritchard) and members (Drs. Decheng Yang and Jian Ye) for their commitments to my many progress meetings and their discussions and suggestions on my research.

Chapter 1 – Introduction

1.1. Overview of myocarditis

Myocarditis is defined clinically as inflammation of the myocardium and necrosis and/or degeneration of adjacent myocytes in the absence of an ischemic event (9, 137). It is a major cause of sudden, unexpected death in individuals less than 40 years old (54). More importantly, it is a potential precursor to dilated cardiomyopathy (DCM), which leads to congestive heart failure (36, 210). Each year ~100,000 new cases of DCM are diagnosed in the United States alone and the 10-year survival rate of the disease is ~40% (202, 204). Unfortunately, there is no specific and effective therapy available to date for the treatment of myocarditis/DCM. Currently, supportive therapies are primarily used for myocarditis/DCM patient care. At end-stage DCM, heart transplantation represents the only definitive therapeutic option (138). According to the International Society of Heart and Lung Transplantation Registry, cardiomyopathy accounts for about half of all patients requiring heart transplants (87).

Myocarditis is originally described by Joseph Sobernheim in 1837 as inflammation of the myocardium (164). Remarkable advances in our understanding, diagnosis, and treatment of myocarditis were made in the last 150 years. Myocarditis is an insidious disease that is typically asymptomatic and subclinical, thus conceals its true incidence. It was post-mortem studies that revealed the astounding prevalence of myocarditis (54). The advent of transvenous endomyocardial biopsy in 1962 by Sakakibara and Konno opened up opportunity to assess the premorbid presence of myocardial inflammation in patients (173). Yet, different biopsy studies derived highly variable incidences of myocarditis, ranging from 0 to 80 percent (122). The disparities were attributed to differences in patient selections, diagnostic criteria, as well as the inherent insensitivity of the biopsy in the detection of inflammatory disease (38, 104, 174). To resolve the disparities and standardize diagnostic evaluation, the Dallas criteria for the histological diagnosis of myocarditis were introduced in 1986 (8). These criteria include categories of acute (lymphocytic infiltration with myocytolysis), borderline (lymphocytic infiltration without myocytolysis), and persistent (repeatedly observed lymphocytic infiltration and myocytolysis on serial biopsies), as well as negative (absent of lymphocytic infiltration and myocytolysis) (8). However, the Dallas criteria probably still underestimates the true incidence of myocarditis.

The causes of myocarditis are diverse (summarized in **Table 1**) and include infectious (viral, bacterial, parasitic, and fungal) agents, toxins, allergens, and immunologic disorders (61, 70, 139). Infectious agents are the most common cause of myocarditis worldwide. The relevance of specific infectious etiologies varies with geographical regions. In Central and South America, myocarditis is

commonly associated with Chagas disease caused by the parasite *Trypanosoma cruzi*, whereas in North America and other developed nations, cardiotropic viruses are the primary infectious agents of myocarditis (5, 151, 204). Routine serological examinations of serum from patients during acute myocarditis and convalescence demonstrated rising antibody titers against selected viruses (27). Furthermore, viral genome has been identified in the myocardium of patients with clinically suspected myocarditis and DCM. Endomyocardial biopsy examinations of myocarditis and DCM patients by polymerase chain reaction (PCR) revealed the presence of viral genomes in one-third of the inspected cases (94, 177). The presence of viral genome is associated with poor prognosis. The two-year mortality rate in patients tested positive for viral genome in their endomyocardial biopsies is nine times higher than those tested negative (202). Taken together, these studies implicated a causal link between viral myocarditis and the development of DCM.

More than twenty common viruses, including enteroviruses, adenovirus, parvovirus, cytomegalovirus, hepatitis C virus, influenza virus, and human immunodeficiency virus, have been associated with myocarditis in humans (77). Among them, enteroviruses have been the most widely studied viruses in the pathogenesis of viral myocarditis. Global surveillance data compiled by the World Health Organization indicate that coxsackievirus of the enterovirus genus is the dominant cause of myocarditis (77). Young children, particularly newborns under 6 months of ages, are extremely susceptible to coxsackievirus infections. Myocarditis is responsible for approximately 20% of sudden unexpected deaths among young children (54, 163). Thus far, no effective vaccine is available for coxsackievirus infection. The only definitive treatment currently available for DCM is heart transplantation.

Table 1. Primary etiological agents of myocarditis

Viruses	Bacteria	Parasites	Fungi
• Adenovirus • **Coxsackievirus** • Cytomegalovirus • Epstein-Barr virus • Hepatitis C virus • Human immunodeficiency virus • Influenza virus • Parvovirus B19	• *Chlamydia pneumonia* • *Corynebacterium diphtheriae* • *Mycoplasma pneumoniae* • *Serratia marcescens* • *Streptococcus pneumoniae* • *Treponema pallidum*	• *Echinococcus granulosus* • *Taenia solium* • *Toxoplasma gondii* • *Trypanosoma cruzi* • Visceral larva migrans • *Wuchereria bancrofti*	• Actinomyces • Aspergillus • Blastomyces • Candida • Coccidioides • Crytoccoccus • Histoplasma • Mucormycoses • Nocardia

Toxins	Allergens	Immunologic disorders	
• Amphetamines • Anthracyclines • Cocaine • Catecholamines • Ethanol • Fluorouracil • Heavy metals • Interleukin-2	• Acetazolamide • Amitriptyline • Cefaclor • Colchicine • Lidocaine • Penicillin • Tetanus toxoid • Tetracycline	• Churg-Strauss syndrome • Inflammatory bowel disease • Insulin-dependent diabetes mellitus • Myasthenia gravis • Sarcoidosis • Systemic lupus erythematosus • Takayasu's arteritis • Thyrotoxicosis • Kawasaki's disease • Wegener's granulomatosis	

Multiple etiologies have been identified for the myocarditis, but cardiotropic viruses are the most common causes of the disease in North America and other developed nations. Among them, coxsackievirus of the enterovirus genus is the dominant cause of myocarditis. Data are from Feldman and McNamara (61).

1.2. Coxsackievirus

1.2.1 Discovery of coxsackievirus

Coxsackievirus was originally isolated by Gilbert Dalldorf and Grace Sickles in 1948 while searching for a cure for polio (45). Previous work by Dalldorf suggested that fluid collected from monkeys infected with a non-poliovirus preparation have protective effect against polio. Dalldorf and Sickles then attempted to isolate such polio-protective viruses using newborn mice and fecal specimens from two young boys suffering from flaccid paralysis (45). These non-polio isolates differed from poliovirus that they were able to infect newborn (suckling) mice in addition to primates. Infection by these non-polio isolates often mimicked mild or non-paralytic poliovirus infection. The newly discovered virus family was eventually given the name Coxsackie, for the Hudson River town of Coxsackie, New York, where Dalldorf obtained the initial fecal specimens. In the following year, Dalldorf and Sickles reported a virus, later called coxsackievirus A (CVA), which induced fatal paralysis and myositis in suckling mice, but not adult mice (43). In the year after, Edward Curnen, Ernest Shaw, and Joseph Melnick discovered the coxsackievirus B (CVB) that confers different antigenicity and pathogenicity from CVA (142). Suckling mice infected with CVB resulted in focal and limited myositis in striated muscles, as well as degeneration of brain, pancreas, heart, and embryonic fat pads (141).

1.2.2 Classification and Properties of coxsackievirus

Coxsackievirus, a family member of *Picornaviridae*, belongs to the human enterovirus (HEV) genus. There are twenty-three known serotypes (1-22, 24) of CVA and six serotypes (1-6) of CVB, which belong to HEV species A (CVA2-8, 10, 12, 14, and16), B (CVB1-6, CVA9 and 23), or C (CVA1, 11, 13, 17, 19-22, and 24) (199). CVA serotypes mainly cause enteric diseases, while the six CVB serotypes are associated with more severe diseases such as aseptic meningitis, pancreatitis, and myocarditis (44). Among the CVBs, only CVB1, 3, and 5 are cardiotropic (72).

Coxsackievirus B3 (CVB3) is a non-enveloped single-positive-stranded RNA virus. The CVB3 genome is a single-stranded sense RNA (ssRNA(+)) molecule of ~7400 nucleotides in length. It comprises a single open reading frame (ORF) flanked on both ends by untranslated regions (UTRs). The ORF encodes 11 viral proteins that are translated into a large polyprotein of 2185 amino acids, including four structural proteins (VP1, VP2, VP3, and VP4), two viral proteases (2A and 3C), an RNA-dependent-RNA-polymerase (3D), a small polypeptide that serve as primer for RNA synthesis initiation (3B, also known as, VPg), an ATPase (2C), two host membrane modifiers (2B and 3A). In addition, there are three functional intermediates (2BC, 3AB, and 3CD) (89). The 5'UTR contains ~800 bases that folds into highly

ordered secondary structures, including the internal ribosome entry site (IRES) that directs viral genome translation initiation. Unlike eukaryotic mRNA, the 5'UTR of viral genome is covalently linked to a small viral polypeptide VPg, instead of the 7-methylguanosine triphosphate cap (63). These structural features of the viral genome 5'UTR serve an important function in cap-independent translation that plays a role in subverting host protein translation machineries for viral replication as discussed in the later sections. On the other hand, the 3'UTR (~100 bases) of viral genome is polyadenylated. The CVB3 genome is encapsulated in an icosahedral protein capsid of ~30 nm in diameter (172). The capsid is composed of 4 viral structural proteins: VP1, VP2, VP3, and VP4. One molecule of each structural protein combines and forms a protomer. Five protomers in turn compose a pentamer and 12 pentamers assemble together to form the capsid.

1.2.3 Lifecycle of coxsackievirus B3

Coxsackievirus lifecycle (summarized in **Figure 1**) begins with its binding and clustering of co-receptor DAF (decay accelerating factor, also known as CD55), which leads CVB3 to its main receptor CAR (coxsackievirus and adenovirus receptor) located in the intercalated disk of cardiomyocyte (179). Its engagement with CAR allows CVB3 to internalize into endosome through the clathrin-dependent endocytosis pathway (39). Subsequent acidification of endosome leads to viral uncoating and release of viral genome (ssRNA(+)) into the cytoplasm. Now, the viral genome translates into a large viral polyprotein, which is processed by viral proteases 2A and 3C embedded within, into 11 viral structural and non-structural proteins, as described previously (172). The RNA-dependent-RNA-polymerase 3D together with primer uridylylated VPg (VPg-pU-pU) transcribe ssRNA(+) into a viral RNA intermediate (ssRNA(-)) that in turn serves as template for the synthesis of multiple viral progeny genomes (ssRNA(+))(150, 152, 168). The viral progeny genomes and structural proteins are integrated to make complete virions. The lifecycle of CVB3 is completed by releasing viral progenies for new rounds of infections.
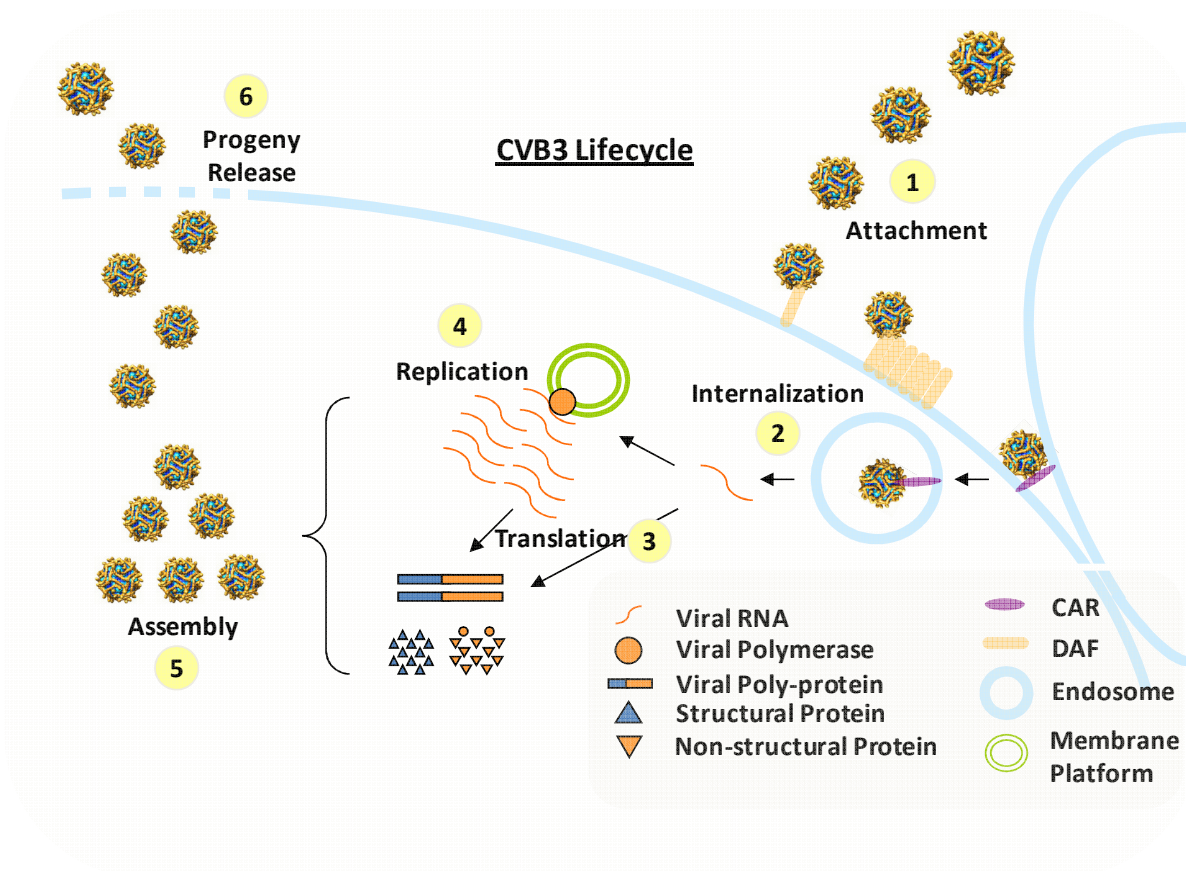
Figure 1. Lifecycle of coxsackievirus.

Coxsackievirus lifecycle begins with its binding and clustering of co-receptor DAF (decay accelerating factor, also known as CD55), which leads CVB3 to its main receptor CAR (coxsackievirus and adenovirus receptor) located in the intercalated disk of cardiomyocyte. Its engagement with CAR allows CVB3 to internalize into endosome. Now, CVB3 uncoats and injects its viral genome (ssRNA(+)) into the cytoplasm. The viral genome translates into a large viral polyprotein, which is processed by viral proteases embedded within, into structural and non-structural proteins. The RNA-dependent-RNA-polymerase 3D transcribe ssRNA(+) into a viral RNA intermediate (ssRNA(-)) that in turn serves as template for the synthesis of multiple viral progeny genomes (ssRNA(+)). The viral progeny genomes and structural proteins are integrated to make complete virions. The lifecycle of CVB3 is completed by releasing viral progenies for infections of nearby cells.

1.2.4 Functions of coxsackievirus-encoded proteins

CVB3, like other family members of *Picornaviridae*, encodes two viral proteases 2A and 3C, as well as intermediate 3CD. Both 2A and 3C are cysteine proteases and are homologous to trypsin-like family of serine proteases. Not only are these viral proteases important in the processing of viral polyprotein (82, 84), but they also contribute to successful viral replication by cleaving multiple host proteins involved in host RNA transcription, host protein translation, cell signalling, and cell structure.

Protease 2A cleaves eukaryotic initiation factor 4G (eIF4G) and poly-A binding protein (PABP) (95, 100, 114, 115). Both eIF4G and PABP are essential for host cap-dependent translation. As a result, cleavage of both proteins halts cellular protein synthesis (100, 115). CVB3 protein synthesis, however, is not affected due to the uncapped nature of viral RNA and its cap-independent translation mechanism conferred by the internal ribosome entry site (IRES) located at the 5'UTR of viral genome (92). This viral strategy, thereby, efficiently subverts host protein synthesis machineries to focus on viral protein synthesis. Furthermore, viral protease 2A cleaves the cytoskeletal proteins dystrophin and cytokeratin-8 (11-13) to facilitate viral progeny release.

Viral protease 3C, on the other hand, supports viral replication by shutting down host gene transcription via cleavage of cAMP response element binding protein (CREB), octamer-binding transcription factor (Oct-1), and cellular TATA-binding protein (TBP), thus adds cellular stress on infected cardiomyocytes (40, 206, 207).

Both viral proteases also contribute to myocyte death by activating host apoptosis by cleaving Bcl-2 family protein Bid and inducing caspase-8-mediated activation of caspase-3 (16, 33, 74). *In vitro* observation of CVB3-infected cells reveals numerous degenerative cellular changes associated with the aforementioned pro-viral events, i.e. host transcription and translation shutdown and disruption of cytoskeleton, during CVB3 replication, collectively referred as cytopathic effect (CPE) (29, 30). Infected cells suffering from CPE undergo morphological changes such as cell rounding and membrane permeability alteration, followed by detachment from cell culture surface, and eventual cell lysis through apoptosis, necrosis, or both.

Non-structural viral proteins other than the polymerase and proteases, such as 2B, 3A, and intermediate 2BC, also play important roles in CVB3 lifecycle. Experimental evidence suggests that viral 2B, 2BC, and 3A initiate intracellular membrane reorganization to support viral replication and increase plasma membrane permeability to facilitate viral progeny release (52, 194). This is supported by the observation that poliovirus carrying a 2B mutation is defective in RNA amplification and viral progeny release in cell culture (96).

1.3.   Pathogenesis of CVB3-induced myocarditis: a tri-phasic disease

Coxsackievirus B3 infection may lead to severe myocardial injury. The outcome of CVB3 infection depends on the complex interaction between pro-viral mechanisms and host anti-viral immune responses (37, 126, 138). Data from murine experimental model of CVB3-induced myocarditis suggests that the disease progression can be characterized in three distinct phases: (I) viremic, (II) inflammatory infiltration, and (III) cardiac remodeling (125, 189). Featured events in each phase of viral myocarditis are summarized in **Figure 2**.

1.3.1   Viremic phase

The viremic phase (0-4 days post infection) features prominent viral replication and early cardiomyocyte damages without significant host immune responses during acute myocarditis (125, 189). It is well documented that CVB3 inflicts direct damages to infected cardiomyocytes, which contributes significantly to subsequent disease development (58, 127). As early as 2 days post infection, cytopathic lesions featuring single or multi-cell vacuolar changes are observed in CVB3-infected immune competent mice. Numerous and widespread islands of cardiomyocytes with cytopathic lesions, contraction band coagulation necrosis, as well as early single-cell calcification are observed from day 3 onwards (37, 138). Furthermore, *in situ* hybridization analysis shows co-localization of viral genome with damaged cardiomyocytes (105, 127). Further evidence of direct virus-induced myocardial injury comes from CVB3 infection of SCID (severe combined immunodeficiency) mice, which has no mature T and B cells due to their inability to complete V(D)J gene recombination. CVB3-infected SCID mice develop an early and extensive cardiomyocyte coagulative necrosis and contraction band necrosis as compared to their wild-type counterparts (37).

1.3.2   Inflammatory phase

The inflammatory infiltration phase (5-14 days post infection) takes place in response to viremia (125, 189). Natural killer (NK) cells and macrophages detect viral invasion and evoke the innate immune response, resulting in inflammatory cell infiltration of the myocardium. The macrophages and NK cells drive viral clearance by mediating cytolysis of infected cells, and by producing pro-inflammatory cytokines including tumour necrosis factor-α (TNF-α), interleukin-1 (IL-1), IL-2, and interferon-γ (IFN-γ) (58, 127). The innate immune response also mounts an adaptive immune response executed by antigen-specific T-lymphocytes (CD8+ cytotoxic T-cells and CD4+ T-helper cells) and antibody-producing B-lymphocytes, which help eliminate viral particles and viral-infected cells (58). However, these well-

intentioned immunologic host defense mechanisms, if persistently activated, become detrimental and exacerbate myocardial injury. Indeed, certain pro-inflammatory cytokines augmented upon CVB3 infection, such as TNF-α and IL-1, are shown to promote CVB3-induced myocarditis in otherwise disease resistant mice (116). Furthermore, specific removal of certain immune cell populations such as T-lymphocytes in experimental myocarditis mouse models proves to be beneficial (165). These mice have markedly reduced inflammatory infiltrates and mortality rate upon CVB3 challenge. The humoral and cellular immune responses become pathologic when they morph into self-attacking entities upon exposure to secluded cardiac-antigens released from damaged cardiomyocytes, such as cardiac myosin, troponin-1, and vimentin (110, 127). Auto-antibodies against these cardiac proteins were detected in the sera of patients with myocarditis and DCM (47). Some of these auto-antibodies are also shown to cross-react with CVB3 particles (131), supporting the "antigenic mimicry" hypothesis in viral myocarditis (71). All in all, these pathologic immune reactions further contribute to myocyte injuries in the subacute and chronic stages of the disease, leading to heart failure and death.

1.3.3 Remodeling phase

The cardiac remodelling phase (15 days post infection onwards) serves to repair the damaged myocardium in the absence or presence of low-level persistent viral genomes (125, 189). Due to the terminally differentiated nature of cardiomyocytes, myocytes loss in the prior phases of viral myocarditis cannot be replaced through cell proliferation. In addition, viral genomes persisted in the forms of replication-defective mutants and double-stranded RNAs (as well as their consequential sporadic viral protein production) may exacerbate myocyte loss in the long term by chronically activate the immune response in the myocardium (62). Progressive fibrotic reparation takes place in regions of myocyte loss, resulting in abundant collagen accumulation in between remaining viable myocytes. The extensive fibrotic scars, however, are ineffective in facilitating contractile force transmission and electrical signal transduction. Still, cardiac output must be maintained. Efforts of the imperfect "band-aids" and remaining myocytes in delivering adequate cardiac output drive the continual restructuring of the myocardium, with deterioration and further reparation of the interstitial collagen network and cardiomyocyte hypertrophy. However, cardiac output cannot be sustained in the long term. Over time, progressive decompensatory molecular and structural changes take place in the myocardium. Ultimately, this results in myocardial wall thinning and left ventricle dilatation, leading to DCM and heart failure (64, 135).
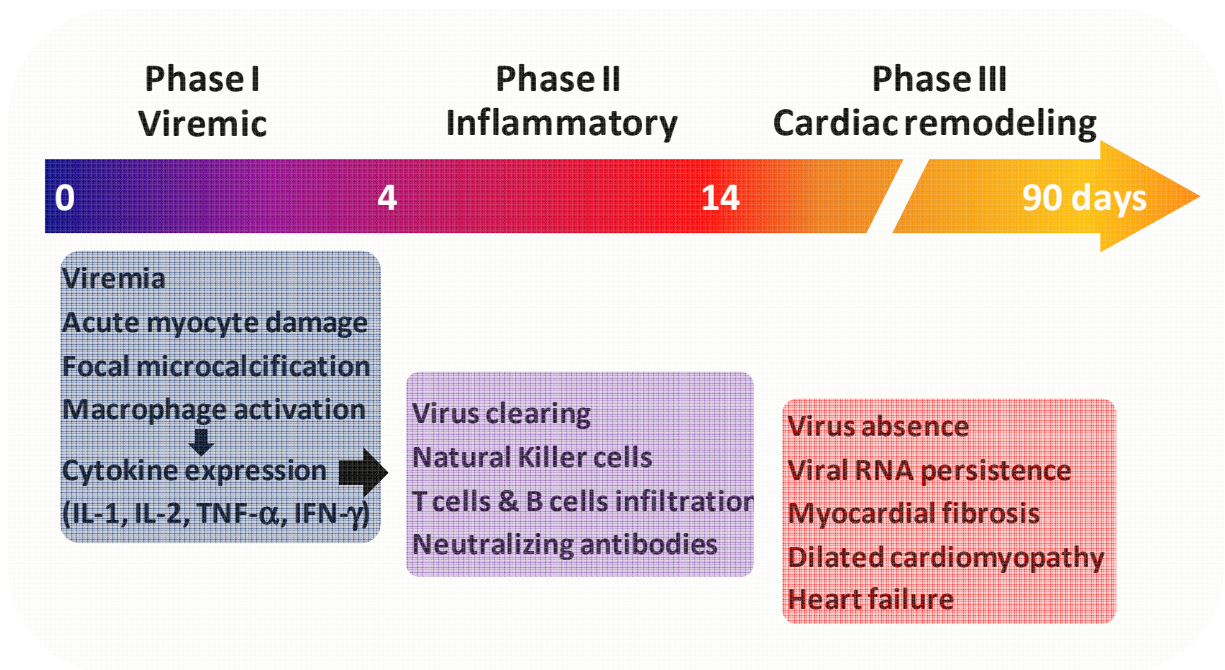
Figure 2. Pathogenesis of viral myocarditis: a tri-phasic disease.

Pathogenesis of viral myocarditis: a tri-phasic disease. In experimental mouse model, three distinct phases of viral myocarditis has been characterized: viremic, inflammatory, and remodeling phases. The viremic phase features prominent viral replication with acute myocyte damage and focal microcalcification in the absence of inflammatory infiltrates. Initial release of cytokines such as IL-1, IL-2, TNF-α, and IFN-γ in infected heart attracted macrophages and NK cells to the sites of injury, which initiates the inflammatory phase characterized by the infiltration of T cells and B cells, as well as the production of neutralizing antibodies for viral clearance. In the remodeling phase of myocarditis, viral particles are typically absent in blood and peripheral tissues. Persistence of viral genome and immune infiltrates may contribute to long-term tissue degeneration and progression of viral myocarditis to DCM and heart failure. This figure is modified from Feldman and McNamara (61).

1.4. Diagnosis and treatment of viral myocarditis

Viral myocarditis is a presumptive diagnosis based on history and clinical features. Viral myocarditis patients may present with a history of recent flu-like symptoms of fever, arthralgia, and malaise. Clinical presentations of viral myocarditis varied widely. Similar to other forms of myocarditis, viral myocarditis is typically asymptomatic and subclinical. However, asymptomatic patients may have electrocardiographic abnormalities. Severe patients with viral myocarditis may have signs and symptoms of clinical heart failure (e.g. shortness of breath, chest pain, and ventricular arrhythmia) and ventricular dilatation. Patients with fulminant viral myocarditis may have severe left ventricular dysfunction, with or without cardiac dilatation (48). Clinical laboratory testing may reveal elevations in leukocyte count, sedimentation rate, and cardiac fraction of creatine kinase, troponin T, as well as troponin I ((49, 118, 181, 195)). Elevated serum levels of cardiac creatine kinase and troponins are indicative of myocardial cell damage. Electrocardiogram may show ventricular arrhythmias. Serological examination may also reveal circulation of anti-viral antibodies (55, 119, 120). Endomyocardial biopsy (EMB) assessed by the Dallas criteria is still the reference standard for diagnosing viral myocarditis, despite its limited sensitivity and specificity (18, 24, 55). Contrast-enhanced magnetic resonance imaging and echocardiography may help localizing and assessing the extent of inflammation in patients with presumed myocarditis (66, 123). Follow-up EMB sampling at the abnormal myocardial area may enhance its diagnostic value. Molecular techniques such as reverse-transcriptional PCR (RT-PCR) and *in situ* hybridization allow detection of the presence of viral genome in EMB specimens (51, 130, 204).

Akin to other forms of myocarditis, the treatment of viral myocarditis is mainly designed around supportive measures, such as inotropic therapy, afterload reduction, arrhythmia management, and adequate tissue oxygenation (61, 192). Although the activation of cellular and humoral autoimmunity may play a role in the long-term progression of myocarditis, immunosuppressive therapy is not recommended in patients with viral myocarditis (1). Various randomized, placebo-controlled trials have failed to demonstrate beneficial effects of immunosuppression (117, 140, 167). Treatment with specific antiviral drugs for viral myocarditis such as Isoxazoles (WIN54954) and Pleconaril (VP63843) has been shown to be beneficial (65, 132). These inhibitors are broad-spectrum viral capsid function inhibitors that block enteroviral attachment, entry, and uncoating. A clinical trial involving Pleconaril usage in children and adults patients with enteroviral meningitis and upper respiratory tract infections were reported to decrease severity and duration of the diseases (19). Still, effective therapeutics for the treatment of viral myocarditis/DCM is greatly needed to improve overall patient survival and cardiac function.

1.5. Research hypothesis and objective

Viral myocarditis, the inflammation of myocardium initiated by viral infection, is an important cause of mortality in newborns and neonates. In addition, it is a precursor to dilated cardiomyopathy. To date, no effective therapy is available for viral myocarditis/DCM. Coxsackievirus B3 is a primary human pathogen of viral myocarditis. Extensive research efforts on CVB3 have broadened our understanding of viral lifecycle. However, the pathogenesis of coxsackievirus-induced myocarditis is not fully understood. The **objective** of this dissertation is to explore the role of host protein manipulation in coxsackieviral replication and pathogenicity. My **hypotheses** are **(1)** coxsackievirus hijacks host's cellular autophagy mechanism to facilitate its own replication; and **(2)** the serum response factor (SRF) is cleaved by viral protease 2A during coxsackievirus infection and contributes to impaired myocardial function and progression to DCM.

As described previously, the general gist of viral lifecycle includes viral particle internalization upon receptor engagement, followed by cytosolic release of viral genomic RNA and viral protein synthesis. Viral proteins manipulate multiple host pathways to facilitate the amplification of viral genomes and viral proteins. Viral proteins 2B, 2BC, and 3A induce massive intracellular membrane reorganization, resulting in vacuolization of host cells. These viral-induced membrane structures are said to support viral replication by serving as physical scaffolds for the assembly of viral replication complexes. However, the nature of these membranes remains unknown. In **Chapter 3**, I explored whether CVB3 manipulates the host autophagy protein degradation pathway to supply membrane platforms for successful viral replication.

Aside from detail events in viral replication, the underlying molecular mechanism that impairs heart function and drives the progression of viral myocarditis and DCM is also vaguely understood. As introduced earlier, the virus-encoded proteases play vital roles in CVB3 lifecycle. Not only are these viral proteases important in the processing of viral polyprotein, but they also contribute to successful viral replication by cleaving multiple host proteins involved in host RNA transcription, host protein translation, cell signalling, and cell structure. Viral proteases have been recognized as important pathogenic factors contributing to the development of DCM. It has been shown that transgenic mice with inducible, cardiac-specific expression of viral protease 2A develop severe cardiac dysfunction and DCM (205). However, the mechanism underlying viral protease-induced DCM is not fully understood. In **Chapter 4**, I explored whether coxsackieviral protease manipulates the expression of serum response factor, an essential transcription factor for the expression of cardiac contractile and regulator genes, and contributes to impaired heart function and progression of viral myocarditis and DCM.

Bridging the existing findings helps create a complete picture of CVB3-induced myocarditis that is valuable to the development of novel therapeutics to attenuate viral replication and ameliorate viral-induced injury. Combinations of antiviral therapies may improve efficacy while minimizing side-effects.

Chapter 2 – Materials and methods

2.1 Materials

Rapamycin, ammonium chloride (NH_4Cl), bafilomycin A, 3-methyladenine (3-MA), monoclonal anti-β-actin antibody, and monoclonal anti-GAPDH antibody were purchased from Sigma. A monoclonal anti-VP1 antibody was obtained from DakoCytomation. Beclin-1 small interfering RNA (siRNA), lysosome-associated membrane protein 2 (LAMP2) siRNA, SRF siRNA, control scramble siRNA, polyclonal anti-SRF C-terminus antibody, anti-FLAG antibody, anti-eIF4γ antibody, and horseradish peroxidase-conjugated secondary antibodies were purchased from Santa Cruz Biotechnology. Polyclonal anti-SRF N-terminus antibody was from Novus Biological. A monoclonal anti-Vps34 antibody was obtained from Life Technologies. Vps34 siRNA, ATG7 siRNA, and scramble control siRNA were obtained from Qiagen. A monoclonal anti-Beclin-1 antibody was purchased from BD Biosciences. Polyclonal guinea pig anti-p62 was purchased from Progen. A polyclonal rabbit anti-LC3 antibody was obtained from MBL International. A polyclonal rabbit anti-phospho-eIF2α antibody was obtained from Cell Signaling. Polyclonal rabbit anti-ATG7 and anti-LAMP2 antibodies were obtained from Cell Signaling and Abcam, respectively. z-VAD-fmk was purchased from EMD Biosciences. z-LKST-fmk was custom synthesized by CPC Scientific.

2.2 Cell culture

HeLa cells and HEK293A cells obtained from the American Type Culture Collection were used for this study. HeLa cells were grown in complete medium (Dulbecco's modified Eagle's medium [DMEM] supplemented with 10% heat-inactivated newborn calf serum). HEK293A cells were maintained in complete medium with the addition of 1% nonessential amino acids. The majority of the experiments in **Chapter 3** were performed with HEK293A cells, and critical experiments were repeated using Hela cells.

The HL-1 cell line, a murine cardiac muscle cell line established from an AT-1 mouse atrial cardiomyocyte tumor lineage, was a generous gift from Dr William C Claycomb (Louisiana State University Medical Center, USA). Cells were plated and maintained in Claycomb medium (JRH Biosciences) supplemented with 10% fetal bovine serum, 100 μg/ml penicillin-streptomycin, 0.1 mM norepinephrine in ascorbic acid, and 2 mM L-glutamine as described previously (129).

2.3 *In vitro* and *In vivo* CVB3 infection

HeLa cells were infected at a multiplicity of infection (MOI) of 10 with CVB3 (Kandolf strain) or sham infected with phosphate-buffered saline (PBS) for 1 h in serum-free DMEM. The cells were then

washed with PBS and cultured in complete medium for various times until they were harvested. HEK293A cells and HL-1 cardiomyocytes were infected in a similar fashion, but with a higher MOI of 100. For autophagy induction, cells were either treated with rapamycin for 3 h or starved in Hank's balanced salt solution (137 mM NaCl, 5.4 mM KCl, 0.8 mM $MgSO_4$, 0.8 mM Na_2HPO_4, 0.4 mM KH_2PO_4, 4.2 mM $NaHCO_3$, 20 mM HEPES, and 1.5 mM $CaCl_2$, pH 7.4) for 2 h prior to virus infection. For inhibition experiments, cells were infected with CVB3 in the presence or absence of various inhibitors or vehicle (dimethyl sulfoxide) for 1 h, washed with PBS, and then incubated with fresh DMEM containing different concentrations of inhibitors unless otherwise specified in the figure legends.

Murine coxsackievirus infection was performed as described (208). Briefly, male A/J mice at the age of ~5 weeks were either infected intraperitoneally with 10^5 plaque-forming unit (PFU) of CVB3 or sham infected with PBS for 3, 9, and 30 days. This study was carried out in strict accordance with the recommendations in the Guide for the Care and Use of Laboratory Animals of the Canadian Council on Animal Care. The protocol was approved by the Animal Care Committee of the University of British Columbia (#A03-0233).

2.4   Heart function measurements

Heart function was measured before infection (day 0) and on days 3, 9, and 30 after CVB3 infection using two-dimensional echocardiography (Sonos 5500, Philips) with a 12 MHz S-12 probe (Sonos 5000). Parasternal long and short axis images at the level of the mitral valve and papillary muscles were taken and these measurements were normalized to changes in body weight and then utilized for calculation of functional parameters. All measurements were averaged for five consecutive cardiac cycles.

2.5   Plaque assay

The virus titer in the cell supernatant was determined by an agar overlay plaque assay performed in triplicate, as described previously (6). In brief, the supernatant from CVB3-infected cells was serially diluted 10-fold and overlaid on a 90 to 95% confluent monolayer of HeLa cells in 6-well plates. After 1 h of incubation (5% CO_2, 37°C), the HeLa cells were washed with PBS to remove non-binding viruses, followed by overlay with 2 ml of warm complete medium containing 0.75% agar in each well. The cells were incubated at 37°C for 72 h and then fixed with Carnoy's fixative (75% ethanol-25% acetic acid) and stained with 1% crystal violet. Plaques were counted, and the viral titer was calculated as PFU per milliliter.

2.6   Western blot analysis

Western blotting was performed as described previously (26, 128). After treatment, the cells were incubated with lysis buffer (50 mM Tris-HCl, pH 7.2, 250 mM NaCl, 0.1% NP-40, 2 mM EDTA, 10% glycerol) containing protease inhibitor cocktail (Roche) on ice for 10 min. Cell lysates were then harvested by scraping, followed by brief sonication and centrifugation at 12,000 × g for 10 min at 4°C. The protein concentration was determined by the Bradford assay (Bio-Rad). Equal amounts of protein were subjected to sodium dodecyl sulfate-polyacrylamide gel electrophoresis and then transferred to nitrocellulose membranes (Amersham). The membranes were blocked for 1 h with 5% nonfat dry milk Tris-buffered saline solution containing 0.1% Tween 20 (TBST). The blots were then incubated for 1 h with the primary antibody prepared in 2.5% milk TBST, followed by three times washing with TBST. The membrane was then incubation for another hour with a HRP-conjugated secondary antibody, followed by washing with TBST. Immunoreactive bands were visualized by enhanced chemiluminescence (SuperSignal West Pico kit; Pierce) and documented by ChemiGenius 2 (Syngene).

2.7   Immunocytochemistry

Immunocytochemical staining was performed as described previously (68). Cells grown on glass slides were washed with PBS and fixed in 4% formaldehyde. Cells were then permeabilized with 0.1% Triton X-100 for 10 min, blocked with 5% bovine serum albumin (BSA) in Tris-buffered saline (TBS) for 30 min. After incubation with primary antibodies at 4 °C overnight and then with anti-rabbit AlexaFluor 594 or anti-mouse AlexaFluor 488 IgG at room temperature for 1 h, cells were washed with PBS and then mounted on slides using VectaShield medium containing 4',6-diamidino-2-phenylindole (DAPI). Cells were imaged and analyzed using a Leica SP2 AOBS confocal fluorescence microscope.

2.8   Transmission electron microscopy

For ultrastructural analysis, HeLa cells and HEK293A cells were sham infected or infected with CVB3 at MOIs of 10 and 100, respectively, for 5 and 7 h. Briefly, cells were fixed in 2.5% glutaraldehyde (Polysciences Inc.) in PBS, pH 7.2, for 10 min at room temperature. Following three washes in PBS, cells were postfixed in 1% osmium tetroxide (Polysciences Inc.), 1% potassium ferrocyanide, 100 mM sodium cacodylate buffer, pH 7.4, for 1 h at room temperature. After several rinses in distilled water, cells were dehydrated in a graded series of acetone washes and embedded in Eponate 12 resin (Ted Pella Inc.). Sections (70 to 80 nm) were cut and viewed on a Tecnai 12 transmission electron microscope (FEI Inc.). Approximately 15 cells were counted, and for each cell the number of double-membrane vesicles was

examined, as previously described (4). Autophagosomes were defined as double-membrane vacuoles measuring 0.2 to 1.0 μm.

2.9 Microscopic monitoring of autophagosome formation

For the detection of autophagosomes, cells were transiently transfected with GFP-LC3 plasmid (a generous gift from Sharon A. Tooze at the Cancer Research UK London Research Institute, United Kingdom), using Lipofectamine 2000 (Life Technologies). After 24 h of transfection, cells were sham or CVB3-infected for 5 h, and the fluorescence of GFP-LC3 was observed under a Leica SP2 AOBS confocal fluorescence microscope. The number of cells with punctate GFP-LC3 localization relative to all green fluorescent protein (GFP)-positive cells was counted (a minimum of 200 GFP-positive cells were counted in total for each condition) and presented as a percentage, as previously described (88).

2.10 RNA interference

HeLa cells were grown at 50% confluence were transiently transfected with various small-interfering RNAs (siRNAs) at a concentration of 50 to 80 nM, using Lipofectamine 2000 or HiPerFect (Qiagen) according to the manufacturer's instructions. A scrambled siRNA was used as a negative control. The silencing efficiency was detected by western blot analyses using the respective antibodies. After 48 h, cells were infected with CVB3 as described above. Cell supernatants and lysates were collected 7 h post infection and analyzed for viral titer and protein expression by plaque assay and western blotting, respectively.

2.11 Generation of SRF mutant constructs

The pCMV-3×FLAG-SRF construct, a generous gift from Dr Ron Prywes (Columbia University, USA), was used as the template for the generation of site-directed mutagenesis (SRFG349E and SRFG327E mutants). Truncated SRF cDNAs were generated by PCR using the following primers: SRF-N forward 5'-GTCGACTCTAGAATGTTACCG-3' and reverse 5'-AGGAGACGGATCCGCTTCATG-3'; SRF-C forward 5'-CTGAAGTCTAGAGGCAGCGG-3' and reverse 5'-ACCCGGGATCCTTTAGATCAT-3'. SRF-N and SRF-C cDNAs were subcloned into pCMV-3×FLAG vector using XbaI and BamHI restriction digestions.

2.12 Luciferase assay

HeLa and HL-1 cells at 90% confluence in 24-well tissue culture plates were transiently co-transfected (using Lipofectamine 2000) with a Firefly luciferase reporter construct containing cardiac α-actin promoter (32) and a Renilla luciferease control vector (Promega) together with plasmids encoding

full-length, truncated, or non-cleavable SRFs, and control LacZ. After 48 h, cell lysates were collected and analyzed for firefly and renilla luciferase activities using a dual luciferase reporter assay system (Promega) as per the manufacturer's instruction. The relative luciferase activities were normalized to the LacZ control group and presented as fold changes.

2.13   Affymetrix array analysis

Microarray analysis of cardiac gene expression was performed as described previously (175). Hearts were harvested at 9 days following CVB3 infection and total RNA was isolated from mouse ventricular tissue using the RNeasy isolation kit (Qiagen) and pooled (n = 4 for each group). Samples were hybridized to a custom mouse GeneChip (Amgen) based on the Affymetrix GeneChip Expression Analysis Technical Manual (Affymetrix). In vitro transcription was performed using an ENZO Bioarray HighYield RNA Transcript Labeling kit as per the manufacturer's instructions. Arrays were washed in the Affymetrix Fluidics Station 450, stained with a streptavidin phycoerythrin solution and scanned using a HP Agilent GeneArray Scanner.

2.14   Real-time quantitative RT-PCR

Total RNAs were extracted from murine HL-1 cardiomyocytes at 24 h post infection using RNeasy isolation kit. Reverse transcription was performed using SuperScript III Reverse Transcriptase (Life Technologies) according to the manufacturer's instructions. mRNA levels of SRF and cardiac genes were measured by real-time quantitative PCR using an ABI Prism 7900HT Sequence Detection System as per the manufacturers' instruction (Perkin-Elmer Applied Biosystems) as previously described (34) and normalized to GAPDH mRNA.

2.15   Statistical analysis

Two-way analysis of variance with multiple comparisons and paired Student's t-tests were performed. Data were shown as the mean plus minus standard deviation (S.D.). P-values < 0.05 were considered to be statistically significant.

For statistical analysis of Affymetrix array data, the gene expression intensity values (averages of two replicates of the microarray analysis) were expressed as $\log_2$ ratios of CVB3- to sham-infected hearts and filtered for fold change cut-off of 1.8. Only genes that exhibited a 1.8-fold change ($\log_2$) or greater were included.

Chapter 3 – Autophagy in coxsackievirus infection

3.1 Background

3.1.1 Autophagy

Autophagy, meaning self-eating, is a conserved process in eukaryotes by which cells removes and recycles cytoplasmic long-lived proteins, misfolded proteins, as well as unwanted or damaged organelles to maintain cellular homeostasis under both normal and stress conditions (106, 109, 161). Autophagy is sub-classified in three forms: macroautophagy, microautophagy, and chaperone-mediated autophagy (42, 56, 67). Among them, macroautophagy, hereafter referred to as autophagy, is the most extensively studied form in both yeast and mammalian cells.

3.1.1.1 Process of autophagy

The hallmark of autophagy is the formation of double-membrane vesicles called autophagosomes, which are derived from the elongation of crescent-shaped double-membrane structures known as isolation membranes or phagophores (106, 109, 161). The process of autophagy (depicted in **Figure 3**) takes place in four sequential steps: initiation, sequestration, fusion, and degradation. During the initiation step, the phagophore nucleates and elongates. Next, the phagophore sequestrates a portion of the cytoplasm including the target misfolded proteins or damaged organelles. The two ends of phagophore eventually fuse to form the autophagosome. Then, the outer membrane of the autophagosome fuses with the lysosomes to form the autolysosome. Finally, the inner membrane and the sequestrated contents of the autophagosome are degraded and recycled by hydrolytic enzymes. The recycled products (i.e. amino acids and fatty acids) are used for biosynthesis or other metabolic activities. Note that autophagosome may also fuse with early or late endosome to form amphisome prior to fusion with lysosome (60).
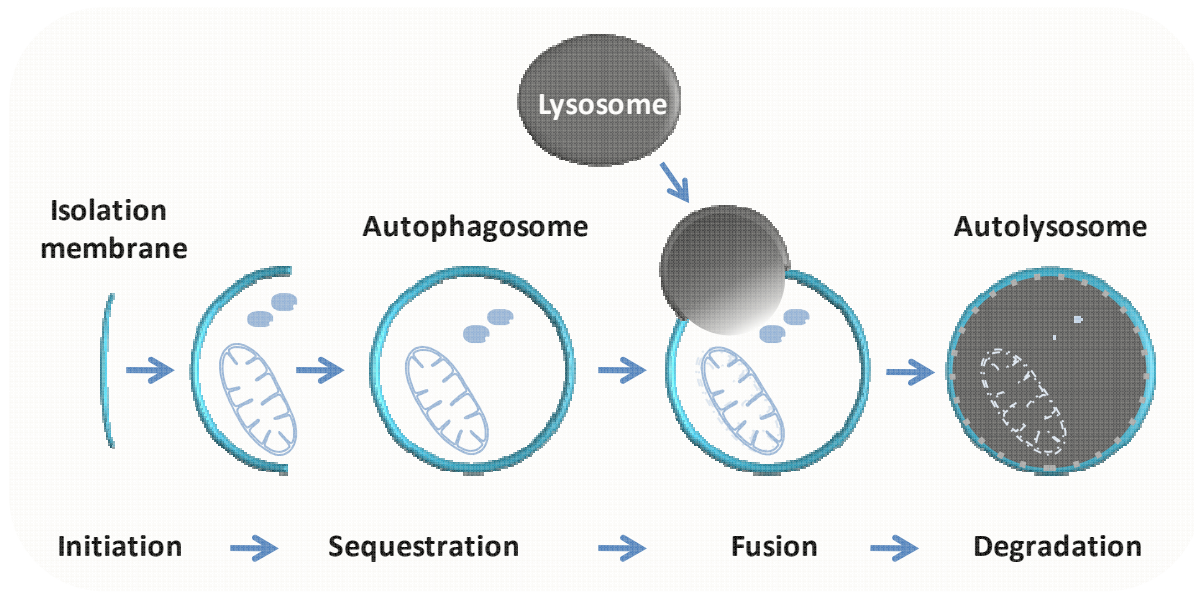
Figure 3. Process of autophagy pathway.

The process of autophagy takes place in four sequential steps: initiation (formation of the isolation membrane), sequestration (elongation and closure of isolation membrane to sequestrate a portion of the cytoplasm), fusion (autophagosome-lysosome fusion), and degradation (formation of autolysosome to eliminate its inner membrane and sequestrated contents).

3.1.1.2 Autophagy pathway components

The autophagy process is orchestrated by autophagy-related gene (ATG) products. More than 30 ATGs have been identified to date (83, 106, 146). The ATG proteins work together in complexes, including the class III phosphoinositide 3-kinase (PI3K) complex, the ULK complex, and two ubiquitination-like conjugation systems (ATG12-ATG5 system and LC3-PE (microtubule-associated protein light-chain 3-phosphatidylethanolamine) system) (83, 106, 146, 161). The ULK complex is made up of uncoordinated 51-like kinase 1/2 (ULK1/2), ATG13, focal adhesion kinase family interacting protein of 200 kD (FIP200), and ATG101. The class III PI3K complex is composed of vacuolar protein sorting-34 (Vps34), p150, beclin-1, ATG14, and Ambra1 (activating molecule in beclin-1-regulated autophagy). The two ubiquitination-like conjugation systems are comprised of ATG7, ATG12, ATG5, ATG16L1, ATG10, ATG4, ATG3, and LC3 (or ATG8 in yeast).

3.1.1.3 Molecular process of autophagosome formation

The molecular process of autophagosome formation (**Figure 4**) is explained as follow. Autophagy is initiated with the activation of ULK complex, which in turn activates the class III PI3K complex (81, 97). Class III PI3K complex is translocated to the ER/trans-Golgi network (101, 211). It then helps the nucleation of isolation membrane by catalyzing the formation of phosphatidylinositol 3-phosphates (PI3Ps), which interact and recruit other ATGs involved in membrane elongation (184). The elongation of the isolation membrane is then mediated by the ubiquitination-like conjugation systems. In the ATG12-ATG5 system, ATG12 is first activated by ATG7 and subsequently transferred to ATG10, then conjugated with ATG5 and subsequently to ATG16 to mediate the formation of LC3-PE (161). The LC3-PE system goes through a similar process in which nascent LC3 is first cleaved by ATG4 to become LC3-I, which is subsequently activated by ATG7, and then transferred to ATG3. Finally, LC3-I is conjugated to PE on the isolation membrane with the help of the ATG16-ATG12-ATG5 complex to form LC3-PE complex, also known as LC3-II (161). The recruitment of LC3-II on autophagic vesicles has been considered a common trait of autophagosome formation (161). Ratio of LC3-I to LC3-II, which measures the rate of LC3 lipidation, has also been widely accepted as a marker for autophagosome formation (98).

3.1.1.4 Regulation of autophagy

The process of autophagy formation is tightly regulated by various kinases, phosphatases, and small GTPases. The serine/threonine protein kinase mTOR (mammalian target of rapamycin) is one key negative regulator of autophagy. Blocking mTOR activity by amino acid deprivation or rapamycin treatment has been shown to induce autophagy (41, 109). On the other hand, the eukaryotic initiation factor 2α (eIF2α) regulates autophagy positively (186). eIF2α is phosphorylated and activated in the event of starvation, endoplasmic reticulum (ER) stress, and the presence of double-stranded viral RNA replication-intermediates. eIF2α phosphorylation drives the formation of autophagosome as well as the inhibition of protein translation process (112, 186). In addition, small GTPases and phosphatases, such as Ras, PTEN, and protein phosphatase 2A, also participate in the regulation of autophagosome formation.
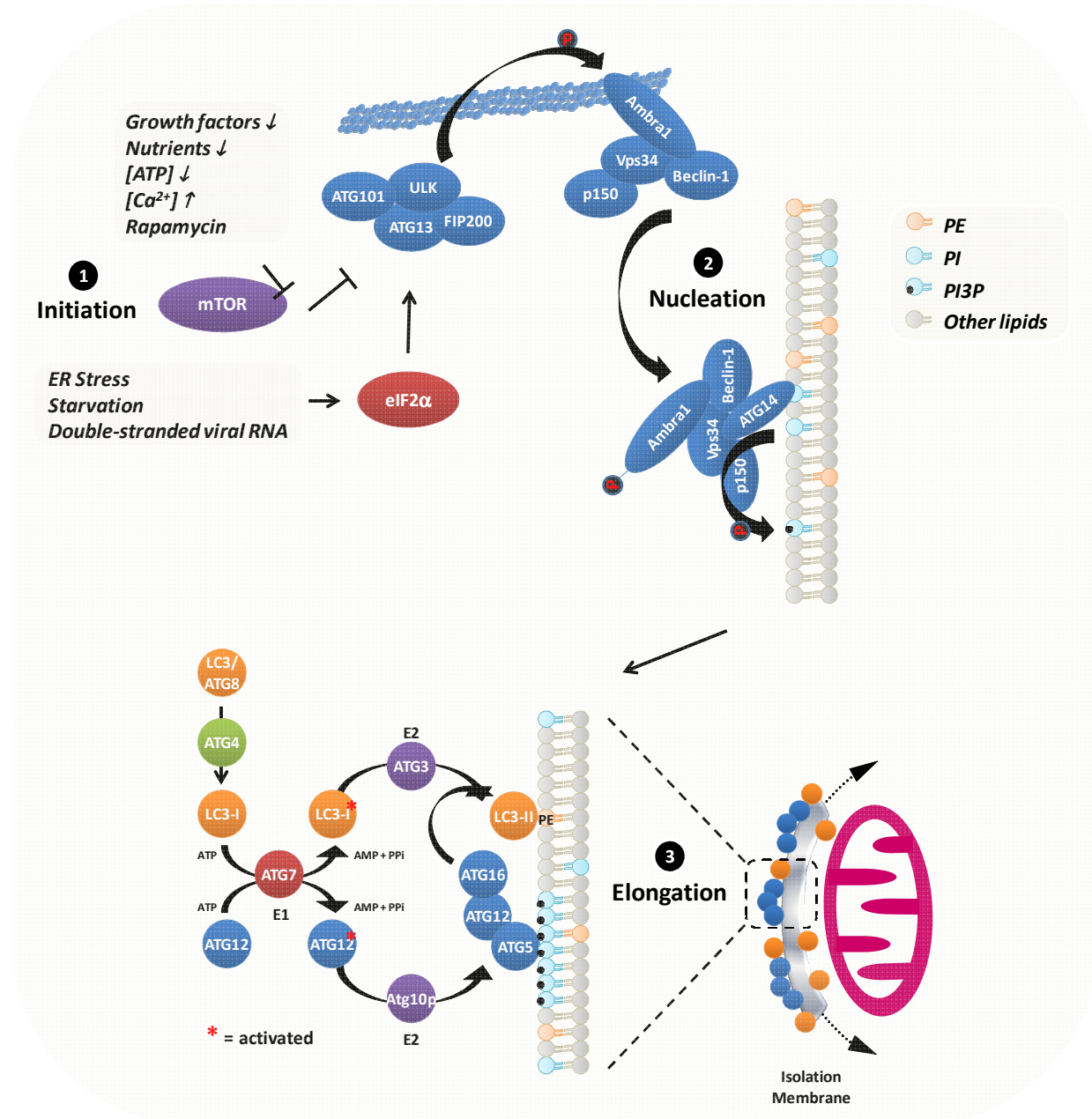
Figure 4. Molecular machineries of autophagy pathway.

Autophagy is initiated during cellular and metabolic stress via mTOR inactivation or eIF2α activation, which allows ULK complex activation. Activated ULK in turn phosphorylates Ambra1, which interacts with the Vps34 and Beclin-1 at the microtubule. Phosphorylation of Ambra1 results in the release of the class III PI3K complex from the microtubule and its translocation to the ER/trans-Golgi network, the major site of autophagosome formation. During autophagosome nucleation, the class III PI3K complex generates PI3Ps, which recruit other ATGs involved in membrane elongation. Elongation of the isolation

membrane is then mediated by two ubiquitination-like conjugation systems. ATG7 and ATG10 mediate ATG12-ATG5 complex formation, which is subsequently bound to ATG16. LC3 is cleaved by ATG4, forming LC3-I. Mediated by ATG7, ATG3, and the ATG16-ATG12-ATG5 complex, LC3-1 is conjugated to PE, generating LC3-PE complex, also known as LC3-II.

3.1.2 Autophagy in cardiac diseases

Autophagy is vital for cardiomyocyte function and viability. Autophagy supplies emergency energy sources by breaking down cytoplasmic proteins and organelles into amino acids and fatty acids. It was shown that cardiomyocyte survival under glucose deprivation is markedly reduced in the presence of autophagy inhibitor 3-methyladenine. Defects in the autophagy pathway lead to the development of cardiac diseases (121, 147, 190). It was reported that cardiac-specific ATG5 knockdown in adult mice results in cardiac hypertrophy, left ventricular dilatation, and contractile dysfunction (154). On the other hand, excessive autophagic activity induced under stress conditions such as ischemia reperfusion and pressure overloading is also detrimental to the heart as it leads into autophagic cell death (78, 134, 185, 197). This is supported by experimental data obtained from beclin-1 knockout mice challenged with either left anterior descending coronary artery ligation plus subsequent reperfusion or aortic banding (136, 216). In both models, disruption of beclin-1 expression results in the attenuation of stress-induced autophagy induction, as well as reduction in myocardial damage and pathological remodelling, underlining the damaging effect of dysregulated autophagy activity in the pathogenesis of various heart diseases.

3.1.3 Autophagy in viral infections

Autophagy has also been suggested to play a part in host immune response by sequestrating invading pathogens (e.g. herpes simplex virus and sindbis virus) and subsequently removing them from host cells (102). Viruses, on the other hand, have evolved various strategies to evade such host defense mechanism. Some viruses such as herpes simplex virus encode gene products that block cellular autophagy (186). Other viruses are able to hijack the autophagy pathway to benefit their own replication (102, 203). Certain positive-stranded RNA viruses such as poliovirus and coronavirus were reported to subvert cellular autophagy to facilitate their own replication (91, 171). Poliovirus proteins have been shown to co-localize with autophagic proteins (91). Induction of autophagy increases poliovirus yield, whereas autophagy inhibition decreases viral yield (91). Similar observations were made in murine hepatitis virus of the coronavirus family (171). Thus, the role of autophagy in the host seems to be dependent on the viral strain, but its overall relevance remains controversial.

3.2   Rationale

Picornavirus infection induces reorganization of intracellular membrane, which serves as a platform for the assembly of viral replication complex. However, the origin and nature of the viral-induced membrane platform remains unclear. Autophagosome, a double-membrane vesicle, is a potential site of viral replication. It has been reported that coronaviruses colocalize with the markers of autophagosome LC3 and ATG12 (171). Coronaviral replication is impaired in autophagy knockout (Atg5-/-) embryonic stem cell lines (171). Additionally, poliovirus proteins have also been shown to colocalize with a co-transfected GFP-LC3 protein (91). Stimulation of autophagy increases poliovirus yield, and inhibition of the autophagosomal pathway decreases viral yield. However, the role of autophagy in CVB3 replication remains unknown. Here, I explored whether CVB3 manipulates the host autophagy protein degradation pathway to supply membrane platforms for successful viral replication.

3.3   Hypothesis and specific aims

The objective of this chapter is to elucidate the molecular mechanisms utilized in viral replication. In this study, my **HYPOTHESIS** is that coxsackievirus hijacks host's cellular autophagy mechanism to facilitate its own replication.

My **SPECIFIC AIMS** are:

Aim 1. Examine whether CVB3 infection facilitates autophagosome formation

**Aim 2.** Define the role of autophagosome in viral replication

Aim 3. Identify the signalling components which stimulates the formation of autophagosome

3.4 Results

3.4.1 CVB3 infection increases autophagosome formation.

To determine whether CVB3 infection triggers cellular autophagy, ultrastructural analysis was performed with sham- or CVB3-infected HeLa and HEK293A cells. Electron micrographs of CVB3-infected cells revealed an increased prevalence of double-membrane vesicles in the perinuclear region compared to that of sham-infected cells (**Figure 5A**). Further quantitative analysis (**Figure 5B**) demonstrated a significant increase in autophagosome-like vesicles, which were characterized as double-membrane vesicles with a diameter of 0.2 to 1.0 μm present in the cytoplasm, in CVB3-infected cells.

To confirm that the observed double-membrane vesicles were indeed related to autophagy, I examined LC3 modification, another hallmark of autophagy (107, 145). Two forms of LC3 have been reported. In quiescent cells, LC3 resides in the cytoplasm in a precursor form, referred to as LC3-I. However, upon exposure to various autophagy stimuli, it is rapidly activated and subsequently conjugated to phosphatidylethanolamine to form an LC3-phosphatidylethanolamine complex, commonly referred as LC3-II, which participates in the formation of autophagosomes and remains attached to matured autophagosomes (98). It has been shown that the LC3-II/LC3-I ratio correlates well with the number of autophagosomes (98). After CVB3 infection, Western blots were performed to detect the LC3-II/LC3-I ratio, using an anti-LC3 antibody which recognizes both forms of LC3. As shown in **Figure 5C**, expression of LC3-II increased with the progression of CVB3 infection, which was accompanied by a decrease of LC3-I expression. The densitometry ratio of LC3-II to LC3-I demonstrated a cumulative increase in autophagosomes during CVB3 infection. Punctate accumulation of LC3, which represents the recruitment of LC3 to autophagic vacuoles, has also been suggested to be a characteristic of autophagy (98). After CVB3 infection, I showed that GFP-LC3-transfected cells with punctate GFP-LC3 distribution were markedly increased (**Figure 5D**), further confirming the increased formation of autophagosomes after viral infection.

A.

B.

27
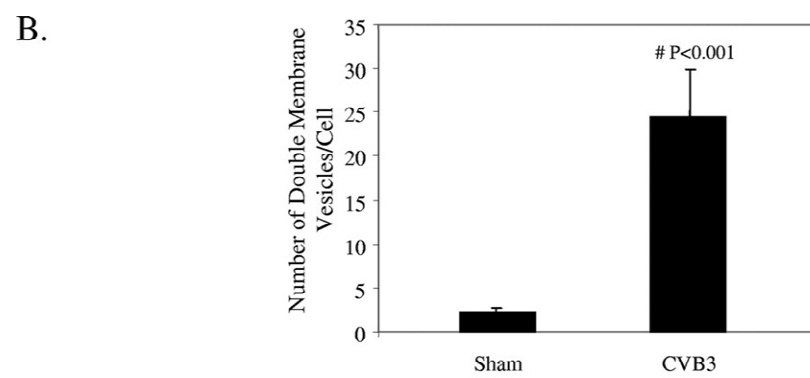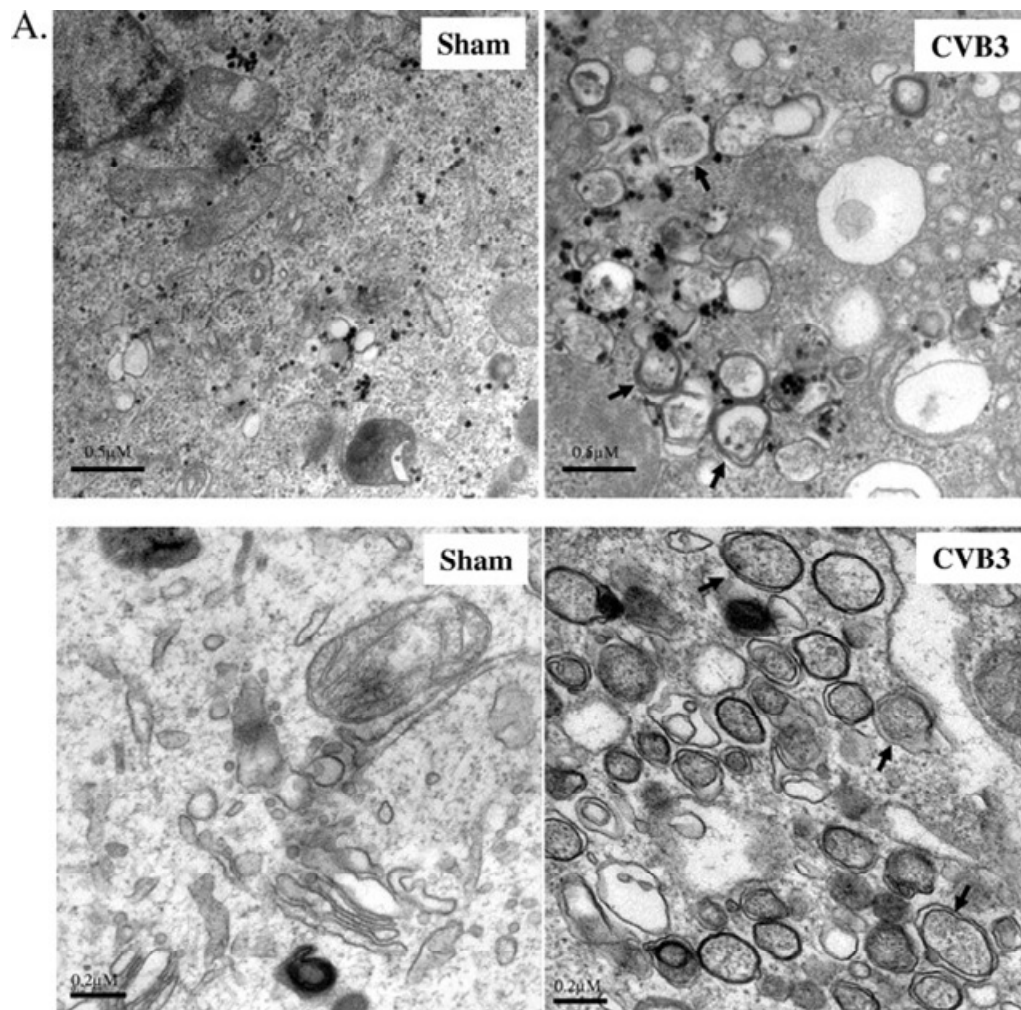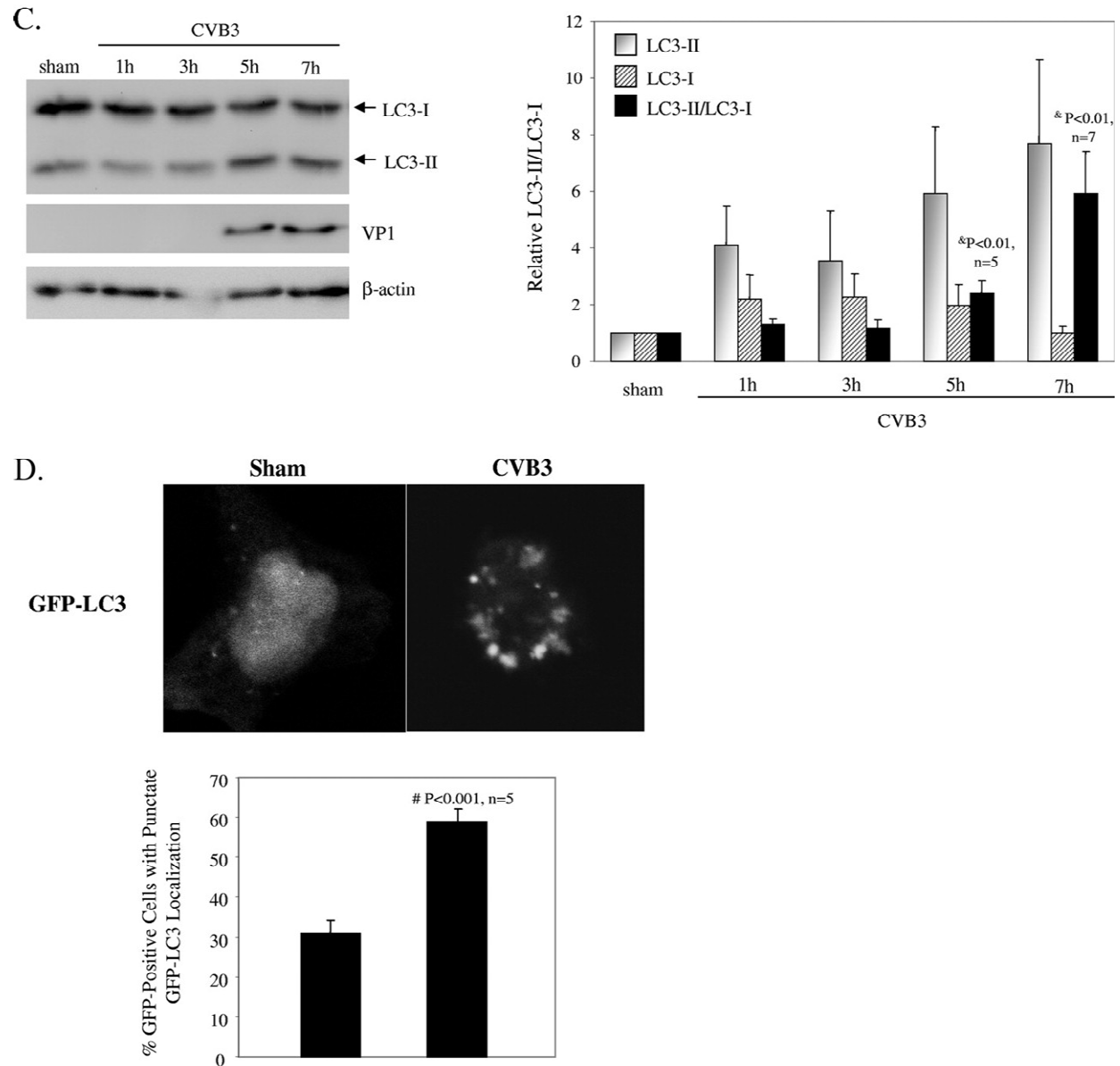
Figure 5. CVB3 infection increases autophagosome formation.

(A) Representative electron micrographs of sham- and CVB3-infected HeLa (top) and HEK293A (bottom) cells at 7 h post infection. Arrows indicate representative autophagosomes that would be scored positive in panel B. (B) Quantitation of the numbers of autophagosomes in sham- and CVB3-infected HEK293A cells. Data shown represent the number of autophagosomes per cell under each condition (mean ± standard error [SE]). #, P < 0.001 compared to sham infection, by Student's t test. (C) The LC3-II/LC3-I ratio, which is a hallmark of autophagy, increases with the progression of CVB3 infection. (Left) Western blot analysis of LC3 and viral capsid protein VP1 expression in CVB3-infected cells at various times post infection. β-Actin expression was examined as a protein loading control. (Right) Expression of LC3-II and LC3-I and ratio of LC3-II to LC3-I at the indicated times after CVB3 infection (means ± SE; n = 5 or 7 [as indicated]). LC3 expression was quantitated by densitometric analysis using NIH ImageJ v1.37

and normalized to sham infection, which was arbitrarily set to a value of 1.0. and, P < 0.01 compared to sham infection. (D) Representative confocal images and quantitation of autophagosomes in GFP-LC3-transfected HEK293A cells after CVB3 infection. HEK293A cells were transfected with GFP-LC3 plasmid for 24 h, followed by CVB3 infection. The GFP fluorescence was analyzed by confocal fluorescence microscopy. The percentage of cells with punctate GFP-LC3 localization relative to all GFP-positive cells was calculated and is presented as the mean ± SE (n = 5). #, P < 0.001 compared to sham infection.

3.4.2 Mechanism of induction of autophagosome formation

To determine the potential mechanism of induction of autophagosome formation, I examined the phosphorylation status of eIF2α and mTOR, two key regulators that control autophagosome formation and maturation. It has been shown that eIF2α phosphorylation positively regulates the autophagic pathway (186), whereas mTOR is a negative regulator of autophagosome formation (41). I found that eIF2α phosphorylation was increased at 5 and 7 h post infection (**Figure 6**), corresponding to an increased formation of autophagosomes in CVB3-infected cells. However, no significant changes in the levels of mTOR phosphorylation were observed after CVB3 infection (data not shown).
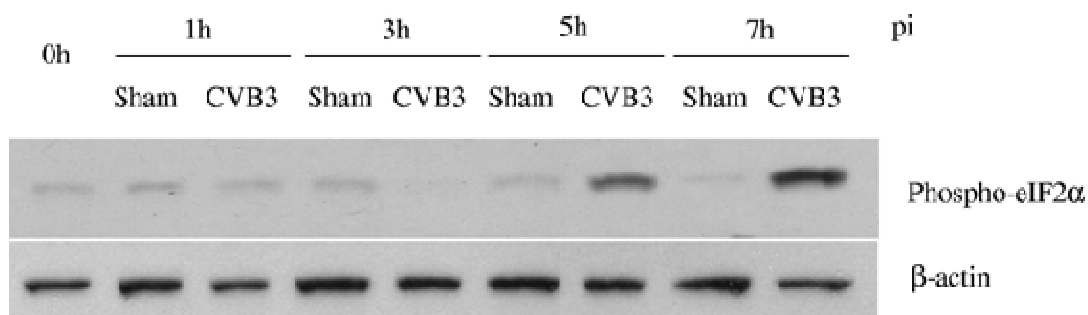
Figure 6. CVB3 infection induces eIF2α phosphorylation.

Western blot analysis of phosphorylated eIF2α and β-actin (loading control) expression was performed at the indicated times post infection. Similar results were obtained in two independent experiments.

3.4.3 Autophagy inhibitor 3-MA reduces CVB3 replication.

To determine whether the autophagosome induction during CVB3 infection was a host antiviral response or a viral replication mechanism, I tested the effect of 3-methyl adenine (3-MA) on CVB3 replication. 3-MA is a widely used selective inhibitor of autophagy which blocks the formation of autophagosomes and inhibits intracellular protein degradation without affecting protein synthesis (178). As shown in **Figure 7**, treatment with 3-MA resulted in a dose-dependent reduction of viral capsid protein (VP1) expression (**Figure 7A**) as well as in a significant reduction in CVB3 viral progeny titer (**Figure 7B**). More importantly, I found that 3-MA treatment led to significant inhibition of viral protein synthesis, even when it was introduced during the later stages of the virus life cycle (**Figure 7C**). This finding suggests that autophagic machinery may not have a destructive role during CVB3 infection and instead may play an important role in the replication of CVB3.
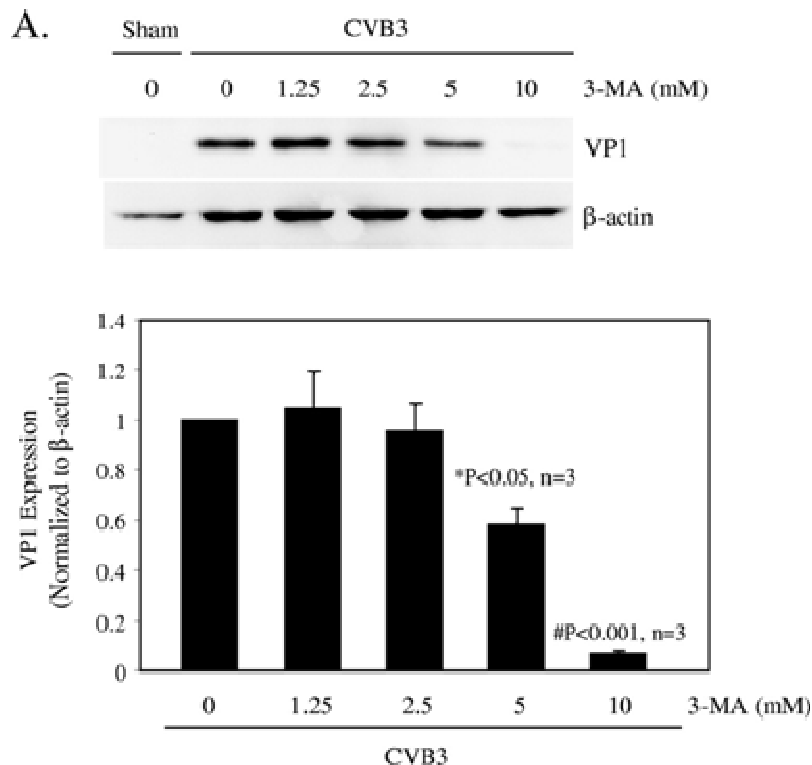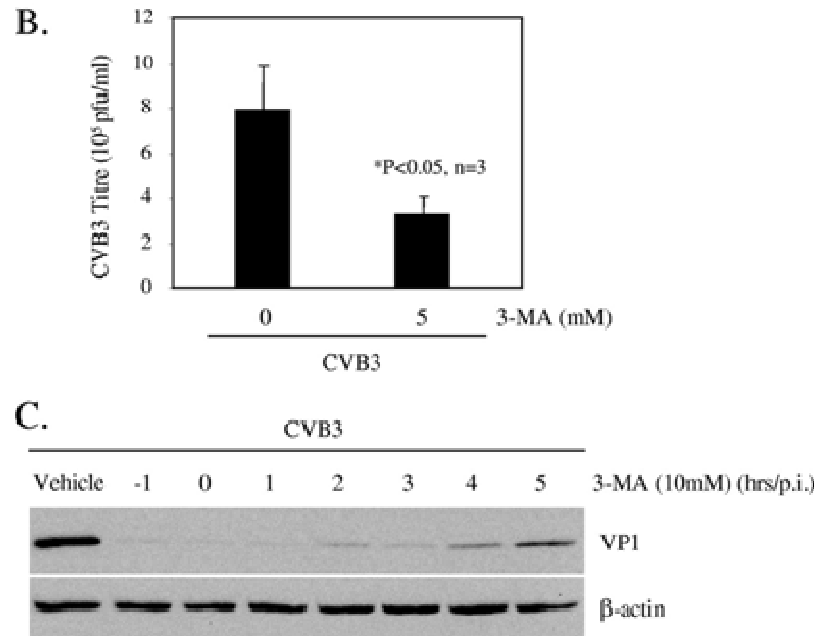
Figure 7. Autophagy inhibitor 3-MA reduces CVB3 replication.

(A) (Top) Western blot analysis of viral protein VP1 and β-actin (loading control) expression 7 h following CVB3 infection, with or without 3-MA treatment, as indicated. (Bottom) VP1 expression was quantitated by densitometric analysis using NIH ImageJ v1.37 and normalized to β-actin expression. The VP1/β-actin ratio was further normalized to the CVB3-infected group without treatment, which was arbitrarily set to a value of 1.0. The data shown are means ± SE (n = 3), and significance was determined by Student's t test. *, P < 0.05; #, P < 0.001 (compared to nontreated cells). (B) Plaque assay measuring the CVB3 viral progeny titers in supernatants collected from infected cells treated with or without 3-MA. The data shown are means ± SE for three independent experiments. *, P < 0.05 compared to nontreated cells. (C) Western blot analysis of CVB3-infected cells treated with 10 mM 3-MA at different times, as indicated.

3.4.4 Induction of autophagy enhances viral growth.

To further determine the role of autophagy, I investigated the effect of autophagosome induction on viral protein expression. Cells were deprived of amino acids (**Figure 8A**), a condition that is known to be able to induce autophagy (41), or treated with the pharmacological reagent rapamycin, which has been shown to induce autophagy by inhibiting the mTOR pathway (23) (**Figure 8B**). I showed that induction of autophagy through either nutrient deprivation or rapamycin treatment significantly increased viral protein expression (**Figure 8**). These results further suggest a critical role of autophagy in the virus life cycle, although I cannot rule out other effects that these treatments might have on viral replication, independent of autophagy.
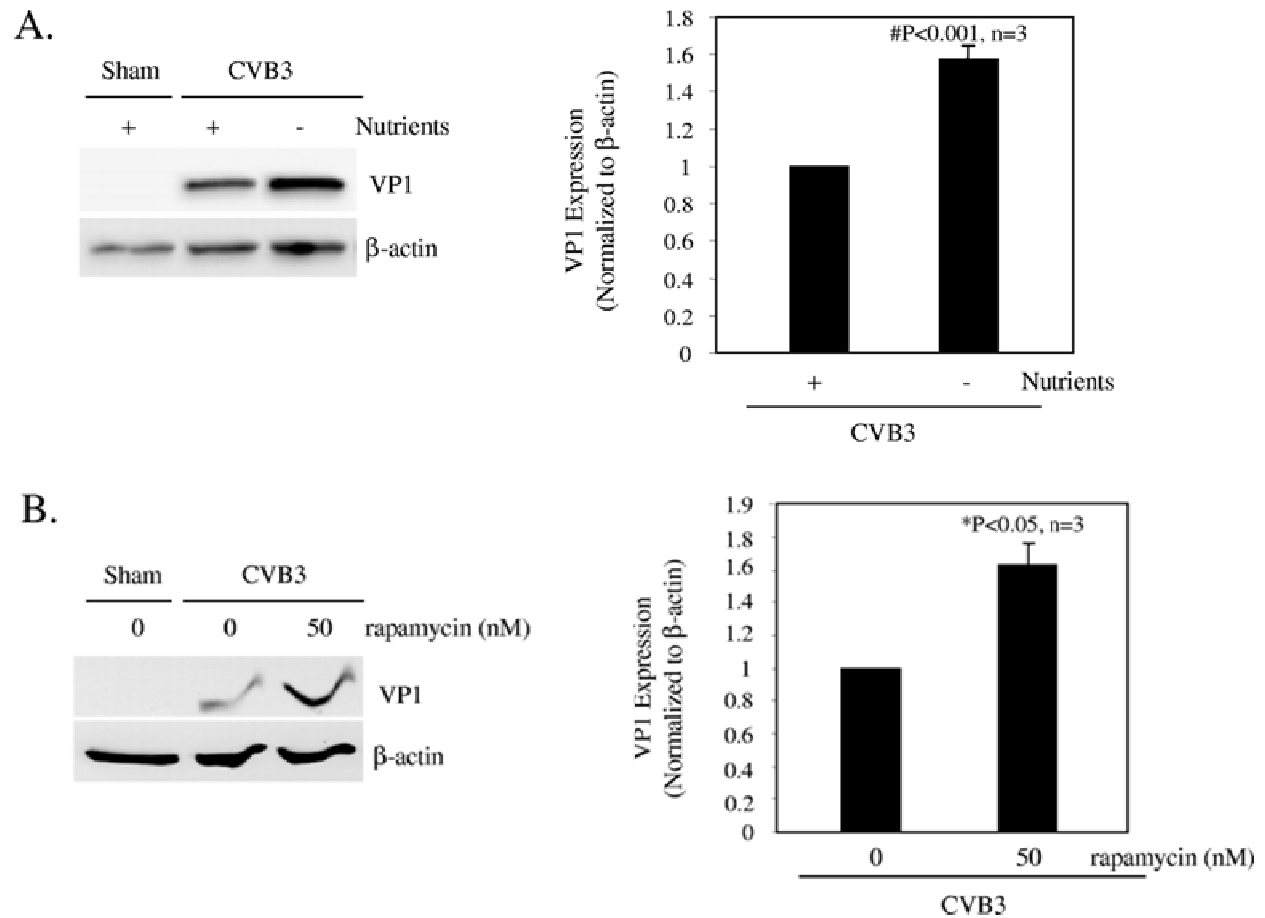
Figure 8. Induction of autophagy enhances viral replication.

Western blot analysis of VP1 and β-actin expression was performed at 7 h post infection. (A) Prior to CVB3 infection, cells were incubated in Hank's balanced salt solution for 2 h to induce cell starvation. (B) Cells were pretreated with rapamycin (50 nM) for 3 h. VP1 expression was quantitated, normalized, and analyzed as described in the legend to Figure 7 (data are means ± SE; n = 3). *, P < 0.05; #, P < 0.001 (compared to nontreated cells).

3.4.5 Knockdown of the genes critical for autophagosome formation reduces CVB replication.

To extend the studies with pharmacological agents, I employed a target-specific RNA interference approach to assess the effect of autophagosome disruption on viral replication. Cells were transfected with siRNAs (for ATG7, Beclin-1, and Vps34) to knock down the genes required for different steps of autophagosome formation. The autophagy protein ATG7 is an enzyme essential for activation of autophagosome formation and maturation machinery (106, 109). Deletion of ATG7 in mice has been shown to result in reduced autophagosome formation and impaired degradation of proteins and organelles induced by starvation (111). As shown in the phase-contrast images in **Figure 9A**, cells transfected with siRNA against ATG7 displayed greater resistance to CVB3 infection and maintained normal cell morphology, unlike the scramble siRNA-treated cells, which displayed severe virus-induced cytopathic effect. In addition, ATG7 siRNA treatment also blocked viral protein synthesis (**Figure 9B**). Similarly, disruption of the class III PI3K signaling complex required for autophagosome formation by Beclin-1 and Vps34 siRNAs resulted in significant reductions in CVB3 replication (**Figure 10**). My results further demonstrate a requirement of autophagy for effective coxsackievirus infection.
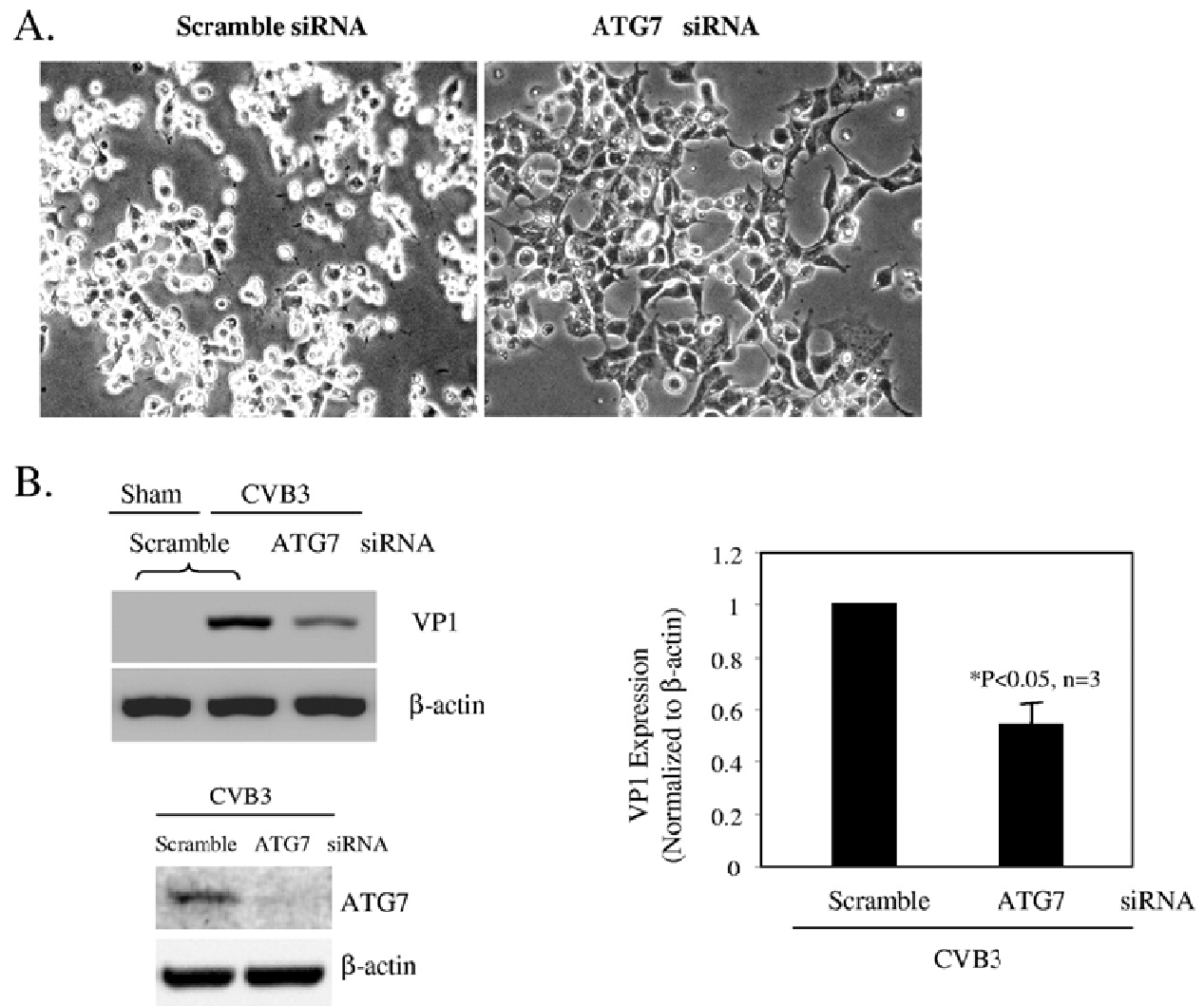
Figure 9. Gene silencing of ATG7 by siRNA inhibits CVB3 replication.

(A) Representative light microscopic images of CVB3-infected cells, with or without ATG7 siRNA transfection. (B) Western blot probing for VP1 and ATG7 expression, with or without ATG7 knockdown. VP1 expression was quantitated, normalized, and analyzed as described in the legend to Figure 7 (data are means ± SE; n = 3). *, P < 0.05 compared to scramble siRNA-transfected cells.
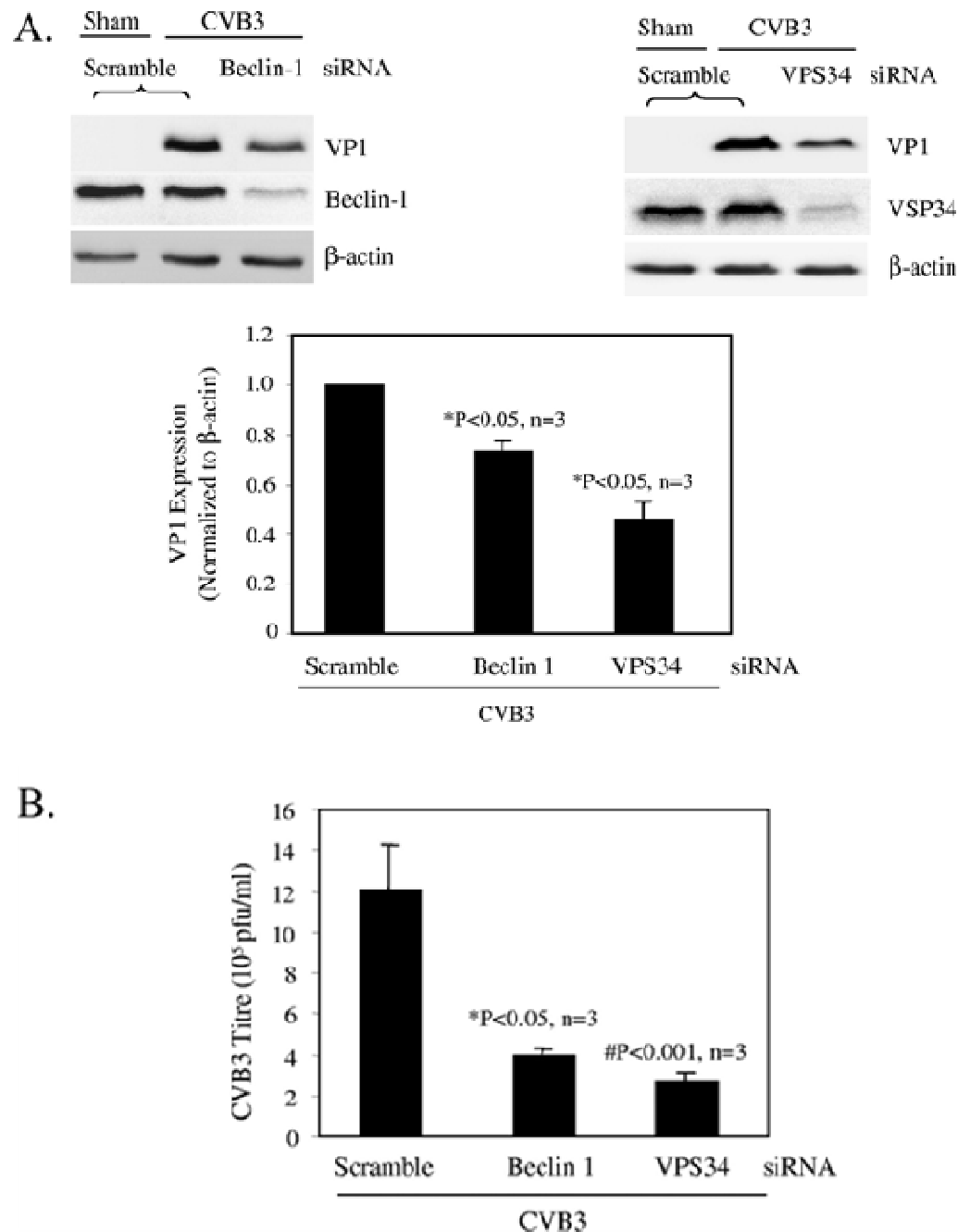
Figure 10. Knockdown of class III PI3K components reduces CVB3 replication.

(A) Western blot analysis of VP1 and Beclin-1 or Vps34 expression in CVB3-infected cells transfected with Beclin-1 (left) or Vps34 (right) siRNA prior to CVB3 infection. VP1 expression was quantitated, normalized, and analyzed as described in the legend to Figure 7 (data are means ± SE; n = 3). *, $P < 0.05$ compared to scramble siRNA control. (B) Plaque assay results for scramble or Beclin-1 and Vps34 siRNA-transfected cells (means ± SE; n = 3). *, $P < 0.05$; #, $P < 0.001$ (compared to scramble siRNA-transfected cells).

3.4.6 Expression of p62 following CVB3 infection.

I next examined the effect of CVB3 infection on autophagy- or lysosome-mediated protein degradation. The protein p62 has been considered a marker for autophagy-mediated protein degradation or autophagic flux (108). As shown in **Figure 11**, inhibition of lysosome function by bafilomycin A and NH_4Cl, two pH-neutralizing agents, resulted in increased expression of p62. However, protein expression of p62 was unchanged during the course of CVB3 infection, suggesting that CVB3 infection triggers increased accumulation of autophagosomes without promoting protein degradation by lysosomes.

A
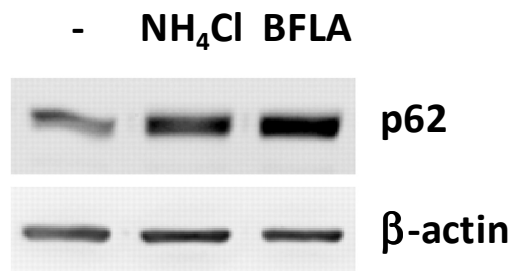
B
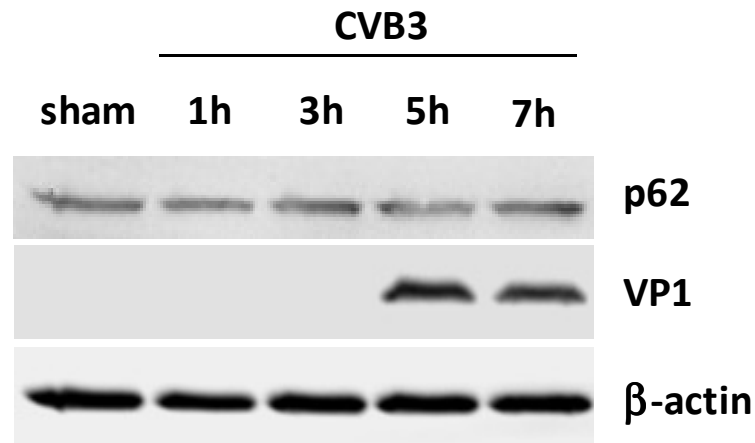
Figure 11. Expression of p62 is not affected by CVB3 infection.

(A) Western blot analysis of p62, a marker of autophagic protein degradation activity, in cells treated with the lysosome inhibitors bafilomycin A (BFLA; 0.1 µM) and NH_4Cl (2.5 mM) for 16 h. (B) Expression of p62 in CVB3-infected cells at the indicated times after virus infection. Similar results were obtained in two independent experiments.

3.4.7 Lysosomal inhibition enhances CVB3 replication.

Finally, I investigated whether prevention of autophagosome-lysosome fusion promotes viral infectivity. Cells were transiently transfected with scramble or LAMP2 (lysosome-associated membrane protein 2) siRNA for 48 h and then infected with CVB3. I showed that knockdown of LAMP2 resulted in significant increases of viral protein expression and virus titer (**Figure 12**). LAMP2 is a lysosomal membrane protein critical for autophagosome-lysosome fusion. Knockdown of LAMP2 has been shown to induce the cytoplasmic accumulation of LC3-associated vesicles (75). It was also reported that LAMP2-deficient mice exhibit a massive accumulation of autophagic vacuoles in various tissues (188). Thus, my results further suggest a key role of autophagosomes in supporting CVB3 replication.
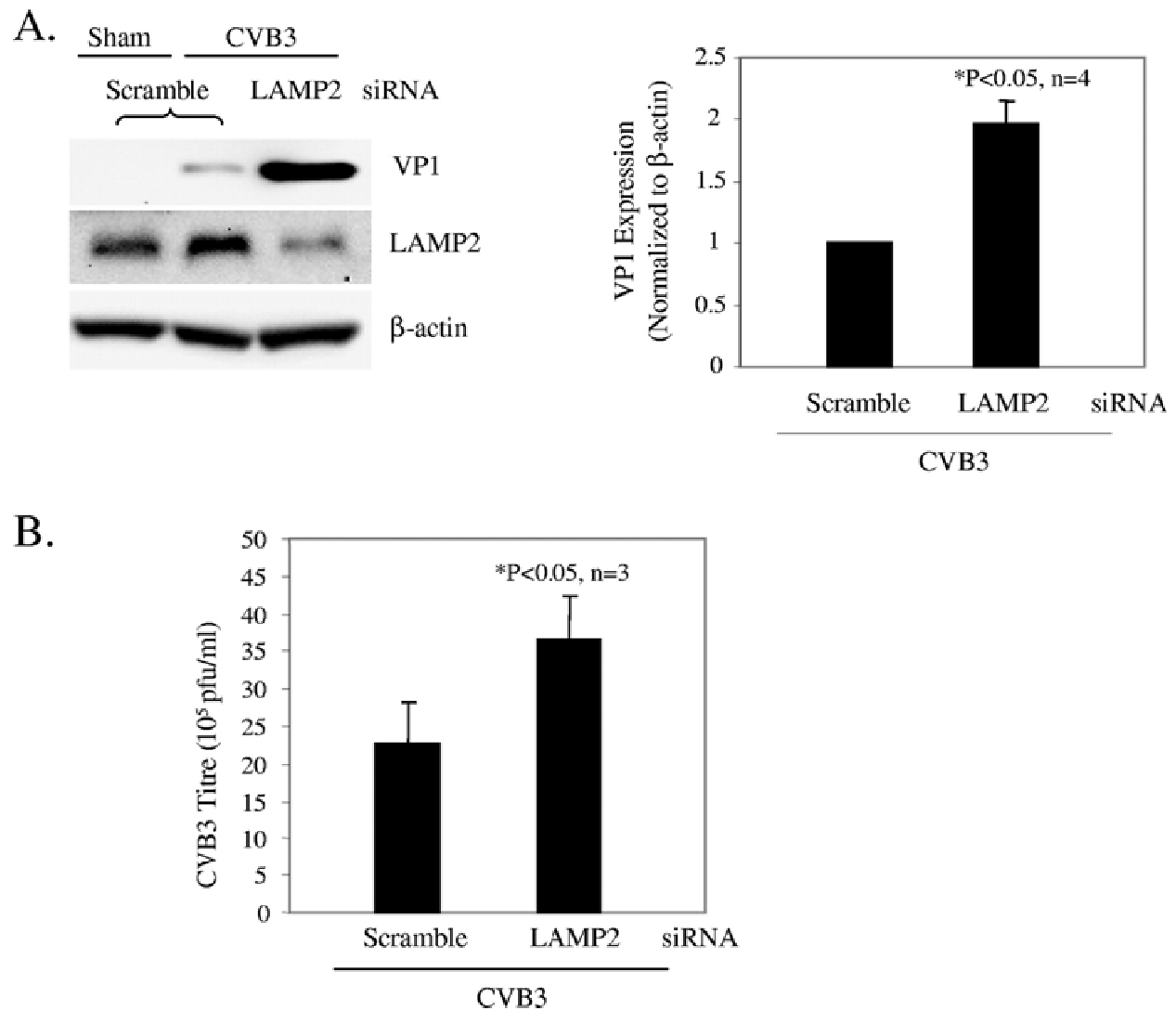
Figure 12. Lysosomal inhibition enhances CVB3 replication.

(A) Western blot analysis of VP1 and LAMP2 expression in CVB3-infected cells transiently transfected with scramble or LAMP2 siRNA. VP1 expression was quantitated, normalized, and analyzed as described in the legend to Figure 7 (data are means ± SE; n = 3 or 4 [as indicated]). (B) Virus titer in scramble or LAMP2 siRNA-transfected cells, determined by plaque assay (mean ± SE; n = 3). *, P < 0.05 compared to scramble siRNA control.

3.5   Discussion

Autophagy is an evolutionarily conserved cellular process that spans the entire spectrum of eukaryotes. It serves a housekeeping role in protein turnover and in the removal of damaged or unnecessary organelles. It also serves an important function in innate host defense by eliminating intracellular pathogens. For example, it has been shown that pharmacological induction of autophagy helps in the clearance of Mycobacterium tuberculosis (79) and that CD40 induction of autophagy promotes elimination of Toxoplasma gondii from macrophages (7). Furthermore, recent studies suggest a role for autophagy in host adaptive immune responses through the delivery of intracellular pathogenic antigens for major histocompatibility complex class II presentation to CD4 T cells (176).

Successful invading pathogens have evolved various strategies to evade host autophagy. For instance, some bacterial or viral proteins, such as IcsB secreted by Shigella flexneri (160) and ICP34.5 encoded by herpes simplex virus type 1 (186), have been documented to block or evade cellular autophagy. Other pathogens adopt different approaches in battling host autophagic defense by subverting it to facilitate their own procreation. In fact, several studies have shown that the autophagosome provides an intracellular compartment that benefits the survival and multiplication of bacteria, including Porphyromonas gingivalis, Brucella abortus, and Coxiella burnetii (176). In addition, some viruses have been reported to induce autophagosome formation to facilitate their own replication (102, 203).

Replication of positive-stranded RNA viruses requires intracellular membrane surfaces on which they assemble their replication complexes. Colocalization of viral RNA replication machineries with double-membrane vesicles in infected cells has been well documented for various positive-stranded RNA viruses, including poliovirus, rhinovirus, equine arterivirus, murine hepatitis virus, and severe acute respiratory syndrome virus (59, 203). Thus, it was speculated that the autophagosome, a double-membrane vesicle, may serve as a site for viral RNA replication. Recent studies on coronavirus and poliovirus seem to support this notion. It was reported that murine hepatitis virus, which belongs to the coronavirus family, colocalizes with the ubiquitin-like autophagy proteins (LC3 and Atg12p) and that viral replication is impaired in autophagy knockout (Atg5−/−) embryonic stem cell lines (171). Additionally, poliovirus proteins have been shown to colocalize with a co-transfected GFP-LC3 protein (91). Stimulation of autophagy increases the poliovirus yield, and inhibition of the autophagosomal pathway decreases the viral yield (91). Despite this exciting observation, recent data on the role of autophagy in positive-stranded RNA virus infection remain contradictory. A recent report showed that infection of rhinovirus type 2, a member of the picornavirus family, does not induce autophagosome formation (25).

That paper further reported that neither induction nor inhibition of autophagy affects viral protein production. In addition, using ATG5-deficient cells, it was recently demonstrated that ATG5 and an intact autophagic pathway are not required for the replication of murine hepatitis virus (214). These studies challenge the view that the autophagosome is a common cellular component utilized by positive-stranded RNA viruses to facilitate their replication.

These discrepancies of the reported data prompted me to explore the role of autophagy in coxsackievirus infection in this study. I report here that CVB3 infection induces the formation of double-membrane vesicles with concurrent LC3 lipidation. I further showed that manipulation of the host autophagy pathway by pharmacological compounds or target-specific RNA interference resulted in significant alterations in the outcome of CVB3 replication. I demonstrated that inhibition of signaling pathways or autophagy genes critical for autophagosome formation reduces viral protein expression and the viral progeny titer. Conversely, increasing the cellular number of autophagosomes prior to viral infection by cellular starvation, rapamycin treatment, or lysosomal inhibition promotes viral replication. Taken together, my data suggest that the host double-membrane autophagosome is likely utilized by CVB3 to facilitate its own replication. Of note, autophagy activation is most prominent at the later stages of viral replication. Increased formation of autophagosome helps the exponential amplification of viral components by supplying sufficient physical scaffolds for the viral components synthesized at earlier time points.

As alluded to earlier, the process of autophagosome formation is tightly controlled. The serine/threonine protein kinase mTOR is one of the key regulators and negatively controls autophagosome formation (41). Class I PI3K is the traditional upstream activator of mTOR. In addition, it has been shown that mTOR can be regulated by intracellular amino acids and ATP, independent of class I PI3K activation. ATP depletion or specific inhibition of mTOR by rapamycin has been shown to activate autophagy, whereas the addition of amino acids inhibits this process. In this study, I showed that levels of mTOR phosphorylation were unchanged after CVB3 infection, suggesting that CVB3-induced autophagy is not triggered by mTOR dephosphorylation.

In contrast, eIF2α kinase positively regulates autophagy in response to nutrient deprivation and viral infection. eIF2α kinase plays a key role in translation inhibition under various stress conditions, through phosphorylation of eIF2α. Restriction of herpes simplex virus growth has been linked to such a function of eIF2α phosphorylation (149). Recently, the eIF2α kinase signaling pathway was also shown to promote autophagy induced by nutrient deprivation or rapamycin treatment, likely through a mechanism that induces LC3 conversion (112, 186). My present study demonstrates that eIF2α is

phosphorylated after CVB3 infection, suggesting a potential signaling mechanism for CVB3-induced autophagosome formation. It is unclear how eIF2α phosphorylation occurs during CVB3 infection. One explanation could be that double-stranded RNA formed from a CVB3 intermediate activates double-stranded RNA-dependent protein kinase and subsequently leads to eIF2α phosphorylation.

Class III PI3K complexes also play a crucial role in the early steps of autophagosome formation. In mammalian cells, the autophagic protein Beclin-1 (a homologue of yeast ATG6) forms the class III PI3K complex with Vps34, a class III PI3K, at the trans-Golgi network (101, 211). This complex promotes autophagosome formation by supplying phosphatidylinositol 3-phosphates to the preautophagosome membrane (184). It has been shown that 3-MA blocks the formation of autophagosomes by inhibiting the activity of class III PI3K (23, 169). I demonstrate that 3-MA blocks CVB3 infection, which is in agreement with previous report from my laboratory that inhibition of PI3K by LY294002 suppresses CVB3 replication (57). LY294002 is an inhibitor of both class I and class III PI3K and has also been shown to be a potent autophagy inhibitor (23).

Although the specific mechanism by which the autophagosome is utilized during coxsackievirus replication in host cells has not been elucidated, it is likely that, as demonstrated for poliovirus (91), the autophagosome provides a physical scaffold where the coxsackieviral complex may reside and viral RNA synthesis may occur. Furthermore, LC3 has been identified to be a binding protein of an AU-rich RNA element in the 3'-untranslated region of fibronectin mRNA, which facilitates the recruitment of RNA to polyribosomes for translation (215). Perhaps AU-rich element-containing viruses, such as CVB3, which carries an AU-rich element in the 3'-untranslated region (170), also adopt LC3-docking double-membrane vesicles as the sites of viral protein translation through the recruitment of polyribosomes. It is plausible to speculate that autophagosome double-membrane vesicles not only act as sites of viral RNA synthesis but also take an active role in CVB3 protein synthesis by bridging the nascent viral RNA with polyribosomes through LC3.

3.6   Limitations and solutions

Multiple experimental methods were conducted in my study to ensure the validity of each finding. For example, I confirmed the induction of autophagosome formation in CVB3 infected cells by transmission electron microscopy and quantification of LC3 conversion. I increased the level of autophagosome in host cells by nutrient starvation, rapamycin treatment, and lysosomal inhibition. I inhibited the autophagy pathway using inhibitor (3-MA) against the Class III PI3K, as well as siRNA against autophagy component ATG7. However, several supplemental experiments could further

strengthen my observations. I could apply immune-gold staining of LC3 to demonstrate the presence of LC3 on CVB3-induced vesicles observed in transmission electron microscopy. I could also monitor the autophagic flux, i.e. the turnover of autophagosome, in CVB3 infected cells. By comparing CVB3-infected cells with or without the introduction of lysosomal inhibitors (e.g. bafilomycin A, NH_4Cl, and choloroquine) an hour prior to cell harvesting, I can gain further insights in the nature of virus-induced autophagosomes. The difference in LC3 conversion between these treatment groups demonstrates whether the autophagosomes mature into autolysosomes or they stay as is. So far, my p62 expression result suggests that the virus-induced autophagosomes are not geared towards degradation. Measuring the autophagic flux would provide a more definitive answer.

Regarding the autophagy inhibition experiments, additional experiments could help validate my observations. In this study, I only achieved successfully knockdown ATG7 expression using siRNA. I tried other siRNAs against ATG5 and LC3, but failed to observe any meaningful knockdown in western blot confirmation. Higher efficiency knockdown of other autophagy components using lentivirus shRNAs or ATG knockout cell lines may help elucidate the specific requirements of autophagy pathway in CVB3 infection. It is possible that CVB3 only utilize part of the autophagy machineries, therefore ATG knockdown beyond the ubiquitination-like conjugation systems (ATG12-ATG5 and LC3-PE) such as the ULK complex components may provide further clarifications.

Autophagy inhibitor 3-MA is particular potent in suppressing CVB3 replication (**Figure 7C**). It effectively inhibited CVB3 protein expression even when introduced at 5 hours post infection. However, 3-MA may have other properties in addition to autophagy inhibition. More specific inhibitors targeting the ubiquitination-like conjugation system should also be used. I did however perform siRNA knockout of the components (Vps34 and beclin-1) of Class III PI3K, the target of 3-MA. Knockdown of these genes also inhibited CVB3 replication. Knockdown of autophagy components linking Class III PI3K to the rest of the autophagic machineries will help further elucidate the role of this complex in CVB3-infection.

Another limitation of the present study is the utilization of tumor cell lines, HEK293 (transformed Human embryonic kidney cells) and HeLa (Human cervical cancer cells). These cell lines are great for the study of molecular pathways due to their ease of cultivation and transfection. However, cardiomyocytes such as rat neonatal cardiomyocytes and HL-1 cells should be used to confirm the findings in this chapter.

3.7 Future directions

In this study, I demonstrated that eIF2α, which is a known positive regulator of the autophagy pathway, is phosphorylated during CVB3 infection. However, it is by no means a conclusive mechanism of autophagy subversion. Future studies are required to clarify the relationship between eIF2α phosphorylation and autophagy induction in CVB3 infection. In addition, the mechanism behind eIF2α phosphorylation in CVB3 infection remains to be explored. Perturbation of its upstream kinases such as dsRNA-dependent protein kinase R (PKR) and protein kinase RNA-like endoplasmic reticulum kinase (PERK), as well as phosphatases such as protein phosphatase 2A and PTEN using chemical inhibitors or RNA interference may reveal the molecular signalling events that lead to autophagosome formation in CVB3-infected cells.

Coxsackieviral proteins are potential molecular drivers of autophagosome formation. As previously described, non-structural proteins 2B, 2BC, and 3A are involved in intracellular membrane rearrangement. 3A plays an important role in membrane trafficking and in manipulating intracellular protein transport from ER to Golgi (200). Mutations in 3A result in defects in viral RNA synthesis (200, 201). Physical association of 3A and viral polymerase 3D has also been shown to play an important role in the initiation of viral RNA synthesis (85). 2B and its precursor 2BC alter membrane permeability (3, 35, 194). 2B was also reported to have anti-apoptotic properties that prevent premature cell death, so as to ensure sufficient time for viral replication (193). However, the exact mechanisms by which 3A, 2B, and 2BC regulate intracellular membrane reorganization are still largely unclear. Future studies correlating the expression and localization of these CVB3 non-structural proteins (alone or in combinations) with the markers of autophagosome, as well as identifying their cellular binding partners may help elucidate the role of these membrane-modifying viral proteins in autophagy subversion.

As described above, LC3 has been shown to bind the AU-rich elements (AUUUA sequence) in the 3'UTR of fibronectin mRNA and facilitate the recruitment of polyribosomes for translation (215). CVB3 genome also contains AU-rich elements in its 3'UTR (170). CVB3's 3'UTR has been shown to play a critical role in viral replication by modulating mRNA stability and translation efficiency (103, 209). I therefore postulated that the autophagosome, harbouring LC3, is an ideal platform for CVB3 replication because it may support the concurrent translation of newly synthesized viral RNA through the recruitment of polyribosomes. Future studies involving the co-localization of viral RNA-dependent RNA polymerase 3D with markers of autophagosome and polyribosome, as well as mutation of AU-rich elements in the 3'UTR of CVB3 genome may help test the speculation.

My *in vitro* observation of autophagy subversion by coxsackievirus warrants further investigation *in vivo*. Confirmation of autophagosome formation *in vivo* is made feasible by the establishment of GFP-LC3 transgenic mice (148). CVB3 infection of GFP-LC3 mice will elucidate the dynamics of autophagy activation in the progression of viral myocarditis. In fact, preliminary observations from my coworkers (unpublished data) and others (99) have demonstrated the activation of autophagy in CVB3-infected heart, liver, and pancreas using GFP-LC3 mice. Further studies using cardiac-specific autophagy knockout mice will reveal the role of autophagy in the pathogenesis of viral myocarditis. My study demonstrated that gene-silencing of ATG7 in cells by siRNA inhibits CVB3 infection. ATG7 is an enzyme essential for both ubiquitination-like conjugation systems required for autophagosome formation and maturation (106, 109). Knockdown of ATG7 was reported to be more efficient in blocking autophagy pathway than the knockdown of other ATGs. Deletion of ATG7 in mice was reported to result in attenuation of autophagosome formation and impaired degradation of proteins and organelles induced by starvation (111). Therefore, cardiac-specific disruption of autophagy pathway through ATG7 knockout in mice will be ideal in studying the role of autophagy in the overall development of viral myocarditis.

3.8   Summary

I demonstrated that CVB3 manipulates the host autophagy protein degradation pathway to supplement viral replication. Autophagy is an evolutionary conserved homeostatic mechanism in eukaryotes that degrades and recycles long-lived cytoplasmic proteins, as well as damaged organelles. The hallmark of autophagy is the formation of double-membrane vesicles known as autophagosomes. I provided the initial evidence that CVB3 infection induces the formation of autophagosomes. Up-regulation of autophagosome formation enhances CVB3 replication, whereas downregulation of autophagy pathway reduces CVB3 replication in host cells. My results help clarify the nature of the intracellular membranes previously shown to be required for viral replication.

Chapter 4 – Serum response factor in CVB3-induced myocarditis

4.1 Background

4.1.1 Mechanisms of CVB3-induced DCM

Although viral myocarditis was originally considered an immune system-mediated disease of the heart, accumulating evidence demonstrates that early direct virus-mediated injury occurring prior to infiltration of immune cells contributes significantly to the pathogenesis of viral myocarditis (37, 86, 138). In cultured cells, CVB3 infection induces a direct cytopathic effect and cell apoptosis (29, 30, 33). CVB3 infection of severe combined immune deficient mice results in early and extensive myocyte coagulative necrosis and contraction band necrosis as compared to their wild-type counterparts (37, 138). Prominent cytopathic alterations co-localize to cells which desmonstrate viral replication by in situ hybridization for viral RNA, reinforcing the importance of direct virus-induced damage (105).

Viral proteases have been recognized as important pathogenic factors contributing to the development of DCM. It has been shown that transgenic mice with inducible, cardiac-specific expression of viral protease 2A develop severe cardiac dysfunction and DCM (205). Experimental evidence from cell culture and cell-free in vitro studies demonstrates that 2A induces the cleavage and functional impairment of dystrophin (11-13). As depicted in **Figure 13**, dystrophin connects the cytoskeletal actin-binding site to the β-dystroglycan extracellular matrix anchor; thus, its cleavage leads to the disruption of the cytoskeletal architecture. It is therefore proposed that 2A-induced DCM is associated with disrupted myocyte membrane integrity through the cleavage of dystrophin (11-13). However, a direct causal relationship between dystrophin cleavage and 2A-induced DCM has not been provided in these studies and other mechanisms may also play pivotal roles. Moreover, mdx (dystrophin-deficient) mice display a relatively mild DCM phenotype (50, 76). The mild phenotype has been attributed to the compensatory up-regulation of the dystrophin homologue, utrophin, as evidenced by severe dystrophic phenotypes in mice with double-knockout of utrophin and dystrophin (50, 76, 80, 93). Previous studies have shown that CVB3 infection does not cleave utrophin (13). Thus, the DCM phenotype induced by dystrophin cleavage may be dampened by the compensatory effect of utrophin. Together, these data suggest that dystrophin-cleavage alone is not sufficient to explain the severe cardiomyopathy phenotype observed in 2A transgenic mice. Thus, I postulate that other substrates of 2A may also play a key role in the development of DCM.
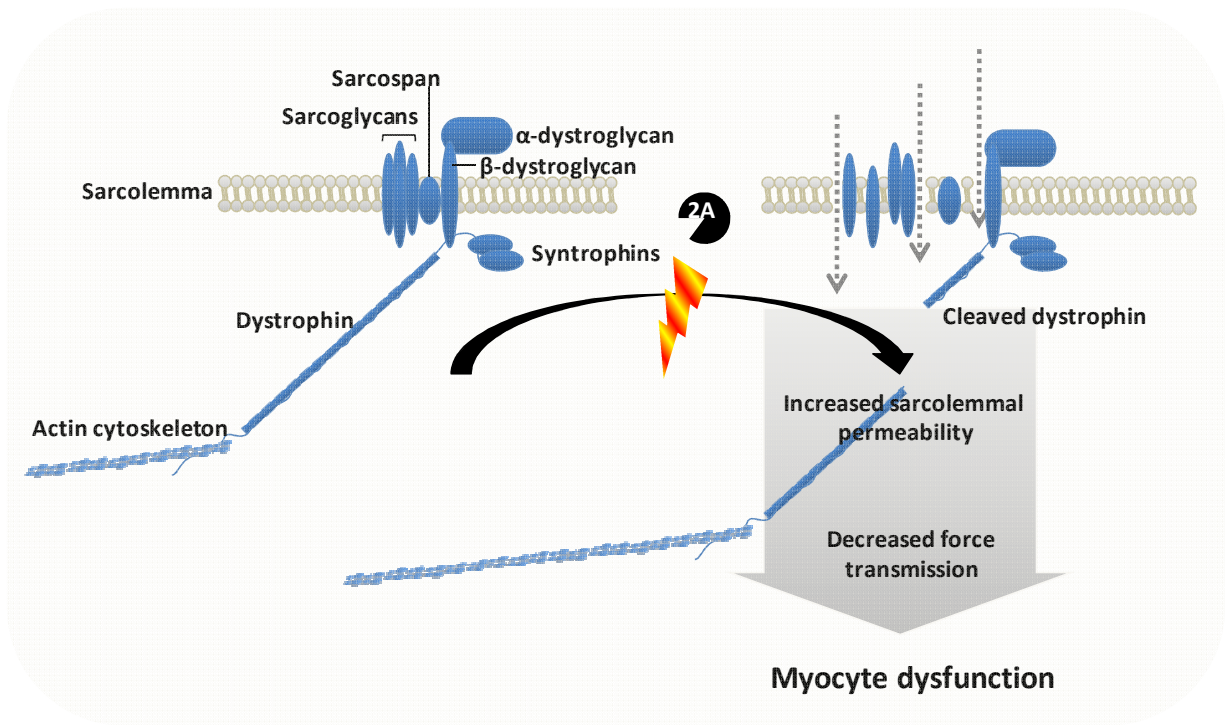
Figure 13. Coxsackieviral protease 2A cleaves dystrophin at its 3' hinge.

Dystrophin is a component of the dystrophin-glycoprotein complex that links the cytoskeleton to the extracellular matrix. Dystrophin cleavage by viral protease 2A contributes to myocyte dysfunction by reducing contractile force transmission and increasing sarcolemmal permeability.

4.1.2   Serum response factor

Serum response factor (SRF), originally identified by Treisman and colleagues, is a founding member of the MADS (MCM1 in yeast, Agamous and Deficiens in plants, and SRF in animals) box family of transcription factors (159, 191). SRF was named after its binding activity to serum response element (SRE, also known as CArG box (CC(A/T)$_6$GG)) located in the promoter region of immediate early transcription factor, c-Fos (159, 191). Similar SREs were subsequently found in the promoter regions of a number of other immediate early genes, as well as contractile genes and microRNA (miRNA) genes (143, 157, 162). A genome-wide search for SRF targets has identified approximately 1 200 genes, which contain single or more copies of this consensus SRE sequence in their promoter regions (termed CArGome) (183). More than 250 of these genes have been validated (183).

3.1.2.1 Important SRF domains

Gene expression regulation property of SRF is conferred by its major domains (**see Figure 14**) (31, 143, 162). Its nuclear localization signal (amino acids 95-100) is required for nuclear translocation of SRF. Its DNA binding and dimerization domain (amino acids 133-222) is highly conserved among eukaryotes and is essential for its binding to SREs of target genes, as well as formation of SRF dimers. Its transactivation domain (amino acids 339-508) carries out transcriptional activation of target genes. It also has multiple phosphorylation sites targeted by several signaling kinases.

3.1.2.2 SRF regulation

SRF by itself has relatively low transcriptional activity. Expression of SRF target genes are controlled in a cell- and context-specific manner through interactions between SRF and its cell-specific cofactors. Examples of SRF cofactors in cardiac tissues are Nkx2.5, GATA4, MEF2, and Myocardin. SRF cofactors may compete for common binding interface on SRF, thus allowing SRF-dependent gene expression in varying contexts. SRF-mediated gene expression can be activated by a variety of agents, including serum, cytokines, mitogens, lipopolysaccharides, and viral activator proteins. All in all, the activity of SRF is governed by various mechanisms including transcription, translation, alternative RNA splicing, association with cofactors, subcellular localization, as well as phosphorylation and cleavage (31, 143, 162).
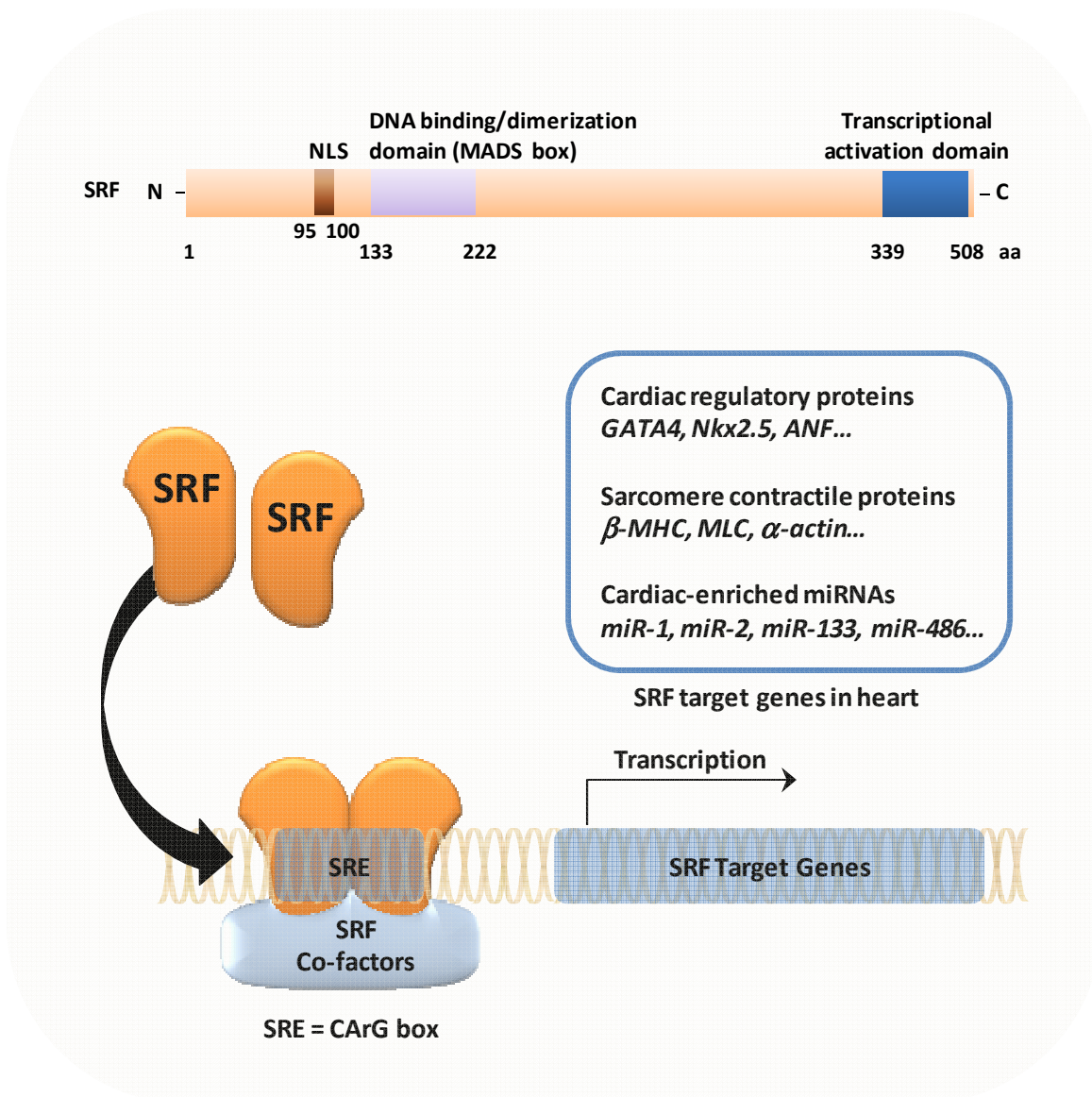
Figure 14. Serum response factor regulates cardiac gene expression.

SRF is a muscle-enriched transcription factor that regulates the expression of cardiac regulatory proteins, sarcomere contractile proteins, as well as cardiac-specific microRNAs (miRNAs). SRF contains three major domains: NLS (nuclear localization signal), DNA binding and dimerization domain, and transcriptional activation domain. SRF dimerizes and associates with co-factors such as GATA4, Nkx2.5, MEF2, and myocardin and binds to serum response element (SRE) (also known as CArG box) to activate gene transcription.

3.1.2.3 SRF in cell growth and differentiation

SRF is an important regulator of cell growth, differentiation, as well as apoptosis. Blocking SRF function by anti-SRF antibodies or by SRF sequence-specific antisense RNA decreases muscle marker gene expression and prevents the differentiation of myoblast to myotube (73, 182). In contrast, activation of SRF through the Rho-GTPases pathway promotes muscle cell differentiation and muscle gene expression (28). It has been demonstrated that caspase-3 activation leads to the cleavage of SRF in human B-cells, whereas the expression of a caspase-resistant form of SRF significantly inhibits apoptosis in these cells (21, 53). Knockout of SRF gene in mice is embryonic lethal due to defects in mesoderm differentiation (10).

4.1.3 SRF-mediated cardiac gene expression

SRF is highly expressed in cardiac muscle and plays a central role in cardiac development and function by regulating genes for cardiac contractile and regulatory proteins as well as silencer miRNAs (124, 144, 155, 156). Cardiac muscle-specific inactivation of SRF in utero results in a dilated, heart failure-like phenotype with embryo demise occurring at ~e11.5 of mouse development (144, 156, 158, 166). Cardiac genes directly under SRF regulation include cytoplasmic cytoskeletons such as desmin and titin, membrane cytoskeletons such as dystrophin and zona occludens, contractile elements such as cardiac α-actin, α-myosin heavy chain (α-MHC), β-MHC, myosin light chain (MLC), and cardiac troponins, contractile regulators such as sarcoplasmic reticulum Ca^{2+}-ATPase (SERCA), Na^+/Ca^{2+} exchanger NCX1, and atrial naturetic factor (ANF), as well as transcription regulators such as nuclear factor of activated T-cells (NFAT), Nkx2.5, myocardin (144, 156, 158, 166, 183). Indirect SRF regulation of cardiac genes has also been reported. Transcription factors with no functional SRE in their promoter regions, such as GATA-4 and myocyte enhancer factor-2 (MEF2), are also reduced in SRF-null hearts and cardiomyocytes (144, 156, 158, 166). Downregulation of these indirect targets is suggested to be secondary to the reduced expression of other SRF targets. Interestingly, SRF-inactivation in cardiomyocytes also activates a subset of genes, which is attributed to the loss of SRF-dependent miRNAs, illustrating an additional gene-silencing function of SRF (14, 156). Recent studies have identified several miRNAs as targets of SRF in the heart, which include miR-486 (180), miR-133a (124, 156), and miR-1 (213). Expression of these miRNAs controls heart development and function by repressing the expression of cardiac regulatory proteins.

4.1.4   SRF in heart diseases

Severe heart failure is associated with the reduced expression of a broad range of cardiac-specific genes. Microarray studies in human end-stage heart failure revealed a significant downregulation of many cardiac genes, including many SRE-containing genes, implicating the importance of SRF in the progression of heart failure (17, 90, 187). It was reported that expression of a dominant-negative splice variant of SRF that lacked portions of the transactivation domain is markedly elevated in human and animal failing hearts (20, 46). The dominant-negative SRF splice variant potently inhibited SRF-dependent gene expression, mirroring the biochemical phenotype seen in SRF-null mice. Interestingly, a recent report showed that SRF cleavage also occurs in the cardiomyocytes of end-stage DCM patients (32). Increased caspase activity during heart failure induces the cleavage of SRF, producing a truncated protein that lacks the C-terminal transactivation domain, and acts as a dominant repressor of SRF-dependent cardiac genes, similar to the alternatively spliced variant (32). Together, these studies suggest that decreased expression of full-length wild-type SRF and/or the increased production of truncated SRF may down-regulate SRF-dependent genes and thereby contribute to the progression of severe heart failure.

On the other hand, sustained elevation of SRF expression is also detrimental to the heart. SRF overexpression induces cardiac hypertrophy, which is a compensatory response to a variety of physiological or pathological stimuli. Re-expression of fetal genes such as ANF, β-myosin heavy chain, and skeletal α-actin, has been considered as a marker of this condition (2, 15, 153). Many of these genes have SREs in their promoter regions suggesting that SRF may be a critical transcription factor in the reprogramming of fetal genes. *In vitro* experiments using isolated cardiomyocytes from SRF-floxed transgenic mice demonstrated the requirement of SRF in the induction of fetal gene expression (155). Transgenic mouse studies showed that cardiac-specific overexpression of SRF induces a pattern of fetal gene re-expression similar to that observed in cardiac hypertrophy, and subsequently causes severe cardiomyopathy characterized by four-chamber dilatation, cardiomyocyte hypertrophy, interstitial fibrosis, and mitochondrial/myofibril damage (212). Most recently, there was a report showing that forced expression of striated muscle activator of Rho signalling sensitizes the heart to pressure overload-induced and calcineurin signalling-induced cardiac hypertrophy by modulating SRF-dependent transcription (113). Collectively, these experimental data suggest that strictly-controlled SRF expression is essential for the maintenance of cardiac homeostasis.

4.2   Rationale

As described previously, enteroviral-encoded proteases have been recognized as important pathogenic factors contributing to the development of DCM. Transgenic mice with cardiac-restricted expression of viral protease 2A develop severe cardiac dysfunction and DCM (205). Disruption of the dystrophin-glycoprotein complex through dystrophin cleavage by 2A has been proposed as one important mechanism for the progression of DCM (11-13). However, dystrophin-null mice do not develop severe cardiomyopathy (50, 76) as observed in 2A transgenic mice, suggesting that other molecular targets for the protease exist and contribute to the viral pathogenesis. In addition, in-house Affymetrix array data (**Figure 15B**) from Dr. Bobby Yanagawa, a previous PhD student in our laboratory, showed that the expression of contractile and regulatory genes in CVB3-infected mouse hearts is significantly decreased, which is also unexplainable by dystrophin cleavage.

4.3   Hypothesis and specific aims

The objective of the present chapter is to explore viral protease substrate that contributes significantly to the impaired heart function and development of DCM. Specifically I **HYPOTHESIZE** that the serum response factor is cleaved by viral protease 2A during CVB3 infection and contributes to impaired myocardial function and progression to DCM.

My **SPECIFIC AIMS** are:

Aim 1. Examine whether SRF is cleaved in CVB3 infection

Aim 2. Determine the mechanisms of SRF cleavage

Aim 3. Determine the functional significance of SRF cleavage

4.4　Results

4.4.1　Cardiac function and cardiac gene expression following CVB3 infection

The mouse model of myocarditis has been well characterized and commonly used to study target organ injury during CVB3 infection (34, 133). Two-dimensional echocardiography was performed to assess functional alterations in CVB3-infected mouse hearts. As shown in **Figure 15A**, virus-infected mice displayed cardiac dysfunction, evidenced by a significant reduction in left ventricular posterior wall (LVPW) thickening and ejection fraction.

Heart failure has been associated with the reduction of a broad range of cardiac-specific genes (17, 90, 187). To confirm the downregulation of contractile and regulatory genes in CVB3-infected mouse heart (as shown in Affymetrix microarray data **Figure 15B**), I performed real-time RT-PCR examination of CVB3-infected cardiomyocytes. Quantitative RT-PCR results in **Figure 15C** demonstrate downregulation of several cardiac genes, including ANP, β-MHC, GATA-4, MEF2, and NFAT, in CVB3-infected cardiomyocytes.
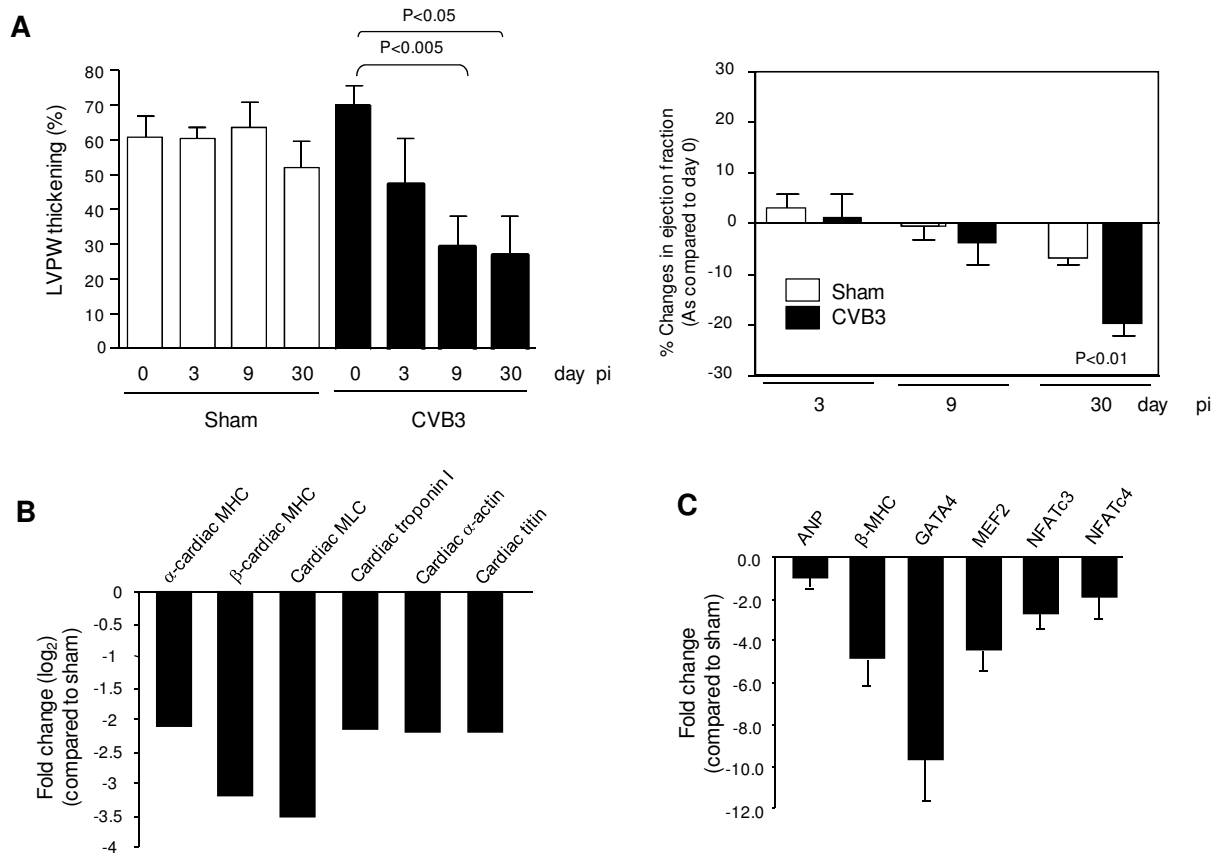
Figure 15. Cardiac function and cardiac gene expression following CVB3 infection.

(A) Cardiac function following CVB3 infection by echocardiography. At day 0 (before infection), and 3, 9, and 30 days following CVB3 or sham infection of A/J mice, systolic and diastolic parasternal long and short axis measurements were obtained. Left ventricular posterior wall (LVPW) thickening and ejection fraction are presented as percentage changes (mean ± SD, n = 4 for each group). pi, post infection. (B) CVB3- or sham-infected mouse hearts (n = 4 for each group, pooled) at 9 days pi were collected for Affymetrix array analysis. Gene changes in intensity (averages of two replicates of the microarray analysis) were plotted as a ratio of CVB3- to sham-infected hearts for visualization. Only genes that exhibited a 1.8-fold change (log_2) or greater were included. MHC, myosin heavy chain; MLC, myosin light chain. (C) Murine HL-1 cardiomyocytes were sham- or CVB3-infected for 24 h. Real-time quantitative RT-PCR was performed to examine the expression of indicated genes. The gene expression was normalized to GAPDH mRNA, and then displayed as fold changes compared to sham infection (mean ± SD, n = 3). ANP, atrial natriuretic peptide; MEF2, myocyte enhancer factor 2; NFATc, nuclear factor of activated T cells.

4.4.2 Expression levels of SRF following CVB3 infection

As alluded to earlier, SRF is a cardiac-enriched transcription factor, regulating the expression of numerous cardiac-specific genes. To explore whether downregulation of cardiac genes is associated with dysregulation of SRF, I examined the expression levels of SRF during CVB3 infection. Using an antibody against the C-terminus of SRF, I found that CVB3 infection of mouse cardiomyocytes (**Figure 16A**, top panel) and hearts (**Figure 16D**) led to marked decreases in the protein expression of SRF (~67 kDa), accompanied by the appearance of ~20 kDa fragments. To validate the results, I used an antibody against the N-terminus of SRF (Novus Biologicals). As shown in **Figure 16A** bottom panel, an extra band at the molecular weight of ~50 kDa was detected in addition to the full-length SRF following CVB3 infection of mouse cardiomyocytes at 20 h and 24 h. These data suggest that SRF is potentially cleaved during CVB3 infection to generate two cleavage products of approximately 50 and 20 kDa, respectively. I further examined the distribution of SRF following CVB3 infection of mouse cardiomyocytes using anti-C-terminal SRF antibody. **Figure 16B** showed that SRF was redistributed from the nucleus to the cytoplasm in CVB3-infected cells, whereas it remained in the nucleus of sham-infected cells.

Real-time RT-PCR was also carried out to examine the gene expression of SRF after CVB3 infection of mouse cardiomyocytes. The results in **Figure 16C** demonstrate unchanged mRNA levels of SRF following CVB3 infection, suggesting that the reduced protein expression of full-length SRF is unlikely due to decreased gene expression, but rather protein cleavage.
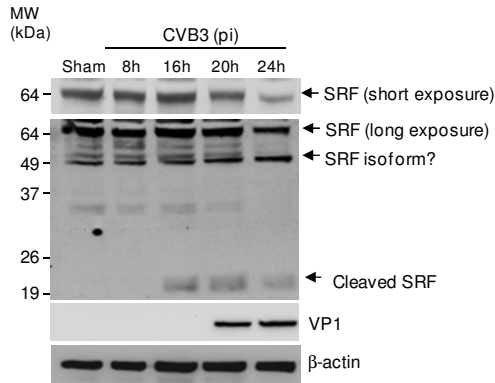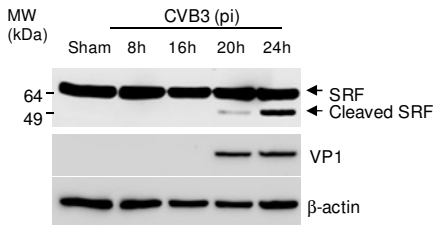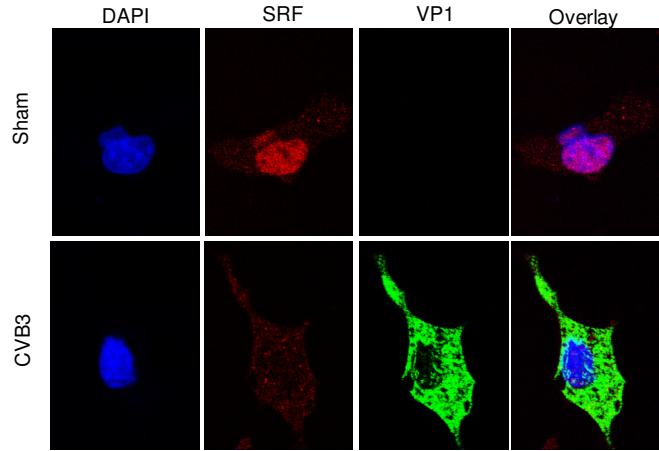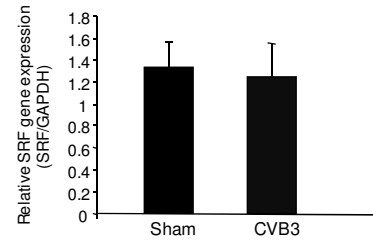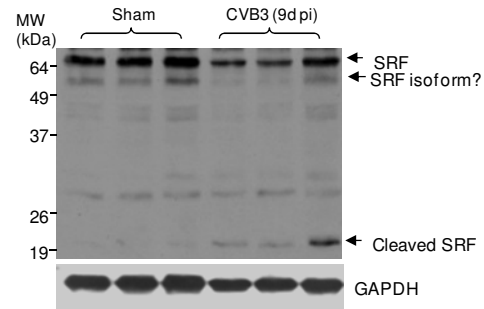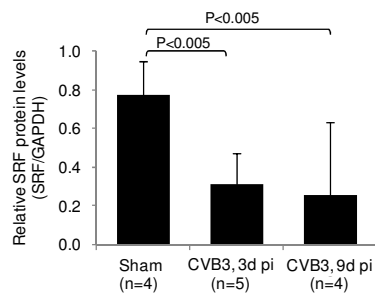
Figure 16. Protein and gene expression of SRF following CVB3 infection.

(A) Protein expression of SRF following CVB3 infection of murine HL-1 cardiomyocytes. HL-1 cells were either sham infected or infected with CVB3 for various times as indicated. Western blotting was performed to examine protein expression of SRF (top, using anti-C-terminal SRF antibody; bottom, using anti-N-terminal SRF antibody), viral protein VP1 and β-actin (loading control). (B) Protein distribution of SRF following CVB3 infection of HL-1 cells. HL-1 cells were infected with CVB3 for 20 h, double-immunocytochemical staining was then performed using anti-C-terminal SRF antibody and anti-VP1

antibody to examine the expression and localization of SRF (red) and viral protein VP1 (green), respectively. The nucleus was counterstained with DAPI (blue). (C) Gene expression of SRF after CVB3 infection. RNA samples were extracted from HL-1 cardiomyocytes at 24 h following CVB3 infection. Gene levels of SRF were measured by real-time quantitative RT-PCR and normalized to GAPDH mRNA (mean ± SD, n = 3). (D) SRF expression in A/J mouse heart following 3 and 9 days of CVB3 infection. Heart extracts were used for western blot analysis of protein expression of SRF (using an anti-C-terminal SRF antibody) and GAPDH (loading control). Left panels, levels of SRF were quantitated by densitometric analysis using NIH ImageJ V1.43, normalized to GAPDH, and presented as mean ± SD. Right panels, representative western blot of SRF expression in mouse heart at 9 days post infection.

4.4.3   Cleavage of SRF following CVB3 infection

To further confirm cleavage of SRF, I utilized a HeLa cell line, a well-characterized model in CVB3 investigations amenable for transfection with plasmids. HeLa cells which express low levels of endogenous SRF were transiently transfected with a 3×FLAG-tagged SRF construct for 48 h followed by CVB3 infection for 7 h. Western blot was performed using anti-FLAG antibody or anti-C-terminal SRF antibody, which showed two cleavage products with molecular weights of ~50 and ~20 kDa, respectively (**Figure 17**). These results correspond well with my observation on endogenous SRF cleavage shown in **Figure 16A**.
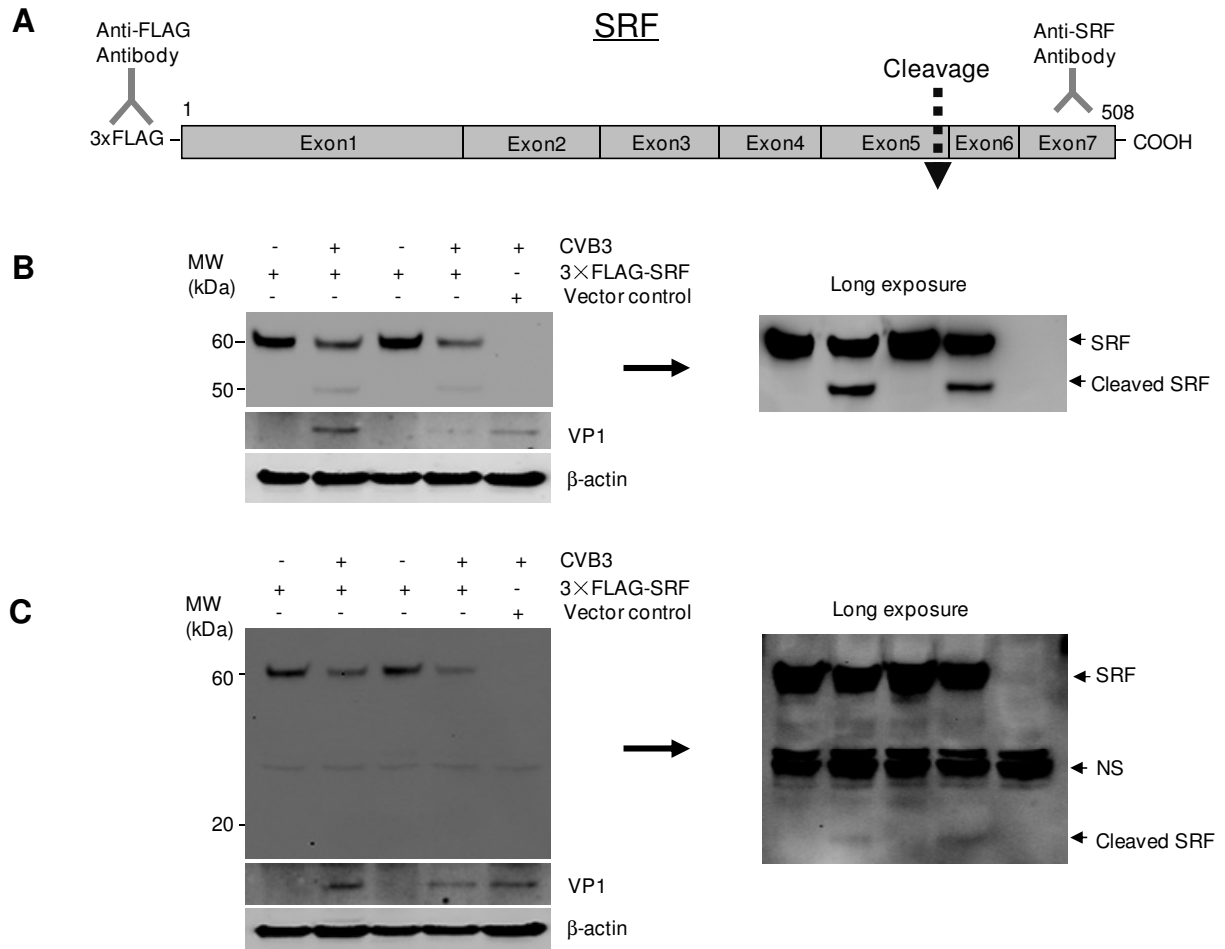
Figure 17. Cleavage of SRF following CVB3 infection.

HeLa cells were transiently transfected with a plasmid expressing 3×FLAG-SRF for 48 h, followed by CVB3 infection for 7 h. (A) Schematic diagram of the 3×FLAG-SRF construct and western blot detection of SRF with the antibodies described in B and C. Western blotting was performed to examine protein expression of viral protein VP1, β-actin (loading control), and SRF using an anti-FLAG antibody that recognizes the N-terminus of SRF (B) or using an anti-C-terminal SRF antibody (C). NS, nonspecific bands.

Caspase-mediated SRF cleavage, which yields a 32-kDa protein fragment, has been reported in both non-cardiac and cardiac cells (21, 32, 53). To determine whether caspases are involved in CVB3-induced cleavage of SRF, I treated cells with z-VAD-fmk, a general caspase inhibitor. As shown in **Figure 18**, following CVB3 infection of SRF-transfected cells (lane 6), two cleavage products (~50 and ~40 kDa using anti-N-terminal FLAG antibody and of ~30 and ~20 kDa using anti-C-terminal SRF antibody) were detected. With addition of z-VAD-fmk (lane 7), the levels of the ~40 kDa (upper panel) and the ~30 kDa (middle panel) fragments were markedly reduced, indicating that they are the cleavage products of SRF by caspases. The appearances of the ~40 kDa (upper panel) and the ~30 kDa (middle panel) bands in SRF-transfected and sham-infected cells (lane 5) are likely due to transfection-induced cytotoxicity. It was noted that inhibition of caspase activation did not prevent the production of the ~50 kDa (lane 7, upper panel) and the ~20 kDa (lane 7, middle panel) fragments, suggesting that these cleavages are independent of caspase activation. Taken together, my results suggest that SRF is cleaved during CVB3 infection by viral protein and caspases at two different sites. Since caspase activation is a late event during viral infection, downregulation of cardiac genes in CVB3-infected mouse heart and cardiomyocytes may be mainly attributable to viral protease-mediated SRF cleavage.
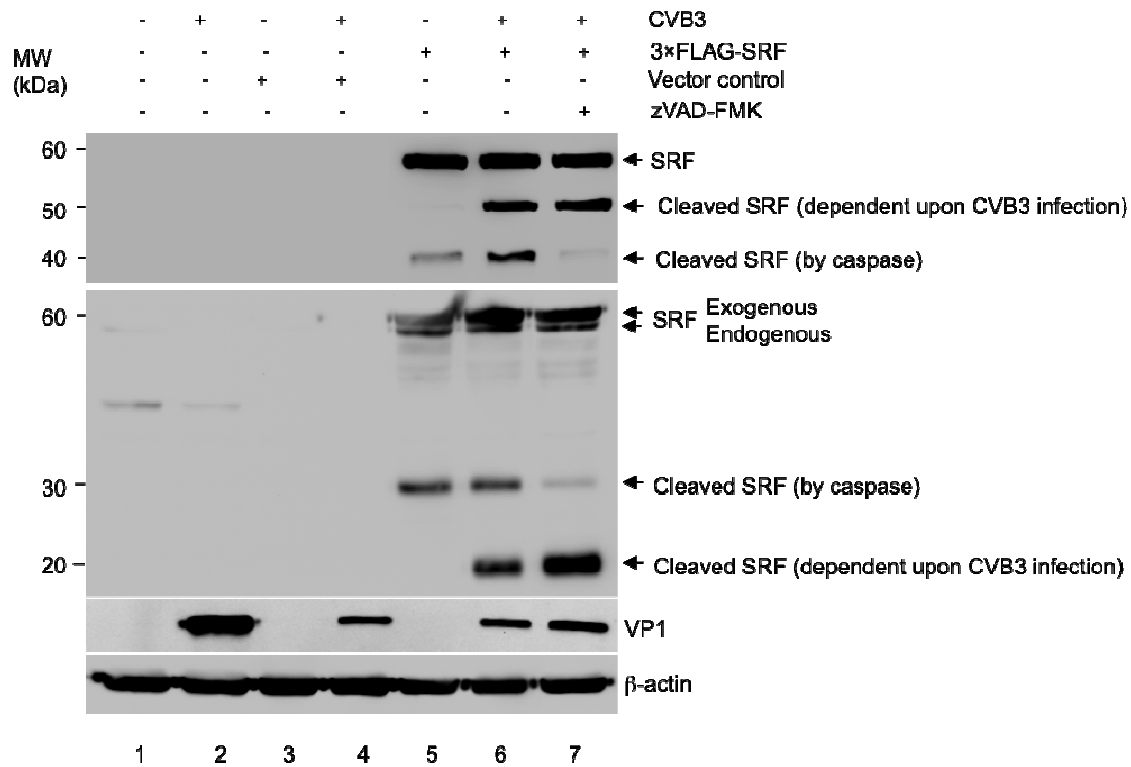
Figure 18. Effect of caspase inhibition on CVB3-induced cleavage of SRF.

HeLa cells were transiently transfected with a plasmid expressing 3×FLAG-SRF or an empty vector for 48 h, followed by CVB3 infection for 7 h in the presence or absence of z-VAD-fmk (50 µM), a pan caspase inhibitor. Western blotting was performed to examine protein expression of SRF (top, using anti-FLAG antibody; middle, using anti-C-terminal SRF antibody), viral protein VP1, and β-actin (loading control).

4.4.4 Identification of SRF cleavage site during CVB3 infection

As illustrated in **Figure 19A**, SRF protein consists of two major domains: the SRE DNA binding and dimerization domain (amino acids 133 to 222) and the transactivation domain (amino acids 339 to 508). Computer prediction algorithm for cleavage sites by enteroviral proteases (NetPicoRNA V1.0 algorithm) revealed potential 2A protease site, which results in two products of ~50 and ~20 kDa (**Figure 19A**), consistent with the SRF fragments detected in CVB3-infected cells. First, I examined whether SRF can be cleaved by viral protease 2A. **Figures 19B** and **19C** showed that overexpression of 2A resulted in two cleavage products of FLAG-tagged SRF with the molecular weights similar to those observed during CVB3 infection. This study suggests that CVB3 induces SRF cleavage through the action of viral protease 2A.

A

SRF	Residue	Pos	Clv*	Surf#	Sequence
Human	G	348	0.582	0.712	FTLMPGGAVAQ
Mouse, Rat	G	344	0.582	0.712	FTLMPGGAVAQ
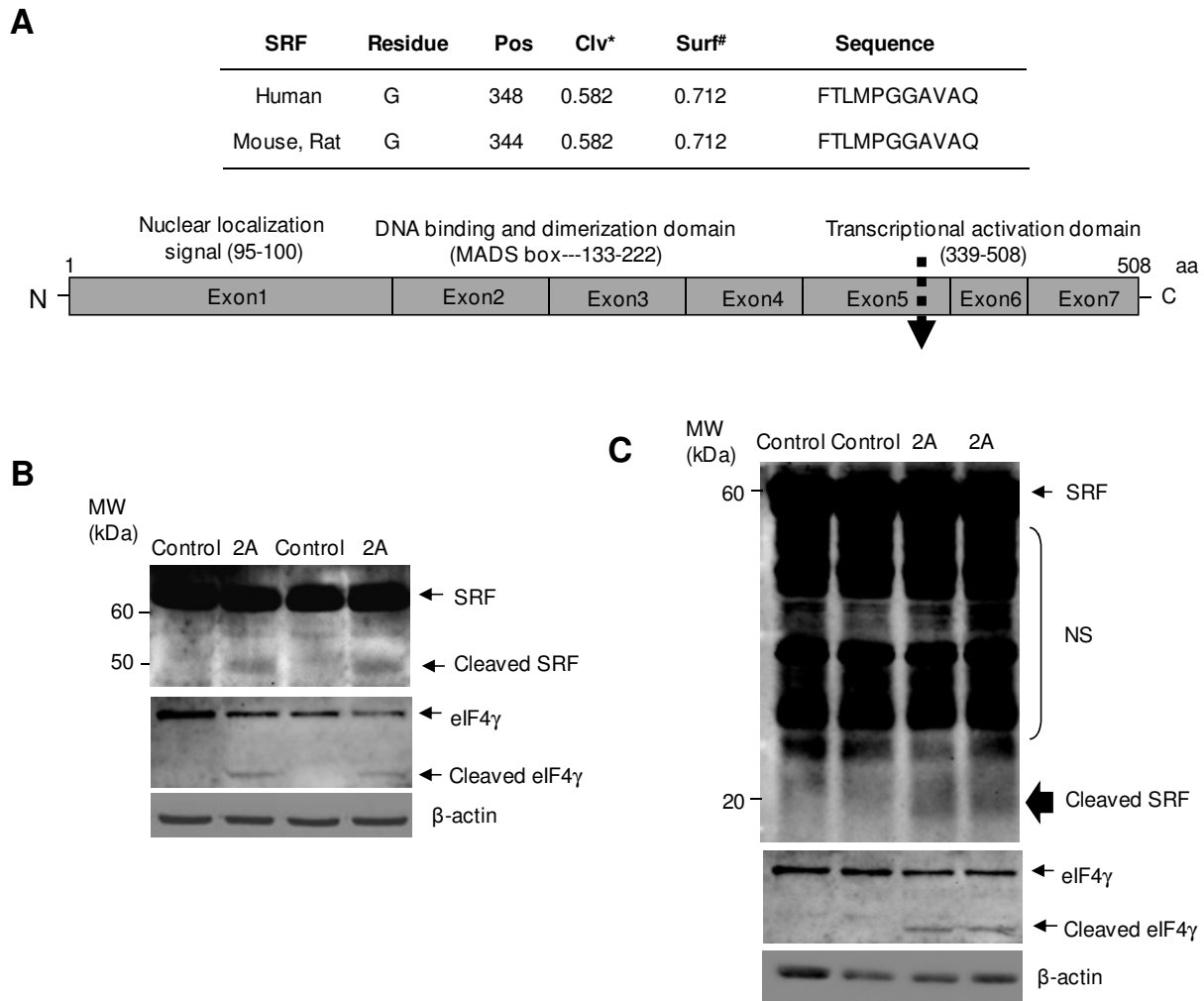
Figure 19. Cleavage of SRF by overexpressing viral protease 2A.

(A) SRF prediction cleavage site for viral protease 2A. The SRF protein sequence was searched for putative cleavage sites of picornavirus proteases using NetPicoRNA V1.0 algorithm. *Cleavage prediction score above 0.500 are predicted as potential cleavage sites. #Surface exposure scores above 0.500 are predicted as surface exposed sites. (B, C) HeLa cells were transiently transfected with 3×FLAG-tagged SRF construct for 48 h, followed by additional transfection with either empty vector (control) or viral protease 2A plasmid for another 48 h. Western blotting was performed to examine protein expression of SRF using anti-FLAG antibody (B) that recognizes the N-terminus of SRF, or by anti-C-terminal SRF antibody (C). The 2A proteolytic activity was confirmed by the cleavage of eIF4γ. Expression of β-actin was shown as a loading control. NS, nonspecific bands.

To confirm the cleavage site predicted by the computer algorithm, I constructed a SRF point mutant, in which the G residue at position 349 was replaced with E (G349E), by site-directed mutagenesis. However, I found that this mutant was still susceptible to cleavage during infection (**Figure 20B**, upper). To further identify the cleavage site of SRF, I constructed three deletion mutants and a series of point mutation plasmids (data not shown). I found that the G327E mutant was resistant to CVB3-induced cleavage (**Figure 20B**, lower), suggesting that SRF is cleaved after T326. Although this cleavage site is not predicted by the NetPicoRNA program, amino acid sequence alignments of SRF with other known 2A substrates at the cleavage region revealed a similar cleavage motif (**Figure 20C**).
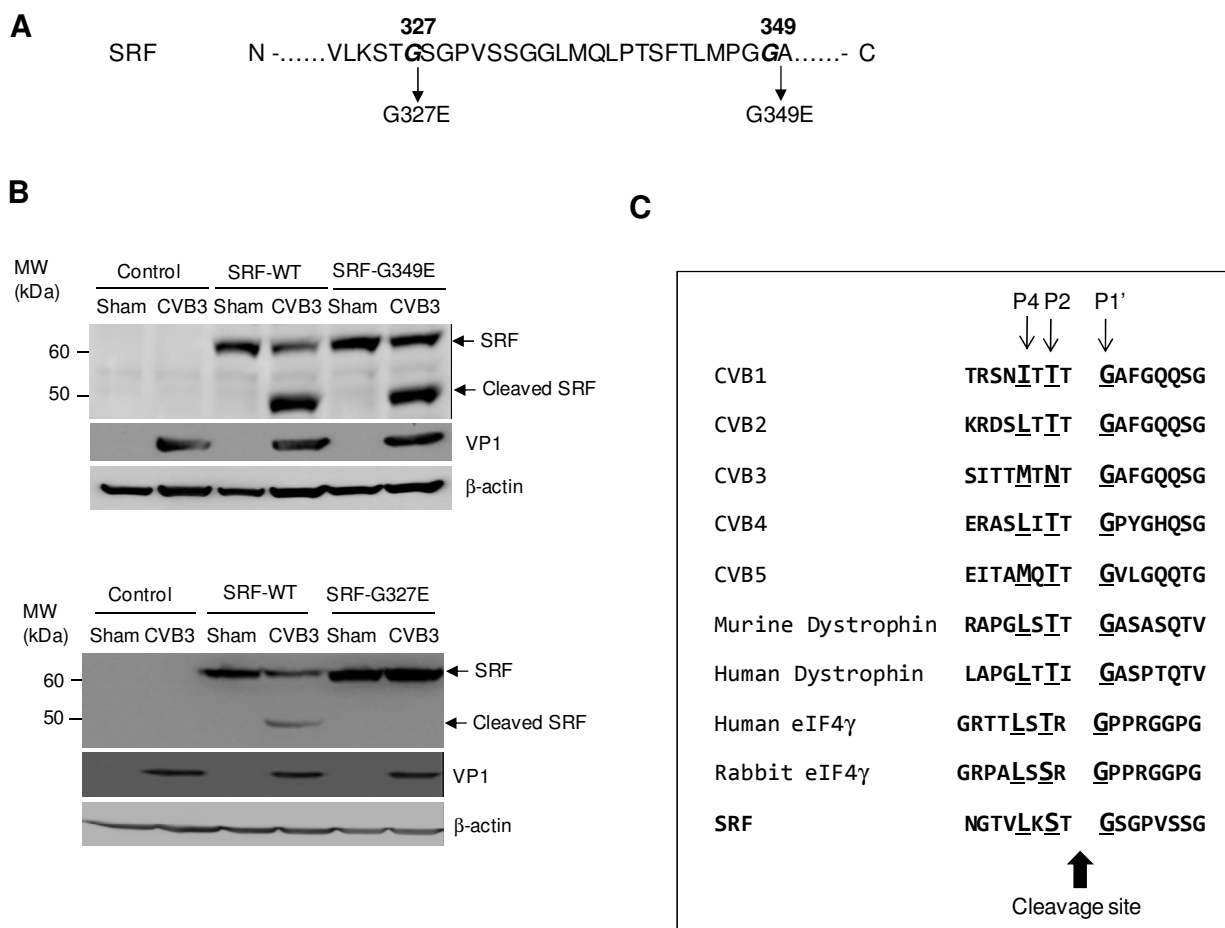
Figure 20. Cleavage of SRF after T326 following CVB3 infection.

(A) Diagram of point mutation constructs of SRF. (B) HeLa cells were transiently transfected with 3×FLAG-tagged SRF-wild-type (SRF-WT) or SRF mutants (SRF-G349E or SRF-G327E as indicated) for 48 h, followed by 7 h CVB3 infection. Transfection of an empty vector (pcDNA) was used as negative controls. Western blotting was performed to examine protein expression of SRF using anti-FLAG antibody and viral protein VP1. Expression of β-actin was shown as a loading control. . (C) Identification of protease 2A substrate cleavage site. Substrate recognition by 2A depends on a degenerate amino acid pattern upstream of the cleavage site. The cleavage recognition site usually contains a T, or S at position P2 and an L, I, or M at position P4. A glycine residue at the P1' C-terminal side of the scissile bond of the cleavage site occurs in all known substrates of the 2A protease.

4.4.5 Cellular localization and transcriptional function of CVB3-mediated SRF cleavage fragments

To understand the functional significance of CVB3-induced SRF cleavage, I generated two constructs expressing the N- and C-terminal SRF fragments, respectively. I showed that the SRF-N truncate harboring a DNA-binding domain and a nuclear localization signal was localized to the nucleus in both HeLa cells (**Figure 21B**) and HL-1 cardiomyocytes (**Figure 21C**) as expected, whereas SRF-C which carries a transcriptional activation domain was distributed in the cytoplasm (**Figure 21B**) or in both cytosol and nucleus (**Figure 21C**).

To determine the transcriptional activities of cleaved or non-cleavable SRFs, HeLa cells (**Figure 21D**) and HL-1 cardiomyocytes (**Figure 21E**) were transiently co-transfected with Firefly luciferase reporter construct containing cardiac α-actin promoter together with plasmids encoding full-length, truncated, or non-cleavable SRFs and LacZ (control). As displayed in **Figure 21D** and **21E**, the cardiac α-actin promoter activities were strikingly increased with the addition of wild-type and non-cleavable forms of SRF. However, both SRF-N and SRF-C mutants lost their gene transcriptional functions. My results suggest that CVB3-induced cleavage of SRF leads to the disruption of SRF-mediated gene transactivation.

In addition to loss of function of SRF, the presence of SRF cleavage products may themselves have detrimental effects on the function of native SRF. The N-terminal fragment of SRF contains an intact DNA-binding domain but lacks the C-terminal transactivation domain. To test whether this fragment can act as a dominant-negative competitor to full-length SRF, I co-transfected wild-type SRF together with SRF-N and SRF-C mutants in the presence of cardiac α-actin reporter and Renilla luciferase control plasmids into HeLa cells (**Figure 21D**) and HL-1 cardiomyocytes (**Figure 21E**). I demonstrated that the SRF-N mutant significantly decreased wild-type SRF-induced promoter activities of cardiac α-actin, suggesting a negative regulatory role of this mutant in regulating SRF function probably by competing for DNA binding.

A

SRF-WT

SRF-N

SRF-C

SRF-G327E

B

C

D

E

68
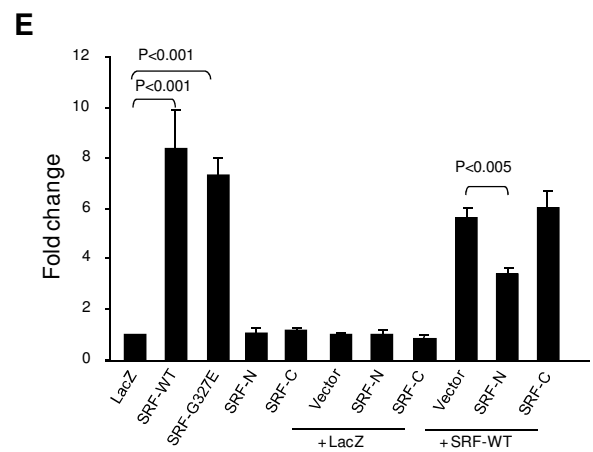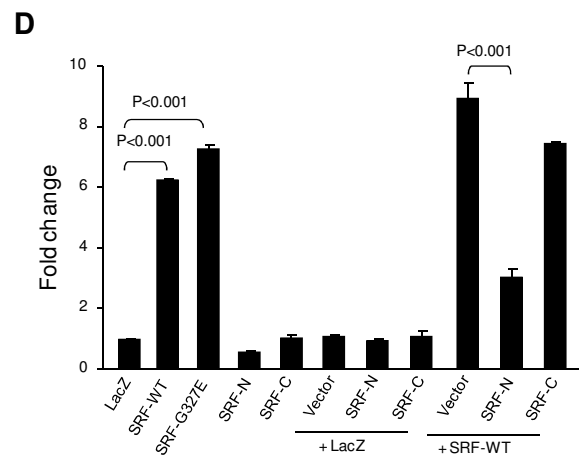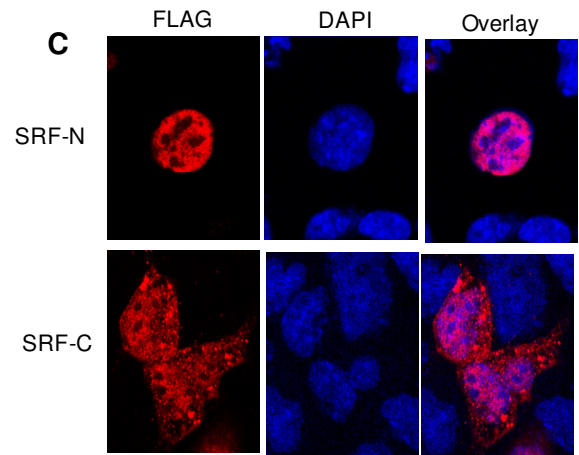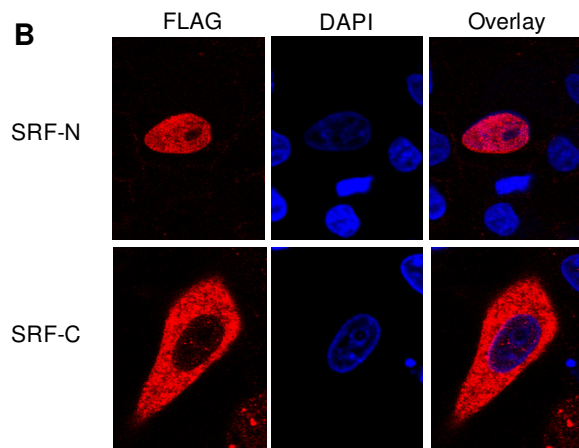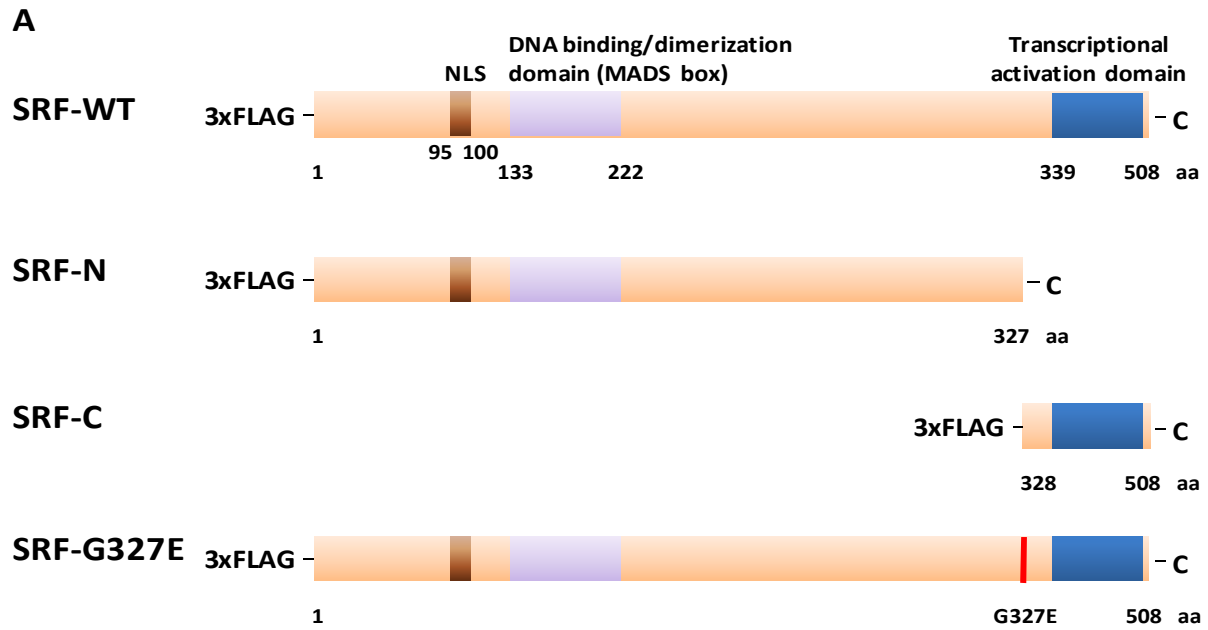
Figure 21. Cellular localization and transcriptional activity of SRF mutants.

(A) Schematic diagram of four 3xFLAG-SRF constructs. NLS, nuclear localization signal. (B, C) HeLa cells (B) or HL-1 cardiomyocytes (C) were transiently transfected with 3×FLAG-tagged SRF-N or SRF-C fragments of the cleaved SRF products for 48 h using Lipofectamine 2000. Immunocytochemical staining for transfected SRF was performed using anti-FLAG antibody. Nucleus was counterstained with DAPI. (D, E) HeLa cells (D) or HL-1 cardiomyocytes (E) were transiently co-transfected with cardiac α-actin luciferase reporter plasmid and constructs expressing SRF-WT or empty vector and/or SRF-G327E, SRF-N, and SRF-C mutants as indicated for 48 h. Luciferase assay was performed and the values are presented as folder changes (mean ± SD, n = 3) over those of control reporter (LacZ), which were arbitrarily set as 1.

4.4.6 Effects of CVB3-mediated SRF cleavage on viral replication

Viruses usually utilize or modulate the host cell infrastructure for their own replication. To test whether cleavage of SRF is beneficial to viral propagation within the host cells, finally, I examined the influences of SRF cleavage on viral replication. **Figure 22** showed that neither knockdown of SRF nor overexpression of wild-type or truncated SRFs affects viral replication, suggesting that cleavage of SRF may not contribute directly to viral benefits.
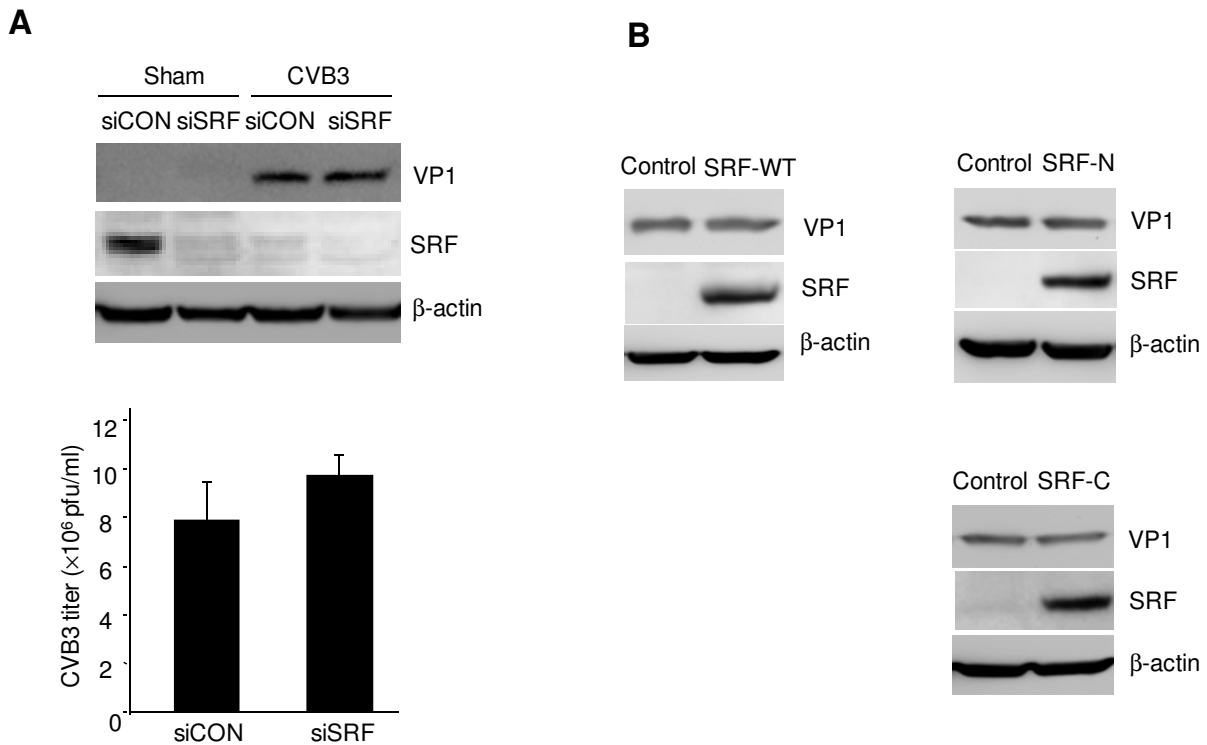
Figure 22. Effects of SRF dysregulation on CVB3 replication.

(A) Effects of knockdown of SRF on CVB3 replication. The gene expression of SRF was knocked down by siRNA. siCON, scramble siRNA control. Upper, western blot analysis was carried out to examine protein level of viral protein VP1, SRF (with anti-FLAG antibody), and β-actin (loading control). Lower, plaque assay was performed to examine virus titers. The results are shown as mean ± SD (n = 3). (B) Effect of overexpression of SRF-wild-type (SRF-WT) and two truncated SRF mutants on CVB3 replication. HeLa cells were transiently transfected with SRF-WT or truncated SRF mutants (SRF-N or SRF-C as indicated) for 48 h, followed by 7 h CVB3 infection. Western blot analysis was carried out to examine protein level of viral protein VP1, SRF (with anti-FLAG antibody) and β-actin (loading control).

4.4.7 Attenuation of SRF cleavage using peptide-based inhibitor

Blocking SRF cleavage is a potential therapeutic strategy in the treatment of viral myocarditis. Viral protease 2A has a catalytic cysteine residue and its substrate recognition is dependent on the 4~6 amino acids upstream of the scissile bond (196). A 2A substrate analogue inhibitor (z-LKST-fmk, shown in **Figure 23A**) was synthesized based on the identified cleavage site of SRF using a strategy described previously (21), which is similar to that used to inhibit caspases (z-VAD-fmk). Fluoromethyl ketone (fmk) can form a covalent bond with the catalytic cysteine leading to protease inactivation. The effectiveness of z-LKST-fmk in blocking SRF cleavage was evaluated. As shown in **Figure 23B**, z-LKST-fmk attenuated CVB3-induced SRF cleavage in a dose dependent manner, which was not observed in the z-VAD-fmk treated murine cardiomyocytes.

A

SRF: ……V<u>LKST</u>**G**SGPVSSGG……

↓

z-LKST-fmk

cbz-leucine-lysine-serine-threonine-fluoromethyl ketone

Chemical Formula: $C_{28}H_{51}FN_5O_8$
Molecular Weight: 604.73
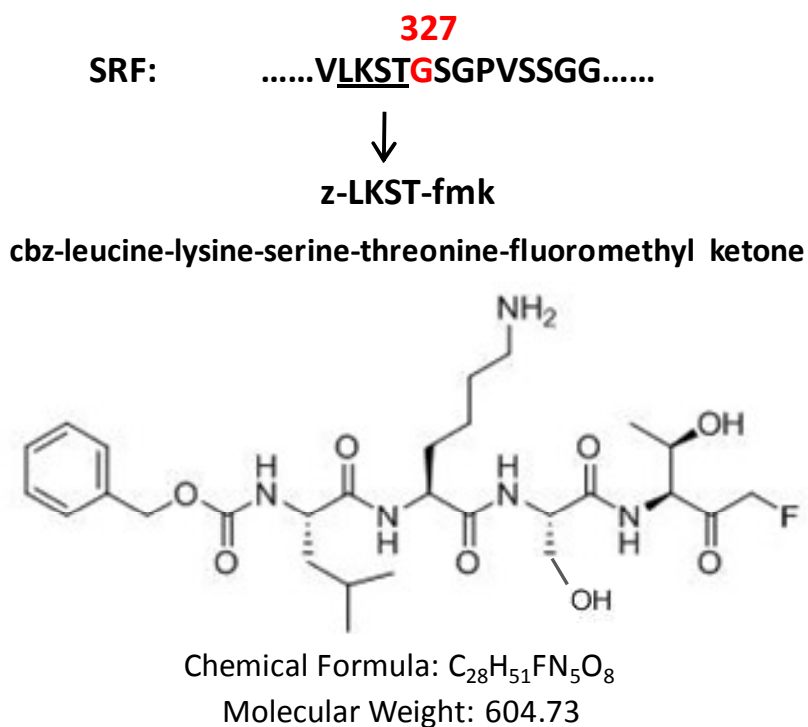
Figure 23. Attenuation of SRF cleavage using peptide-based inhibitor.

(A) Design and structure of 2A substrate analogue inhibitor (z-LKST-fmk). (B) Western blot analysis of SRF, VP1, and β-actin (loading control) expression in CVB3-infected HL-1 murine cardiomyocytes treated various dosage of SRF-based 2A inhibitor (z-LKST-fmk) as indicated, or general caspase inhibitor z-VAD-fmk (50 μM).

4.5   Discussion

Enteroviral proteases have been recognized as an important contributor to viral pathogenesis and resultant myocardial dysfunction via the cleavage of important host proteins. Using a Cre/LoxP-inducible system, it has been shown that transgenic mice with cardiac-specific overexpression of protease 2A develop severe cardiac dysfunction and DCM (205). Experimental evidence from cell culture and cell-free in vitro studies demonstrates that viral protease 2A induces the cleavage and functional impairment of dystrophin (11-13). Dystrophin connects the cytoskeletal actin-binding site to the β-dystroglycan extracellular matrix anchor, thus its cleavage leads to the disruption of the cytoskeletal architecture. It is therefore proposed that protease 2A-induced DCM is associated with disrupted myocyte integrity via the cleavage of dystrophin (13). However, the mdx (dystrophin deficient) mice display a relatively mild dilated phen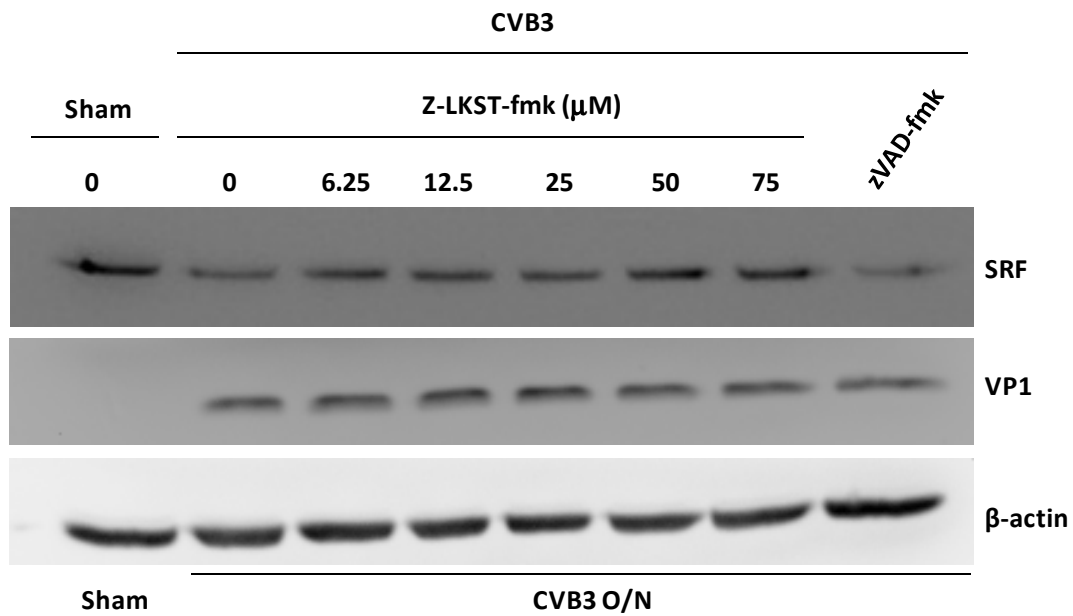otype. This is attributed to the compensatory upregulation of the dystrophin homolog utrophin, as evidenced by severe dystrophic phenotype in mice with double knockout of utrophin and dystrophin (50, 76, 80, 93). Previous study has shown that CVB3 infection does not lead to cleavage of utrophin (13), thus the DCM phenotype induced by dystrophin cleavage may be dampened by the compensatory effect of utrophin in the CVB3-infected heart. All of these suggest that dystrophin cleavage alone may not be sufficient to explain the severe cardiomyopathy phenotype observed in 2A-transgenic mice. This prompts us to postulate that other substrate(s) of 2A may also play a role in the progression of virus-induced cardiomyopathy.

The major findings of this study are as follows: (1) cardiac-specific contractile and regulatory genes are downregulated in CVB3-infected mouse heart and cardiomyocytes, (2) SRF is cleaved by viral protease 2A during CVB3 infection, and (3) cleavage of SRF leads to the disruption of SRF-mediated gene transactivation and production of a dominant-negative competitor to native SRF. These findings suggest that SRF cleavage may contribute to cardiac dysfunction and subsequent progression to DCM in enteroviral myocarditis by disturbing the expression of cardiac contractile and regulatory genes.

Microarray studies in human end-stage heart failure revealed a significant downregulation of numerous cardiac genes, including genes with SRF-binding sites, implicating an important role of SRF in the progression of heart failure (17, 90, 187). Furthermore, as illustrated in this chapter, many cardiac-specific genes are also downregulated in enterovirus-infected heart and cultured cardiomyocytes. All these genes shown in **Figure 15** have either been previously reported to be targets of SRF or contain SREs in their promoter regions (14, 31, 183).

It was reported that expression of an alternatively spliced SRF variant lacking portions of the transactivation domain is markedly increased in human and animal failing hearts (20, 46). This isoform functions as a dominant-negative mutant that inhibits SRF-dependent activation of cardiac muscle genes. Interestingly, my collaborator's recent report showed that SRF cleavage also occurs in myocytes of severely failing human hearts. Increased caspase activity during heart failure induces the cleavage of SRF, producing a truncated protein that lacks the C-terminal transactivation domain, and acts as a dominant inhibitory transcription factor, similar to the alternatively spliced variant (32). These studies suggest that decreased production of full-length SRF, or increased accumulation of truncated SRF, may downregulate SRF-dependent genes and contribute to the progression of severe heart failure. In this study, I have identified a new cleavage site in SRF by viral protease 2A during virus infection and demonstrated a dominant-negative effect of the cleaved SRF on the expression of cardiac genes. With this knowledge, I developed a peptide-based SRF cleavage inhibitor (z-LKST-fmk) that effectively attenuated CVB3-induced SRF cleavage in murine cardiomyocytes. Future studies are required to investigate the therapeutic potential of the peptide-based inhibitor.

Coxsackievirus infection of heart results in focal lesions accompanied by severe fibrosis. Interestingly, recent research on mosaic regional inactivation of SRF in mouse hearts was found to be sufficient in inducing focal lesions and resulting in fatal DCM (69). In these mice, wild-type cardiomyocytes adjacent to the SRF-null myocytes undergo compensatory hypertrophy, which further triggers a hypertrophic response in remote wild-type cardiomyocytes to preserve cardiac output. This mosaic SRF inactivation model provides some insights into the possible pathophysiological consequences of non-functional SRF and dominant-negative SRF truncates presented in patches of CVB3-infected cardiomyocytes and their subsequent influences on the disease progression and outcome.

Overexpression of SRF has also been associated with cardiac hypertrophy. Transgenic mouse studies showed that the cardiac-specific overexpression of SRF induces a pattern of fetal gene re-expression similar to that observed in cardiac hypertrophy and subsequently causes a severe hypertrophic phenotype (212). Therefore, in the future, establishment of a knockin mouse model expressing non-cleavable SRF in the heart will be crucial to determine whether this form of SRF can rescue cardiomyocytes from CVB3-induced dysfunction.

4.6   Limitations and solutions

In this study I tried to apply multiple experimental methods to ensure the validity of each finding. For example, I confirmed CVB3-induced SRF cleavage and the expression of its cleavage products in three different models (mouse hearts, murine cardiomyocytes, and HeLa cells expressing exogenous SRF), as well as using different antibodies against SRF to ensure the validity of western blot results. I differentiated viral protease 2A-induced SRF cleavage from caspase 3-induced SRF cleavage using the pan caspase inhibitor z-VAD-fmk. To assess the consequence of SRF cleavage, I studied the intracellular localization and the transcription activation function of SRF cleavage fragments. However, several supplemental experiments could further strengthen my observations. In particular, my data demonstrating viral protease 2A expression is sufficient in inducing SRF cleavage can be supported by further experiments. The expression of SRF cleavage products is low in HeLa cells transfected with viral protease 2A constructs (**Figure 19**), which is attributed to the inherent limitation of the 2A construct. Protein expression of viral protease from this construct requires the cap-dependent mRNA translation machinery. As described previously, protease 2A effectively shuts down the cap-dependent translation pathway by cleaving eIF4G and PABP. As a result, existing 2A will terminate further expression of 2A. This may be circumvented by constructing an internal ribosome entry site (IRES)-regulated 2A construct, which directs protease 2A expression via the cap-independent translation pathway. Alternatively, an *in vitro* cleavage assay involving purified viral protease 2A and SRF will help confirm 2A-induced SRF cleavage. Additional specificity can be achieved with the addition of cleavage inhibitor z-LKST-fmk.

Regarding to the functional consequences of CVB3-induced SRF cleavage, several supplementary experiments will help strengthen my finding. An electrophoretic mobility shift assay (EMSA) can be conducted to examine the DNA binding activity of truncated SRFs. Other experiments for assessing the functional consequence of SRF cleavage include measuring cardiomyocytes contractility and cardiac gene expression in myocytes transfected with adenovirus constructs overexpressing truncated or non-cleavable SRFs.

Intracellular localization difference of SRF-C in HeLa cells and HL-1 cells (**Figure 21B and 21C**) implies different SRF activity in these cell lines. SRF-C, which lacks nuclear localization signal, should reside predominantly in the cytosol as observed in HeLa cells (**Figure 21B**). However, SRF-C is present evenly in both nucleus and cytosol in HL-1 cells (**Figure 21C**). As previously described, SRF interacts with its cell-specific cofactors to control gene expression in a cell- and context-specific manner. It is likely certain muscle specific cofactors present in HL-1 cells may still interact with the truncated SRF-C and

assist its nuclear shuttling. In this regard, further experiments should be performed to confirm the findings of the effects of CVB3-mediated SRF cleavage on viral replication. HeLa cells were used in this set of experiments to achieve high transfection efficiency. However, HeLa cells are less dependent on SRF-mediated gene expression as reflected from their low endogenous expression level of SRF. Similarly, the expression profile of SRF cofactors is also different in HeLa cells as compared to cardiomyocytes. Therefore, it is important to repeat the same SRF knockdown and overexpression study in cardiac cells such as rat neonatal cardiomyocytes and HL-1 cells to verify the effect of SRF cleavage on CVB3 replication.

4.7 Future directions

This study demonstrated a novel viral mechanism in the downregulation of cardiac gene expression in CVB3-infected host. Coxsackieviral protease 2A-induced SRF cleavage represses cardiac gene expression through the loss of full-length SRF proteins, as well as the generation of dominant negative SRF-N. Future research is required to clarify the role of CVB3-induced SRF cleavage in the progression of viral myocarditis using animal models. The significance of dominant negative SRF-N in the development of viral-induced DCM can be investigated by establishing a transgenic mouse model with cardiac-restricted expression of SRF-N. It answers the question whether SRF-N alone is sufficient to induce cardiomyopathy. Furthermore, the significance of SRF cleavage in the overall development of viral myocarditis can be examined by generating a non-cleavable-SRF-mutant knockin transgenic mouse model. Specifically, a knockin non-cleavable-SRF-mutant mouse model, i.e. homologous replacement of endogenous SRF alleles, is necessary because SRF expression must be strictly controlled in order to maintain cardiac homeostasis. Either overexpression or knockdown manipulation of SRF gene expression in mouse heart results in cardiomyopathy.

Based on the identified SRF cleavage site, a peptide-based 2A inhibitor (z-LKST-fmk) was synthesized. This inhibitor effectively attenuated CVB3-induced SRF cleavage in murine cardiomyocytes. The therapeutic potential of this inhibitor in the treatment of CVB3-induced myocarditis warrants further evaluation. Various cell-free assays (e.g. *in vitro* SRF cleavage assays, as well as caspase, calpain, and proteasome activity assays) will help validate the efficacy and specificity of z-LKST-fmk in blocking protease 2A-induced SRF cleavage. Moreover, functional assessments, such as gene expression and contractility assays, will help evaluate the effectiveness of z-LKST-fmk in preserving the viability of CVB3-infected cardiomyocytes. Eventually, *in vivo* application of z-LKST-fmk will help examine its therapeutic potential in the overall development of coxsackieviral myocarditis/DCM.

4.8   Summary

I demonstrated that CVB3 manipulates SRF expression via protein cleavage (summarized in **Figure 24**). SRF is a transcription factor vital for the expression of cardiac contractile and regulator genes, as well as gene silencing microRNAs. Cardiac-specific knockout of SRF in adult transgenic mice results in disruption of cardiac gene expression and development of severe DCM. I showed that SRF is cleaved in CVB3-infected mouse hearts and cardiomyocytes. Further studies revealed that SRF is cleaved at the 327 amino acids position by CVB3-encoded protease 2A. I demonstrated that SRF cleavage contributes to DCM by abolishing the transactivation property of SRF and generating dominant-negative SRF-truncates. These results provide new insights into the mechanisms by which virus infection impairs heart function and may further the development of new therapeutic approaches to ameliorating myocardial damage and progression to DCM.
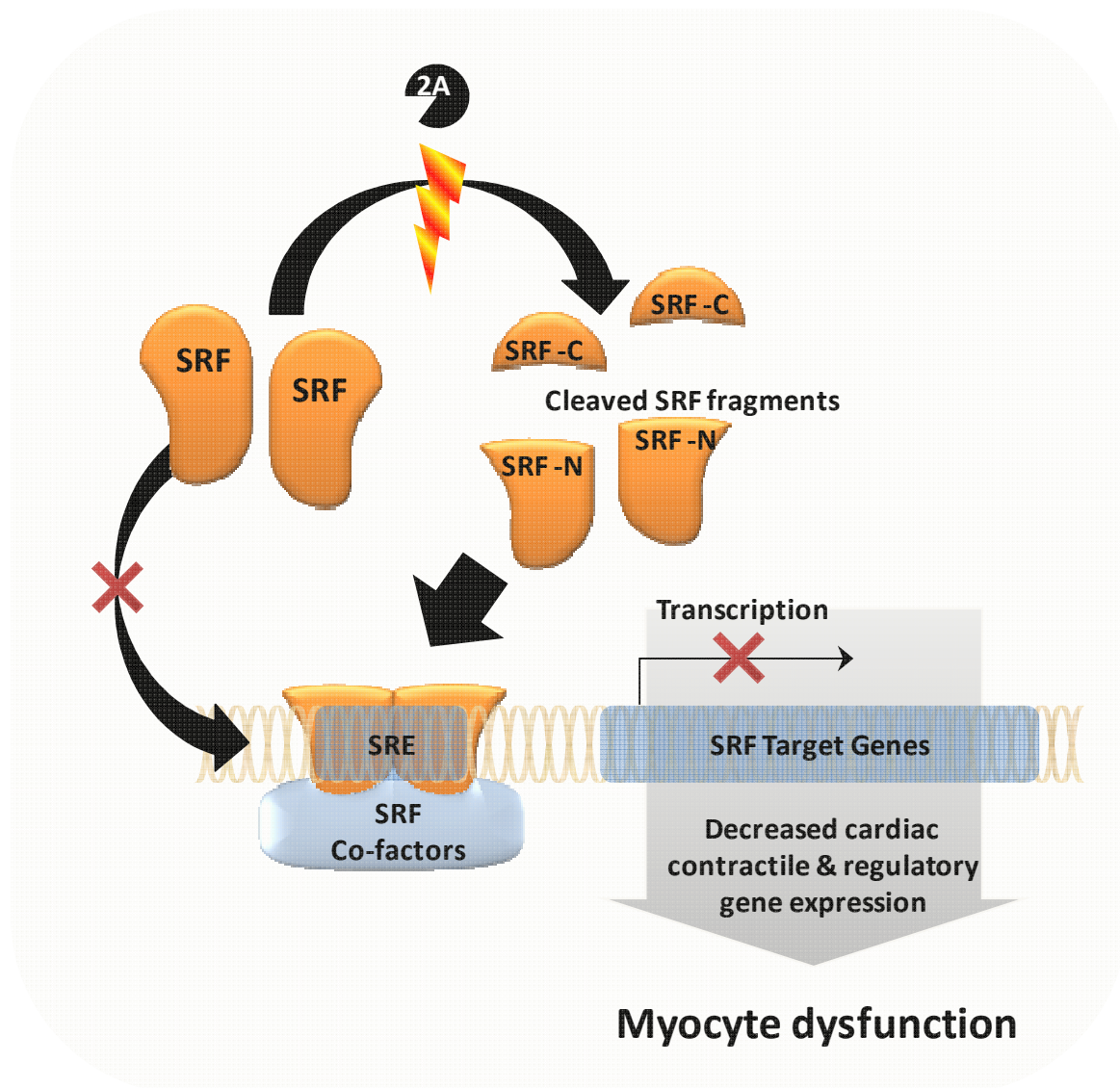
Figure 24. Cleavage of SRF by viral protease 2A leads to myocyte dysfunction.

SRF cleavage by viral protease 2A contributes to myocyte dysfunction by the dissociating of the N-terminal DNA binding/dimerization domain from the C-terminal transcriptional activation domain, thus abolishing SRF-mediated gene expression. Furthermore, the N-terminal fragment (SRF-N) exhibits a dominant-negative effect on endogenous SRF function by competing for DNA binding.

Chapter 5 – Closing remarks

5.1 Research summary and conclusion

In this dissertation, I reported novel host protein manipulation strategies in coxsackievirus-induced cardiomyopathy. Specifically, my work focused on CVB3's strategic subversion of the autophagy pathway to support its replication, as well as its cleavage of the serum response factor that contributes to its pathogenicity. A **summary** of the major findings from my thesis project is listed below:

Chapter 3: Autophagy in coxsackievirus infection

1a) CVB3 infection induces the formation of autophagosomes.

1b) Inhibition of autophagy pathway reduces CVB3 replication – Application of autophagy inhibitor 3-methyladenine or siRNA against autophagy pathway components (ATG7, Beclin-1, and Vps34) reduces CVB3 replication.

1c) Increase autophagosome formation enhances CVB3 replication – Autophagy induction by nutrient starvation and treatment with autophagy inducer rapamycin, or Lysosomal inhibition by RNAi against lysosomal protein LAMP2 enhances CVB3 replication.

Chapter 4: SRF in coxsackieviral cardiomyopathy

2a) SRF is cleaved in CVB3-infected mouse hearts and murine cardiomyocytes.

2b) SRF is cleaved at the 327 amino acids position by viral protease 2A into two fragments: nuclear N-terminal fragment (SRF-N, ~50 kD) and cytoplasmic C-terminal fragment (SRF-C, ~20 kD).

2c) SRF cleavage contributes to CVB3-induced cardiomyopathy in two folds: 1) SRF cleavage abolishes the transcription activation function of SRF, and 2) it generates the dominant negative SRF-N that inhibits wild-type SRF.

Based on these results, I **conclude** that the subversion of host autophagy protein degradation pathway and the cleavage of serum response factor serve critical roles in the pathogenesis of CVB3-induced myocarditis. Strategic subversion of host autophagy machinery is important for efficient viral replication, whereas cleavage of SRF is central to CVB3-induced myocardial dysfunction. Target intervention of these viral strategies may help limit viral replication, ameliorate cardiomyocyte injury, and preserve cardiac function in viral myocarditis.

5.2 Research significance

The newly discovered viral strategies reported in this dissertation may serve as potential therapeutic targets for the treatment of viral myocarditis/DCM. As previously described, viral myocarditis is subdivided into three phases: viremic, inflammatory, and remodeling. At viremic phase, where active viral replication takes place, temporal application of autophagy inhibitor may help control viral replication and limit direct viral-induced myocyte damage. As demonstrated in **Figure 7**, autophagy inhibitor (3-MA) treatment potently inhibited CVB3 replication *in vitro*, even when introduced at 5 hours post infection. However, the impact of autophagy inhibition beyond the viremic phase requires further investigations. Since the outcome of viral myocarditis also depends on the complex interactions between virus infection and host immune system, the effect of autophagy inhibition on immune response must be considered. Recent studies suggest a role for autophagy in host adaptive immune responses through the delivery of intracellular pathogenic antigens for major histocompatibility complex class II presentation to CD4 T cells (176). *In vivo* application of autophagy inhibitor will help evaluate its therapeutic potential in viral myocarditis. Autophagy inhibition in the remodeling phase is cautioned since impairment of protein degradation system has been reported in human failing hearts (22, 198). Application of autophagy inhibitor in the later phases of viral myocarditis may further exacerbate myocardial damage by shutting down this alternative protein degradation pathway. As shown in transgenic mice with cardiac-specific ATG5 knockdown, autophagy is essential to cardiac viability (154). These mice developed cardiac hypertrophy, left ventricular dilatation, and contractile dysfunction (154). Therefore, pharmacological interventions of host autophagy pathway must be carefully designed and stringently evaluated to ensure outstanding benefits with minimal side-effects.

Viral-induced SRF cleavage represents an important mechanism in cardiac gene downregulation in viral myocarditis/DCM. Blocking SRF-cleavage may be a promising therapeutic strategy in the management of viral myocarditis patients. Based on the catalytic requirement and substrate recognition pattern of viral protease 2A, I designed a SRF-based 2A substrate analogue inhibitor (z-LKST-fmk). Fluoromethyl ketone (fmk) can form a covalent bond with the catalytic cysteine leading to protease inactivation. Preliminary study revealed that z-LKST-fmk attenuates CVB3-induced SRF cleavage in a dose dependent manner. Blocking the cleavage of SRF concurrently eliminated the production of dominant negative SRF-N. Preserving functional SRF will likely enhance the recovery of injured cardiomyocyte by allowing the expression of necessary cardiac proteins. Of note, caspase-mediated SRF cleavage is also reported, which generates similar version of dominant negative SRF-N. Although SRF cleavage by caspase is secondary to viral protease, a dual inhibition of SRF cleavage by both mechanisms

using inhibitory peptides z-LKST-fmk and z-VAD-fmk will minimize any SRF cleavage events. Blocking SRF cleavage may help limit preserve myocyte function and limit myocyte loss in all stages of viral myocarditis.

Bibliography

1. 1999. Heart Failure Society of America (HFSA) practice guidelines. HFSA guidelines for management of patients with heart failure caused by left ventricular systolic dysfunction--pharmacological approaches. J Card Fail **5:**357-382.
2. **Akazawa, H., and I. Komuro.** 2003. Roles of cardiac transcription factors in cardiac hypertrophy. Circ Res **92:**1079-1088.
3. **Aldabe, R., and L. Carrasco.** 1995. Induction of membrane proliferation by poliovirus proteins 2C and 2BC. Biochem Biophys Res Commun **206:**64-76.
4. **Alexander, D. E., S. L. Ward, N. Mizushima, B. Levine, and D. A. Leib.** 2007. Analysis of the role of autophagy in replication of herpes simplex virus in cell culture. J Virol **81:**12128-12134.
5. **Amorim, D. S.** 1985. Current status of myocarditis and endomyocardial biopsy in Brazil. Heart Vessels Suppl **1:**79-82.
6. **Anderson, D. R., J. E. Wilson, C. M. Carthy, D. Yang, R. Kandolf, and B. M. McManus.** 1996. Direct interactions of coxsackievirus B3 with immune cells in the splenic compartment of mice susceptible or resistant to myocarditis. J Virol **70:**4632-4645.
7. **Andrade, R. M., M. Wessendarp, M. J. Gubbels, B. Striepen, and C. S. Subauste.** 2006. CD40 induces macrophage anti-Toxoplasma gondii activity by triggering autophagy-dependent fusion of pathogen-containing vacuoles and lysosomes. J Clin Invest **116:**2366-2377.
8. **Aretz, H. T.** 1987. Myocarditis: the Dallas criteria. Hum Pathol **18:**619-624.
9. **Aretz, H. T., M. E. Billingham, W. D. Edwards, S. M. Factor, J. T. Fallon, J. J. Fenoglio, Jr., E. G. Olsen, and F. J. Schoen.** 1987. Myocarditis. A histopathologic definition and classification. Am J Cardiovasc Pathol **1:**3-14.
10. **Arsenian, S., B. Weinhold, M. Oelgeschlager, U. Ruther, and A. Nordheim.** 1998. Serum response factor is essential for mesoderm formation during mouse embryogenesis. EMBO J **17:**6289-6299.
11. **Badorff, C., N. Berkely, S. Mehrotra, J. W. Talhouk, R. E. Rhoads, and K. U. Knowlton.** 2000. Enteroviral protease 2A directly cleaves dystrophin and is inhibited by a dystrophin-based substrate analogue. J Biol Chem **275:**11191-11197.
12. **Badorff, C., B. Fichtlscherer, R. E. Rhoads, A. M. Zeiher, A. Muelsch, S. Dimmeler, and K. U. Knowlton.** 2000. Nitric oxide inhibits dystrophin proteolysis by coxsackieviral protease 2A through S-nitrosylation: A protective mechanism against enteroviral cardiomyopathy. Circulation **102:**2276-2281.
13. **Badorff, C., G. H. Lee, B. J. Lamphear, M. E. Martone, K. P. Campbell, R. E. Rhoads, and K. U. Knowlton.** 1999. Enteroviral protease 2A cleaves dystrophin: evidence of cytoskeletal disruption in an acquired cardiomyopathy. Nat Med **5:**320-326.
14. **Balza, R. O., Jr., and R. P. Misra.** 2006. Role of the serum response factor in regulating contractile apparatus gene expression and sarcomeric integrity in cardiomyocytes. J Biol Chem **281:**6498-6510.
15. **Barbosa, M. E., N. Alenina, and M. Bader.** 2005. Induction and analysis of cardiac hypertrophy in transgenic animal models. Methods Mol Med **112:**339-352.
16. **Barco, A., E. Feduchi, and L. Carrasco.** 2000. Poliovirus protease 3C(pro) kills cells by apoptosis. Virology **266:**352-360.
17. **Barrans, J. D., P. D. Allen, D. Stamatiou, V. J. Dzau, and C. C. Liew.** 2002. Global gene expression profiling of end-stage dilated cardiomyopathy using a human cardiovascular-based cDNA microarray. Am J Pathol **160:**2035-2043.
18. **Batra, A. S., and A. B. Lewis.** 2001. Acute myocarditis. Curr Opin Pediatr **13:**234-239.

19. **Bauer, S., G. Gottesman, L. Sirota, I. Litmanovitz, S. Ashkenazi, and I. Levi.** 2002. Severe Coxsackie virus B infection in preterm newborns treated with pleconaril. Eur J Pediatr **161:**491-493.

20. **Belaguli, N. S., W. Zhou, T. H. Trinh, M. W. Majesky, and R. J. Schwartz.** 1999. Dominant negative murine serum response factor: alternative splicing within the activation domain inhibits transactivation of serum response factor binding targets. Mol Cell Biol **19:**4582-4591.

21. **Bertolotto, C., J. E. Ricci, F. Luciano, B. Mari, J. C. Chambard, and P. Auberger.** 2000. Cleavage of the serum response factor during death receptor-induced apoptosis results in an inhibition of the c-FOS promoter transcriptional activity. J Biol Chem **275:**12941-12947.

22. **Birks, E. J., N. Latif, K. Enesa, T. Folkvang, A. Luong le, P. Sarathchandra, M. Khan, H. Ovaa, C. M. Terracciano, P. J. Barton, M. H. Yacoub, and P. C. Evans.** 2008. Elevated p53 expression is associated with dysregulation of the ubiquitin-proteasome system in dilated cardiomyopathy. Cardiovasc Res **79:**472-480.

23. **Blommaart, E. F., U. Krause, J. P. Schellens, H. Vreeling-Sindelarova, and A. J. Meijer.** 1997. The phosphatidylinositol 3-kinase inhibitors wortmannin and LY294002 inhibit autophagy in isolated rat hepatocytes. Eur J Biochem **243:**240-246.

24. **Bowles, N. E., and J. A. Towbin.** 2000. Molecular Aspects of Myocarditis. Curr Infect Dis Rep **2:**308-314.

25. **Brabec-Zaruba, M., U. Berka, D. Blaas, and R. Fuchs.** 2007. Induction of autophagy does not affect human rhinovirus type 2 production. J Virol **81:**10815-10817.

26. **Burnette, W. N.** 1981. "Western blotting": electrophoretic transfer of proteins from sodium dodecyl sulfate--polyacrylamide gels to unmodified nitrocellulose and radiographic detection with antibody and radioiodinated protein A. Anal Biochem **112:**195-203.

27. **Cambridge, G., C. G. MacArthur, A. P. Waterson, J. F. Goodwin, and C. M. Oakley.** 1979. Antibodies to Coxsackie B viruses in congestive cardiomyopathy. Br Heart J **41:**692-696.

28. **Carnac, G., M. Primig, M. Kitzmann, P. Chafey, D. Tuil, N. Lamb, and A. Fernandez.** 1998. RhoA GTPase and serum response factor control selectively the expression of MyoD without affecting Myf5 in mouse myoblasts. Mol Biol Cell **9:**1891-1902.

29. **Carthy, C. M., D. J. Granville, K. A. Watson, D. R. Anderson, J. E. Wilson, D. Yang, D. W. Hunt, and B. M. McManus.** 1998. Caspase activation and specific cleavage of substrates after coxsackievirus B3-induced cytopathic effect in HeLa cells. J Virol **72:**7669-7675.

30. **Carthy, C. M., B. Yanagawa, H. Luo, D. J. Granville, D. Yang, P. Cheung, C. Cheung, M. Esfandiarei, C. M. Rudin, C. B. Thompson, D. W. Hunt, and B. M. McManus.** 2003. Bcl-2 and Bcl-xL overexpression inhibits cytochrome c release, activation of multiple caspases, and virus release following coxsackievirus B3 infection. Virology **313:**147-157.

31. **Chai, J., and A. S. Tarnawski.** 2002. Serum response factor: discovery, biochemistry, biological roles and implications for tissue injury healing. J Physiol Pharmacol **53:**147-157.

32. **Chang, J., L. Wei, T. Otani, K. A. Youker, M. L. Entman, and R. J. Schwartz.** 2003. Inhibitory cardiac transcription factor, SRF-N, is generated by caspase 3 cleavage in human heart failure and attenuated by ventricular unloading. Circulation **108:**407-413.

33. **Chau, D. H., J. Yuan, H. Zhang, P. Cheung, T. Lim, Z. Liu, A. Sall, and D. Yang.** 2007. Coxsackievirus B3 proteases 2A and 3C induce apoptotic cell death through mitochondrial injury and cleavage of eIF4GI but not DAP5/p97/NAT1. Apoptosis **12:**513-524.

34. **Cheung, C., D. Marchant, E. K. Walker, Z. Luo, J. Zhang, B. Yanagawa, M. Rahmani, J. Cox, C. Overall, R. M. Senior, H. Luo, and B. M. McManus.** 2008. Ablation of matrix metalloproteinase-9 increases severity of viral myocarditis in mice. Circulation **117:**1574-1582.

35.   **Cho, M. W., N. Teterina, D. Egger, K. Bienz, and E. Ehrenfeld.** 1994. Membrane rearrangement and vesicle induction by recombinant poliovirus 2C and 2BC in human cells. Virology **202:**129-145.

36.   **Chow, L. C., H. C. Dittrich, and R. Shabetai.** 1988. Endomyocardial biopsy in patients with unexplained congestive heart failure. Ann Intern Med **109:**535-539.

37.   **Chow, L. H., K. W. Beisel, and B. M. McManus.** 1992. Enteroviral infection of mice with severe combined immunodeficiency. Evidence for direct viral pathogenesis of myocardial injury. Lab Invest **66:**24-31.

38.   **Chow, L. H., S. J. Radio, T. D. Sears, and B. M. McManus.** 1989. Insensitivity of right ventricular endomyocardial biopsy in the diagnosis of myocarditis. J Am Coll Cardiol **14:**915-920.

39.   **Chung, S. K., J. Y. Kim, I. B. Kim, S. I. Park, K. H. Paek, and J. H. Nam.** 2005. Internalization and trafficking mechanisms of coxsackievirus B3 in HeLa cells. Virology **333:**31-40.

40.   **Clark, M. E., P. M. Lieberman, A. J. Berk, and A. Dasgupta.** 1993. Direct cleavage of human TATA-binding protein by poliovirus protease 3C in vivo and in vitro. Mol Cell Biol **13:**1232-1237.

41.   **Codogno, P., and A. J. Meijer.** 2005. Autophagy and signaling: their role in cell survival and cell death. Cell Death Differ **12 Suppl 2:**1509-1518.

42.   **Cuervo, A. M., and J. F. Dice.** 1998. Lysosomes, a meeting point of proteins, chaperones, and proteases. J Mol Med (Berl) **76:**6-12.

43.   **Dalldorf, G.** 1949. The Coxsackie group of viruses. Science **110:**594.

44.   **Dalldorf, G.** 1955. The Coxsackie viruses. Annu Rev Microbiol **9:**277-296.

45.   **Dalldorf, G., and G. M. Sickles.** 1948. An Unidentified, Filtrable Agent Isolated From the Feces of Children With Paralysis. Science **108:**61-62.

46.   **Davis, F. J., M. Gupta, S. M. Pogwizd, E. Bacha, V. Jeevanandam, and M. P. Gupta.** 2002. Increased expression of alternatively spliced dominant-negative isoform of SRF in human failing hearts. Am J Physiol Heart Circ Physiol **282:**H1521-1533.

47.   **De Scheerder, I. K., M. De Buyzere, J. Delanghe, A. Maas, D. L. Clement, and R. Wieme.** 1991. Humoral immune response against contractile proteins (actin and myosin) during cardiovascular disease. Eur Heart J **12 Suppl D:**88-94.

48.   **Dec, G. W., Jr., I. F. Palacios, J. T. Fallon, H. T. Aretz, J. Mills, D. C. Lee, and R. A. Johnson.** 1985. Active myocarditis in the spectrum of acute dilated cardiomyopathies. Clinical features, histologic correlates, and clinical outcome. N Engl J Med **312:**885-890.

49.   **Dec, G. W., Jr., H. Waldman, J. Southern, J. T. Fallon, A. M. Hutter, Jr., and I. Palacios.** 1992. Viral myocarditis mimicking acute myocardial infarction. J Am Coll Cardiol **20:**85-89.

50.   **Deconinck, A. E., J. A. Rafael, J. A. Skinner, S. C. Brown, A. C. Potter, L. Metzinger, D. J. Watt, J. G. Dickson, J. M. Tinsley, and K. E. Davies.** 1997. Utrophin-dystrophin-deficient mice as a model for Duchenne muscular dystrophy. Cell **90:**717-727.

51.   **Dettmeyer, R., A. Baasner, M. Schlamann, C. Haag, and B. Madea.** 2002. Coxsackie B3 myocarditis in 4 cases of suspected sudden infant death syndrome: diagnosis by immunohistochemical and molecular-pathologic investigations. Pathol Res Pract **198:**689-696.

52.   **Doedens, J. R., and K. Kirkegaard.** 1995. Inhibition of cellular protein secretion by poliovirus proteins 2B and 3A. EMBO J **14:**894-907.

53.   **Drewett, V., A. Devitt, J. Saxton, N. Portman, P. Greaney, N. E. Cheong, T. F. Alnemri, E. Alnemri, and P. E. Shaw.** 2001. Serum response factor cleavage by caspases 3 and 7 linked to apoptosis in human BJAB cells. J Biol Chem **276:**33444-33451.

54.   **Drory, Y., Y. Turetz, Y. Hiss, B. Lev, E. Z. Fisman, A. Pines, and M. R. Kramer.** 1991. Sudden unexpected death in persons less than 40 years of age. The American journal of cardiology **68:**1388-1392.

55. **Drucker, N. A., and J. W. Newburger.** 1997. Viral myocarditis: diagnosis and management. Adv Pediatr **44:**141-171.

56. **Dunn, W. A., Jr.** 1994. Autophagy and related mechanisms of lysosome-mediated protein degradation. Trends Cell Biol **4:**139-143.

57. **Esfandiarei, M., H. Luo, B. Yanagawa, A. Suarez, D. Dabiri, J. Zhang, and B. M. McManus.** 2004. Protein kinase B/Akt regulates coxsackievirus B3 replication through a mechanism which is not caspase dependent. J Virol **78:**4289-4298.

58. **Esfandiarei, M., and B. M. McManus.** 2008. Molecular biology and pathogenesis of viral myocarditis. Annu Rev Pathol **3:**127-155.

59. **Espert, L., P. Codogno, and M. Biard-Piechaczyk.** 2007. Involvement of autophagy in viral infections: antiviral function and subversion by viruses. J Mol Med (Berl) **85:**811-823.

60. **Fader, C. M., and M. I. Colombo.** 2009. Autophagy and multivesicular bodies: two closely related partners. Cell Death Differ **16:**70-78.

61. **Feldman, A. M., and D. McNamara.** 2000. Myocarditis. N Engl J Med **343:**1388-1398.

62. **Feuer, R., and J. L. Whitton.** 2008. Preferential coxsackievirus replication in proliferating/activated cells: implications for virus tropism, persistence, and pathogenesis. Current topics in microbiology and immunology **323:**149-173.

63. **Flanegan, J. B., R. F. Petterson, V. Ambros, N. J. Hewlett, and D. Baltimore.** 1977. Covalent linkage of a protein to a defined nucleotide sequence at the 5'-terminus of virion and replicative intermediate RNAs of poliovirus. Proc Natl Acad Sci U S A **74:**961-965.

64. **Florea, V. G., V. Y. Mareyev, A. N. Samko, I. A. Orlova, A. J. Coats, and Y. N. Belenkov.** 1999. Left ventricular remodelling: common process in patients with different primary myocardial disorders. Int J Cardiol **68:**281-287.

65. **Fohlman, J., K. Pauksen, T. Hyypia, G. Eggertsen, A. Ehrnst, N. G. Ilback, and G. Friman.** 1996. Antiviral treatment with WIN 54 954 reduces mortality in murine coxsackievirus B3 myocarditis. Circulation **94:**2254-2259.

66. **Friedrich, M. G., O. Strohm, J. Schulz-Menger, H. Marciniak, F. C. Luft, and R. Dietz.** 1998. Contrast media-enhanced magnetic resonance imaging visualizes myocardial changes in the course of viral myocarditis. Circulation **97:**1802-1809.

67. **Fujita, N., and T. Yoshimori.** 2011. Ubiquitination-mediated autophagy against invading bacteria. Curr Opin Cell Biol **23:**492-497.

68. **Gao, G., J. Wong, J. Zhang, I. Mao, J. Shravah, Y. Wu, A. Xiao, X. Li, and H. Luo.** 2010. Proteasome activator REGgamma enhances coxsackieviral infection by facilitating p53 degradation. J Virol **84:**11056-11066.

69. **Gary-Bobo, G., A. Parlakian, B. Escoubet, C. A. Franco, S. Clement, P. Bruneval, D. Tuil, D. Daegelen, D. Paulin, Z. Li, and M. Mericskay.** 2008. Mosaic inactivation of the serum response factor gene in the myocardium induces focal lesions and heart failure. Eur J Heart Fail **10:**635-645.

70. **Gauntt, C. J.** 2003. Introduction and historical perspective on experimental myocarditis. Humana Press, Totowa, N.J.

71. **Gauntt, C. J., H. M. Arizpe, A. L. Higdon, H. J. Wood, D. F. Bowers, M. M. Rozek, and R. Crawley.** 1995. Molecular mimicry, anti-coxsackievirus B3 neutralizing monoclonal antibodies, and myocarditis. J Immunol **154:**2983-2995.

72. **Gauntt, C. J., R. E. Paque, M. D. Trousdale, R. J. Gudvangen, D. T. Barr, G. J. Lipotich, T. J. Nealon, and P. S. Duffey.** 1983. Temperature-sensitive mutant of coxsackievirus B3 establishes resistance in neonatal mice that protects them during adolescence against coxsackievirus B3-induced myocarditis. Infect Immun **39:**851-864.

73. **Gauthier-Rouviere, C., M. Vandromme, D. Tuil, N. Lautredou, M. Morris, M. Soulez, A. Kahn, A. Fernandez, and N. Lamb.** 1996. Expression and activity of serum response factor is required for expression of the muscle-determining factor MyoD in both dividing and differentiating mouse C2C12 myoblasts. Mol Biol Cell **7:**719-729.

74. **Goldstaub, D., A. Gradi, Z. Bercovitch, Z. Grosmann, Y. Nophar, S. Luria, N. Sonenberg, and C. Kahana.** 2000. Poliovirus 2A protease induces apoptotic cell death. Mol Cell Biol **20:**1271-1277.

75. **Gonzalez-Polo, R. A., P. Boya, A. L. Pauleau, A. Jalil, N. Larochette, S. Souquere, E. L. Eskelinen, G. Pierron, P. Saftig, and G. Kroemer.** 2005. The apoptosis/autophagy paradox: autophagic vacuolization before apoptotic death. J Cell Sci **118:**3091-3102.

76. **Grady, R. M., H. Teng, M. C. Nichol, J. C. Cunningham, R. S. Wilkinson, and J. R. Sanes.** 1997. Skeletal and cardiac myopathies in mice lacking utrophin and dystrophin: a model for Duchenne muscular dystrophy. Cell **90:**729-738.

77. **Grist, N. R., and D. Reid.** 1997. Organisms in myocarditis/endocarditis viruses. J Infect **34:**155.

78. **Gustafsson, A. B., and R. A. Gottlieb.** 2008. Recycle or die: the role of autophagy in cardioprotection. J Mol Cell Cardiol **44:**654-661.

79. **Gutierrez, M. G., S. S. Master, S. B. Singh, G. A. Taylor, M. I. Colombo, and V. Deretic.** 2004. Autophagy is a defense mechanism inhibiting BCG and Mycobacterium tuberculosis survival in infected macrophages. Cell **119:**753-766.

80. **Hainsey, T. A., S. Senapati, D. E. Kuhn, and J. A. Rafael.** 2003. Cardiomyopathic features associated with muscular dystrophy are independent of dystrophin absence in cardiovasculature. Neuromuscul Disord **13:**294-302.

81. **Hara, T., and N. Mizushima.** 2009. Role of ULK-FIP200 complex in mammalian autophagy: FIP200, a counterpart of yeast Atg17? Autophagy **5:**85-87.

82. **Harris, K. S., S. R. Reddigari, M. J. Nicklin, T. Hammerle, and E. Wimmer.** 1992. Purification and characterization of poliovirus polypeptide 3CD, a proteinase and a precursor for RNA polymerase. J Virol **66:**7481-7489.

83. **He, C., and D. J. Klionsky.** 2009. Regulation mechanisms and signaling pathways of autophagy. Annu Rev Genet **43:**67-93.

84. **Hellen, C. U., M. Facke, H. G. Krausslich, C. K. Lee, and E. Wimmer.** 1991. Characterization of poliovirus 2A proteinase by mutational analysis: residues required for autocatalytic activity are essential for induction of cleavage of eukaryotic initiation factor 4F polypeptide p220. J Virol **65:**4226-4231.

85. **Hope, D. A., S. E. Diamond, and K. Kirkegaard.** 1997. Genetic dissection of interaction between poliovirus 3D polymerase and viral protein 3AB. J Virol **71:**9490-9498.

86. **Horwitz, M. S., A. La Cava, C. Fine, E. Rodriguez, A. Ilic, and N. Sarvetnick.** 2000. Pancreatic expression of interferon-gamma protects mice from lethal coxsackievirus B3 infection and subsequent myocarditis. Nat Med **6:**693-697.

87. **Hosenpud, J. D., L. E. Bennett, B. M. Keck, M. M. Boucek, and R. J. Novick.** 2001. The Registry of the International Society for Heart and Lung Transplantation: eighteenth Official Report-2001. J Heart Lung Transplant **20:**805-815.

88. **Hoyer-Hansen, M., L. Bastholm, P. Szyniarowski, M. Campanella, G. Szabadkai, T. Farkas, K. Bianchi, N. Fehrenbacher, F. Elling, R. Rizzuto, I. S. Mathiasen, and M. Jaattela.** 2007. Control of macroautophagy by calcium, calmodulin-dependent kinase kinase-beta, and Bcl-2. Mol Cell **25:**193-205.

89. **Huber, S. A., C. J. Gauntt, and P. Sakkinen.** 1998. Enteroviruses and myocarditis: viral pathogenesis through replication, cytokine induction, and immunopathogenicity. Adv Virus Res **51:**35-80.

90. **Hwang, J. J., P. D. Allen, G. C. Tseng, C. W. Lam, L. Fananapazir, V. J. Dzau, and C. C. Liew.** 2002. Microarray gene expression profiles in dilated and hypertrophic cardiomyopathic end-stage heart failure. Physiol Genomics **10:**31-44.

91. **Jackson, W. T., T. H. Giddings, Jr., M. P. Taylor, S. Mulinyawe, M. Rabinovitch, R. R. Kopito, and K. Kirkegaard.** 2005. Subversion of cellular autophagosomal machinery by RNA viruses. PLoS Biol **3:**e156.

92. **Jang, S. K., and E. Wimmer.** 1990. Cap-independent translation of encephalomyocarditis virus RNA: structural elements of the internal ribosomal entry site and involvement of a cellular 57-kD RNA-binding protein. Genes Dev **4:**1560-1572.

93. **Janssen, P. M., N. Hiranandani, T. A. Mays, and J. A. Rafael-Fortney.** 2005. Utrophin deficiency worsens cardiac contractile dysfunction present in dystrophin-deficient mdx mice. Am J Physiol Heart Circ Physiol **289:**H2373-2378.

94. **Jin, O., M. J. Sole, J. W. Butany, W. K. Chia, P. R. McLaughlin, P. Liu, and C. C. Liew.** 1990. Detection of enterovirus RNA in myocardial biopsies from patients with myocarditis and cardiomyopathy using gene amplification by polymerase chain reaction. Circulation **82:**8-16.

95. **Joachims, M., P. C. Van Breugel, and R. E. Lloyd.** 1999. Cleavage of poly(A)-binding protein by enterovirus proteases concurrent with inhibition of translation in vitro. J Virol **73:**718-727.

96. **Johnson, K. L., and P. Sarnow.** 1991. Three poliovirus 2B mutants exhibit noncomplementable defects in viral RNA amplification and display dosage-dependent dominance over wild-type poliovirus. J Virol **65:**4341-4349.

97. **Jung, C. H., C. B. Jun, S. H. Ro, Y. M. Kim, N. M. Otto, J. Cao, M. Kundu, and D. H. Kim.** 2009. ULK-Atg13-FIP200 complexes mediate mTOR signaling to the autophagy machinery. Mol Biol Cell **20:**1992-2003.

98. **Kabeya, Y., N. Mizushima, T. Ueno, A. Yamamoto, T. Kirisako, T. Noda, E. Kominami, Y. Ohsumi, and T. Yoshimori.** 2000. LC3, a mammalian homologue of yeast Apg8p, is localized in autophagosome membranes after processing. EMBO J **19:**5720-5728.

99. **Kemball, C. C., M. Alirezaei, C. T. Flynn, M. R. Wood, S. Harkins, W. B. Kiosses, and J. L. Whitton.** 2010. Coxsackievirus infection induces autophagy-like vesicles and megaphagosomes in pancreatic acinar cells in vivo. Journal of virology **84:**12110-12124.

100. **Kerekatte, V., B. D. Keiper, C. Badorff, A. Cai, K. U. Knowlton, and R. E. Rhoads.** 1999. Cleavage of Poly(A)-binding protein by coxsackievirus 2A protease in vitro and in vivo: another mechanism for host protein synthesis shutoff? J Virol **73:**709-717.

101. **Kihara, A., Y. Kabeya, Y. Ohsumi, and T. Yoshimori.** 2001. Beclin-phosphatidylinositol 3-kinase complex functions at the trans-Golgi network. EMBO Rep **2:**330-335.

102. **Kirkegaard, K., M. P. Taylor, and W. T. Jackson.** 2004. Cellular autophagy: surrender, avoidance and subversion by microorganisms. Nat Rev Microbiol **2:**301-314.

103. **Klausner, R. D., and J. B. Harford.** 1989. cis-trans models for post-transcriptional gene regulation. Science **246:**870-872.

104. **Kleinert, S., R. G. Weintraub, J. L. Wilkinson, and C. W. Chow.** 1997. Myocarditis in children with dilated cardiomyopathy: incidence and outcome after dual therapy immunosuppression. J Heart Lung Transplant **16:**1248-1254.

105. **Klingel, K., P. Rieger, G. Mall, H. C. Selinka, M. Huber, and R. Kandolf.** 1998. Visualization of enteroviral replication in myocardial tissue by ultrastructural in situ hybridization: identification of target cells and cytopathic effects. Lab Invest **78:**1227-1237.

106. **Klionsky, D. J.** 2007. Autophagy: from phenomenology to molecular understanding in less than a decade. Nat Rev Mol Cell Biol **8:**931-937.

107. **Klionsky, D. J.** 2005. The correct way to monitor autophagy in higher eukaryotes. Autophagy **1:**65.

108. **Klionsky, D. J., H. Abeliovich, P. Agostinis, D. K. Agrawal, G. Aliev, D. S. Askew, M. Baba, E. H. Baehrecke, B. A. Bahr, A. Ballabio, B. A. Bamber, D. C. Bassham, E. Bergamini, X. Bi, M. Biard-Piechaczyk, J. S. Blum, D. E. Bredesen, J. L. Brodsky, J. H. Brumell, U. T. Brunk, W. Bursch, N. Camougrand, E. Cebollero, F. Cecconi, Y. Chen, L. S. Chin, A. Choi, C. T. Chu, J. Chung, P. G. Clarke, R. S. Clark, S. G. Clarke, C. Clave, J. L. Cleveland, P. Codogno, M. I. Colombo, A. Coto-Montes, J. M. Cregg, A. M. Cuervo, J. Debnath, F. Demarchi, P. B. Dennis, P. A. Dennis, V. Deretic, R. J. Devenish, F. Di Sano, J. F. Dice, M. Difiglia, S. Dinesh-Kumar, C. W. Distelhorst, M. Djavaheri-Mergny, F. C. Dorsey, W. Droge, M. Dron, W. A. Dunn, Jr., M. Duszenko, N. T. Eissa, Z. Elazar, A. Esclatine, E. L. Eskelinen, L. Fesus, K. D. Finley, J. M. Fuentes, J. Fueyo, K. Fujisaki, B. Galliot, F. B. Gao, D. A. Gewirtz, S. B. Gibson, A. Gohla, A. L. Goldberg, R. Gonzalez, C. Gonzalez-Estevez, S. Gorski, R. A. Gottlieb, D. Haussinger, Y. W. He, K. Heidenreich, J. A. Hill, M. Hoyer-Hansen, X. Hu, W. P. Huang, A. Iwasaki, M. Jaattela, W. T. Jackson, X. Jiang, S. Jin, T. Johansen, J. U. Jung, M. Kadowaki, C. Kang, A. Kelekar, D. H. Kessel, J. A. Kiel, H. P. Kim, A. Kimchi, T. J. Kinsella, K. Kiselyov, K. Kitamoto, E. Knecht, et al.** 2008. Guidelines for the use and interpretation of assays for monitoring autophagy in higher eukaryotes. Autophagy **4:**151-175.

109. **Klionsky, D. J., and S. D. Emr.** 2000. Autophagy as a regulated pathway of cellular degradation. Science **290:**1717-1721.

110. **Knowlton, K. U., and C. Badorff.** 1999. The immune system in viral myocarditis: maintaining the balance. Circ Res **85:**559-561.

111. **Komatsu, M., S. Waguri, T. Ueno, J. Iwata, S. Murata, I. Tanida, J. Ezaki, N. Mizushima, Y. Ohsumi, Y. Uchiyama, E. Kominami, K. Tanaka, and T. Chiba.** 2005. Impairment of starvation-induced and constitutive autophagy in Atg7-deficient mice. J Cell Biol **169:**425-434.

112. **Kouroku, Y., E. Fujita, I. Tanida, T. Ueno, A. Isoai, H. Kumagai, S. Ogawa, R. J. Kaufman, E. Kominami, and T. Momoi.** 2007. ER stress (PERK/eIF2alpha phosphorylation) mediates the polyglutamine-induced LC3 conversion, an essential step for autophagy formation. Cell Death Differ **14:**230-239.

113. **Kuwahara, K., G. C. Teg Pipes, J. McAnally, J. A. Richardson, J. A. Hill, R. Bassel-Duby, and E. N. Olson.** 2007. Modulation of adverse cardiac remodeling by STARS, a mediator of MEF2 signaling and SRF activity. J Clin Invest **117:**1324-1334.

114. **Lamphear, B. J., R. Kirchweger, T. Skern, and R. E. Rhoads.** 1995. Mapping of functional domains in eukaryotic protein synthesis initiation factor 4G (eIF4G) with picornaviral proteases. Implications for cap-dependent and cap-independent translational initiation. J Biol Chem **270:**21975-21983.

115. **Lamphear, B. J., and R. E. Rhoads.** 1996. A single amino acid change in protein synthesis initiation factor 4G renders cap-dependent translation resistant to picornaviral 2A proteases. Biochemistry **35:**15726-15733.

116. **Lane, J. R., D. A. Neumann, A. Lafond-Walker, A. Herskowitz, and N. R. Rose.** 1992. Interleukin 1 or tumor necrosis factor can promote Coxsackie B3-induced myocarditis in resistant B10.A mice. J Exp Med **175:**1123-1129.

117. **Latham, R. D., J. P. Mulrow, R. Virmani, M. Robinowitz, and J. M. Moody.** 1989. Recently diagnosed idiopathic dilated cardiomyopathy: incidence of myocarditis and efficacy of prednisone therapy. Am Heart J **117:**876-882.

118. **Lauer, B., C. Niederau, U. Kuhl, M. Schannwell, M. Pauschinger, B. E. Strauer, and H. P. Schultheiss.** 1997. Cardiac troponin T in patients with clinically suspected myocarditis. J Am Coll Cardiol **30:**1354-1359.

119. **Leonard, E. G.** 2004. Viral myocarditis. Pediatr Infect Dis J **23:**665-666.

120. **Levi, D., and J. Alejos.** 2001. Diagnosis and treatment of pediatric viral myocarditis. Curr Opin Cardiol **16:**77-83.

121. **Levine, B., and G. Kroemer.** 2008. Autophagy in the pathogenesis of disease. Cell **132:**27-42.
122. **Lie, J. T.** 1988. Myocarditis and endomyocardial biopsy in unexplained heart failure: a diagnosis in search of a disease. Ann Intern Med **109:**525-528.
123. **Lieback, E., I. Hardouin, R. Meyer, J. Bellach, and R. Hetzer.** 1996. Clinical value of echocardiographic tissue characterization in the diagnosis of myocarditis. Eur Heart J **17:**135-142.
124. **Liu, N., S. Bezprozvannaya, A. H. Williams, X. Qi, J. A. Richardson, R. Bassel-Duby, and E. N. Olson.** 2008. microRNA-133a regulates cardiomyocyte proliferation and suppresses smooth muscle gene expression in the heart. Genes Dev **22:**3242-3254.
125. **Liu, P. P., and J. W. Mason.** 2001. Advances in the understanding of myocarditis. Circulation **104:**1076-1082.
126. **Lodge, P. A., M. Herzum, J. Olszewski, and S. A. Huber.** 1987. Coxsackievirus B-3 myocarditis. Acute and chronic forms of the disease caused by different immunopathogenic mechanisms. Am J Pathol **128:**455-463.
127. **Luo, H., J. Wong, and B. Wong.** 2010. Protein degradation systems in viral myocarditis leading to dilated cardiomyopathy. Cardiovasc Res **85:**347-356.
128. **Luo, H., B. Yanagawa, J. Zhang, Z. Luo, M. Zhang, M. Esfandiarei, C. Carthy, J. E. Wilson, D. Yang, and B. M. McManus.** 2002. Coxsackievirus B3 replication is reduced by inhibition of the extracellular signal-regulated kinase (ERK) signaling pathway. J Virol **76:**3365-3373.
129. **Luo, H., J. Zhang, C. Cheung, A. Suarez, B. M. McManus, and D. Yang.** 2003. Proteasome inhibition reduces coxsackievirus B3 replication in murine cardiomyocytes. Am J Pathol **163:**381-385.
130. **Magnani, J. W., and G. W. Dec.** 2006. Myocarditis: current trends in diagnosis and treatment. Circulation **113:**876-890.
131. **Maisch, B., E. Bauer, M. Cirsi, and K. Kochsiek.** 1993. Cytolytic cross-reactive antibodies directed against the cardiac membrane and viral proteins in coxsackievirus B3 and B4 myocarditis. Characterization and pathogenetic relevance. Circulation **87:**IV49-65.
132. **Makarov, V. A., O. B. Riabova, V. G. Granik, P. Wutzler, and M. Schmidtke.** 2005. Novel [(biphenyloxy)propyl]isoxazole derivatives for inhibition of human rhinovirus 2 and coxsackievirus B3 replication. J Antimicrob Chemother **55:**483-488.
133. **Marchant, D., Y. Dou, H. Luo, F. S. Garmaroudi, J. E. McDonough, X. Si, E. Walker, Z. Luo, A. Arner, R. G. Hegele, I. Laher, and B. M. McManus.** 2009. Bosentan enhances viral load via endothelin-1 receptor type-A-mediated p38 mitogen-activated protein kinase activation while improving cardiac function during coxsackievirus-induced myocarditis. Circ Res **104:**813-821.
134. **Martinet, W., M. W. Knaapen, M. M. Kockx, and G. R. De Meyer.** 2007. Autophagy in cardiovascular disease. Trends Mol Med **13:**482-491.
135. **Martino, T. A., P. Liu, and M. J. Sole.** 1994. Viral infection and the pathogenesis of dilated cardiomyopathy. Circ Res **74:**182-188.
136. **Matsui, Y., H. Takagi, X. Qu, M. Abdellatif, H. Sakoda, T. Asano, B. Levine, and J. Sadoshima.** 2007. Distinct roles of autophagy in the heart during ischemia and reperfusion: roles of AMP-activated protein kinase and Beclin 1 in mediating autophagy. Circ Res **100:**914-922.
137. **McManus, B., and R. Kandolf.** 2000. Myocarditis, p. 168-183. *In* B. McManus (ed.), Atlas of Cardiovascular Pathology for the Clinician. Curr. Med., Philadelphia
138. **McManus, B. M., L. H. Chow, J. E. Wilson, D. R. Anderson, J. M. Gulizia, C. J. Gauntt, K. E. Klingel, K. W. Beisel, and R. Kandolf.** 1993. Direct myocardial injury by enterovirus: a central role in the evolution of murine myocarditis. Clin Immunol Immunopathol **68:**159-169.
139. **McManus, B. M., Wood, S. M.** 1997. Inflammatory manifestations of toxic and allergic injury to heart and blood vessels, vol. 6. Elsevier, New York.

140. **McNamara, D. M., R. Holubkov, R. C. Starling, G. W. Dec, E. Loh, G. Torre-Amione, A. Gass, K. Janosko, T. Tokarczyk, P. Kessler, D. L. Mann, and A. M. Feldman.** 2001. Controlled trial of intravenous immune globulin in recent-onset dilated cardiomyopathy. Circulation **103:**2254-2259.

141. **Melnick, J. L.** 1983. Portraits of viruses: the picornaviruses. Intervirology **20:**61-100.

142. **Melnick, J. L., E. W. Shaw, and E. C. Curnen.** 1949. A virus isolated from patients diagnosed as non-paralytic poliomyelitis or aseptic meningitis. Proc Soc Exp Biol Med **71:**344-349.

143. **Miano, J. M.** 2003. Serum response factor: toggling between disparate programs of gene expression. J Mol Cell Cardiol **35:**577-593.

144. **Miano, J. M., N. Ramanan, M. A. Georger, K. L. de Mesy Bentley, R. L. Emerson, R. O. Balza, Jr., Q. Xiao, H. Weiler, D. D. Ginty, and R. P. Misra.** 2004. Restricted inactivation of serum response factor to the cardiovascular system. Proc Natl Acad Sci U S A **101:**17132-17137.

145. **Mizushima, N.** 2004. Methods for monitoring autophagy. Int J Biochem Cell Biol **36:**2491-2502.

146. **Mizushima, N., and B. Levine.** 2010. Autophagy in mammalian development and differentiation. Nat Cell Biol **12:**823-830.

147. **Mizushima, N., B. Levine, A. M. Cuervo, and D. J. Klionsky.** 2008. Autophagy fights disease through cellular self-digestion. Nature **451:**1069-1075.

148. **Mizushima, N., A. Yamamoto, M. Matsui, T. Yoshimori, and Y. Ohsumi.** 2004. In vivo analysis of autophagy in response to nutrient starvation using transgenic mice expressing a fluorescent autophagosome marker. Mol Biol Cell **15:**1101-1111.

149. **Mohr, I.** 2004. Neutralizing innate host defenses to control viral translation in HSV-1 infected cells. Int Rev Immunol **23:**199-220.

150. **Morasco, B. J., N. Sharma, J. Parilla, and J. B. Flanegan.** 2003. Poliovirus cre(2C)-dependent synthesis of VPgpUpU is required for positive- but not negative-strand RNA synthesis. J Virol **77:**5136-5144.

151. **Morris, S. A., H. B. Tanowitz, M. Wittner, and J. P. Bilezikian.** 1990. Pathophysiological insights into the cardiomyopathy of Chagas' disease. Circulation **82:**1900-1909.

152. **Murray, K. E., and D. J. Barton.** 2003. Poliovirus CRE-dependent VPg uridylylation is required for positive-strand RNA synthesis but not for negative-strand RNA synthesis. J Virol **77:**4739-4750.

153. **Nadal-Ginard, B., J. Kajstura, A. Leri, and P. Anversa.** 2003. Myocyte death, growth, and regeneration in cardiac hypertrophy and failure. Circ Res **92:**139-150.

154. **Nakai, A., O. Yamaguchi, T. Takeda, Y. Higuchi, S. Hikoso, M. Taniike, S. Omiya, I. Mizote, Y. Matsumura, M. Asahi, K. Nishida, M. Hori, N. Mizushima, and K. Otsu.** 2007. The role of autophagy in cardiomyocytes in the basal state and in response to hemodynamic stress. Nat Med **13:**619-624.

155. **Nelson, T. J., R. Balza, Jr., Q. Xiao, and R. P. Misra.** 2005. SRF-dependent gene expression in isolated cardiomyocytes: regulation of genes involved in cardiac hypertrophy. J Mol Cell Cardiol **39:**479-489.

156. **Niu, Z., D. Iyer, S. J. Conway, J. F. Martin, K. Ivey, D. Srivastava, A. Nordheim, and R. J. Schwartz.** 2008. Serum response factor orchestrates nascent sarcomerogenesis and silences the biomineralization gene program in the heart. Proc Natl Acad Sci U S A **105:**17824-17829.

157. **Niu, Z., A. Li, S. X. Zhang, and R. J. Schwartz.** 2007. Serum response factor micromanaging cardiogenesis. Curr Opin Cell Biol **19:**618-627.

158. **Niu, Z., W. Yu, S. X. Zhang, M. Barron, N. S. Belaguli, M. D. Schneider, M. Parmacek, A. Nordheim, and R. J. Schwartz.** 2005. Conditional mutagenesis of the murine serum response factor gene blocks cardiogenesis and the transcription of downstream gene targets. J Biol Chem **280:**32531-32538.

159. **Norman, C., M. Runswick, R. Pollock, and R. Treisman.** 1988. Isolation and properties of cDNA clones encoding SRF, a transcription factor that binds to the c-fos serum response element. Cell **55:**989-1003.

160. **Ogawa, M., T. Yoshimori, T. Suzuki, H. Sagara, N. Mizushima, and C. Sasakawa.** 2005. Escape of intracellular Shigella from autophagy. Science **307:**727-731.

161. **Ohsumi, Y.** 2001. Molecular dissection of autophagy: two ubiquitin-like systems. Nat Rev Mol Cell Biol **2:**211-216.

162. **Oka, T., J. Xu, and J. D. Molkentin.** 2007. Re-employment of developmental transcription factors in adult heart disease. Semin Cell Dev Biol **18:**117-131.

163. **Okuni, M., T. Yamada, S. Mochizuki, and I. Sakurai.** 1975. Studies on myocarditis in childhood, with special reference to the possible role of immunological process and the thymus in the chronicity of the disease. Jpn Circ J **39:**463-470.

164. **Olsen, E. G.** 1985. What is myocarditis? Heart and Vessels Suppl **1:**1-3.

165. **Opavsky, M. A., J. Penninger, K. Aitken, W. H. Wen, F. Dawood, T. Mak, and P. Liu.** 1999. Susceptibility to myocarditis is dependent on the response of alphabeta T lymphocytes to coxsackieviral infection. Circ Res **85:**551-558.

166. **Parlakian, A., D. Tuil, G. Hamard, G. Tavernier, D. Hentzen, J. P. Concordet, D. Paulin, Z. Li, and D. Daegelen.** 2004. Targeted inactivation of serum response factor in the developing heart results in myocardial defects and embryonic lethality. Mol Cell Biol **24:**5281-5289.

167. **Parrillo, J. E., R. E. Cunnion, S. E. Epstein, M. M. Parker, A. F. Suffredini, M. Brenner, G. L. Schaer, S. T. Palmeri, R. O. Cannon, 3rd, D. Alling, and et al.** 1989. A prospective, randomized, controlled trial of prednisone for dilated cardiomyopathy. N Engl J Med **321:**1061-1068.

168. **Paul, A. V., J. H. van Boom, D. Filippov, and E. Wimmer.** 1998. Protein-primed RNA synthesis by purified poliovirus RNA polymerase. Nature **393:**280-284.

169. **Petiot, A., E. Ogier-Denis, E. F. Blommaart, A. J. Meijer, and P. Codogno.** 2000. Distinct classes of phosphatidylinositol 3'-kinases are involved in signaling pathways that control macroautophagy in HT-29 cells. J Biol Chem **275:**992-998.

170. **Pilipenko, E. V., S. V. Maslova, A. N. Sinyakov, and V. I. Agol.** 1992. Towards identification of cis-acting elements involved in the replication of enterovirus and rhinovirus RNAs: a proposal for the existence of tRNA-like terminal structures. Nucleic Acids Res **20:**1739-1745.

171. **Prentice, E., W. G. Jerome, T. Yoshimori, N. Mizushima, and M. R. Denison.** 2004. Coronavirus replication complex formation utilizes components of cellular autophagy. J Biol Chem **279:**10136-10141.

172. **Rueckert, R. R.** 1996. Picornaviridae: the viruses and their replication, 3 ed. Lippincott-Raven, Philadelphia, Pa.

173. **Sakakibara, S., and S. Konno.** 1962. Endomyocardial biopsy. Jpn Heart J **3:**537-543.

174. **Saphir, O.** 1960. Nonrheumatic inflammatory diseases of heart, p. 779-823. *In* S. Gould (ed.), Pathology of the heart, 2 ed. Thomas, Springfield, Ill.

175. **Schena, M., D. Shalon, R. W. Davis, and P. O. Brown.** 1995. Quantitative monitoring of gene expression patterns with a complementary DNA microarray. Science **270:**467-470.

176. **Schmid, D., and C. Munz.** 2007. Innate and adaptive immunity through autophagy. Immunity **27:**11-21.

177. **Schwaiger, A., F. Umlauft, K. Weyrer, C. Larcher, J. Lyons, V. Muhlberger, O. Dietze, and K. Grunewald.** 1993. Detection of enteroviral ribonucleic acid in myocardial biopsies from patients with idiopathic dilated cardiomyopathy by polymerase chain reaction. Am Heart J **126:**406-410.

178. **Seglen, P. O., and P. B. Gordon.** 1982. 3-Methyladenine: specific inhibitor of autophagic/lysosomal protein degradation in isolated rat hepatocytes. Proc Natl Acad Sci U S A **79:**1889-1892.

179. **Selinka, H. C., A. Wolde, M. Sauter, R. Kandolf, and K. Klingel.** 2004. Virus-receptor interactions of coxsackie B viruses and their putative influence on cardiotropism. Med Microbiol Immunol **193:**127-131.

180. **Small, E. M., J. R. O'Rourke, V. Moresi, L. B. Sutherland, J. McAnally, R. D. Gerard, J. A. Richardson, and E. N. Olson.** 2010. Regulation of PI3-kinase/Akt signaling by muscle-enriched microRNA-486. Proc Natl Acad Sci U S A **107:**4218-4223.

181. **Smith, S. C., J. H. Ladenson, J. W. Mason, and A. S. Jaffe.** 1997. Elevations of cardiac troponin I associated with myocarditis. Experimental and clinical correlates. Circulation **95:**163-168.

182. **Soulez, M., C. G. Rouviere, P. Chafey, D. Hentzen, M. Vandromme, N. Lautredou, N. Lamb, A. Kahn, and D. Tuil.** 1996. Growth and differentiation of C2 myogenic cells are dependent on serum response factor. Mol Cell Biol **16:**6065-6074.

183. **Sun, Q., G. Chen, J. W. Streb, X. Long, Y. Yang, C. J. Stoeckert, Jr., and J. M. Miano.** 2006. Defining the mammalian CArGome. Genome Res **16:**197-207.

184. **Suzuki, K., T. Kirisako, Y. Kamada, N. Mizushima, T. Noda, and Y. Ohsumi.** 2001. The pre-autophagosomal structure organized by concerted functions of APG genes is essential for autophagosome formation. EMBO J **20:**5971-5981.

185. **Takagi, H., Y. Matsui, and J. Sadoshima.** 2007. The role of autophagy in mediating cell survival and death during ischemia and reperfusion in the heart. Antioxid Redox Signal **9:**1373-1381.

186. **Talloczy, Z., W. Jiang, H. W. t. Virgin, D. A. Leib, D. Scheuner, R. J. Kaufman, E. L. Eskelinen, and B. Levine.** 2002. Regulation of starvation- and virus-induced autophagy by the eIF2alpha kinase signaling pathway. Proc Natl Acad Sci U S A **99:**190-195.

187. **Tan, F. L., C. S. Moravec, J. Li, C. Apperson-Hansen, P. M. McCarthy, J. B. Young, and M. Bond.** 2002. The gene expression fingerprint of human heart failure. Proc Natl Acad Sci U S A **99:**11387-11392.

188. **Tanaka, Y., G. Guhde, A. Suter, E. L. Eskelinen, D. Hartmann, R. Lullmann-Rauch, P. M. Janssen, J. Blanz, K. von Figura, and P. Saftig.** 2000. Accumulation of autophagic vacuoles and cardiomyopathy in LAMP-2-deficient mice. Nature **406:**902-906.

189. **Taylor, L. A., C. M. Carthy, D. Yang, K. Saad, D. Wong, G. Schreiner, L. W. Stanton, and B. M. McManus.** 2000. Host gene regulation during coxsackievirus B3 infection in mice: assessment by microarrays. Circ Res **87:**328-334.

190. **Terman, A., and U. T. Brunk.** 2005. Autophagy in cardiac myocyte homeostasis, aging, and pathology. Cardiovasc Res **68:**355-365.

191. **Treisman, R.** 1986. Identification of a protein-binding site that mediates transcriptional response of the c-fos gene to serum factors. Cell **46:**567-574.

192. **Uhl, T. L.** 2008. Viral myocarditis in children. Crit Care Nurse **28:**42-63; quiz 64.

193. **van Kuppeveld, F. J., A. S. de Jong, W. J. Melchers, and P. H. Willems.** 2005. Enterovirus protein 2B po(u)res out the calcium: a viral strategy to survive? Trends Microbiol **13:**41-44.

194. **van Kuppeveld, F. J., J. G. Hoenderop, R. L. Smeets, P. H. Willems, H. B. Dijkman, J. M. Galama, and W. J. Melchers.** 1997. Coxsackievirus protein 2B modifies endoplasmic reticulum membrane and plasma membrane permeability and facilitates virus release. EMBO J **16:**3519-3532.

195. **Vignola, P. A., K. Aonuma, P. S. Swaye, J. J. Rozanski, R. L. Blankstein, J. Benson, A. J. Gosselin, and J. W. Lister.** 1984. Lymphocytic myocarditis presenting as unexplained ventricular arrhythmias: diagnosis with endomyocardial biopsy and response to immunosuppression. J Am Coll Cardiol **4:**812-819.

196. **Wang, Q. M., R. B. Johnson, W. Sommergruber, and T. A. Shepherd.** 1998. Development of in vitro peptide substrates for human rhinovirus-14 2A protease. Arch Biochem Biophys **356:**12-18.

197. **Wang, X., H. Su, and M. J. Ranek.** 2008. Protein quality control and degradation in cardiomyocytes. J Mol Cell Cardiol **45:**11-27.

198. **Weekes, J., K. Morrison, A. Mullen, R. Wait, P. Barton, and M. J. Dunn.** 2003. Hyperubiquitination of proteins in dilated cardiomyopathy. Proteomics **3:**208-216.

199. **Wei, C., G. Wang, X. Chen, H. Huang, B. Liu, Y. Xu, and F. Li.** 2011. Identification and typing of human enterovirus: a genomic barcode approach. PloS one **6:**e26296.

200. **Wessels, E., D. Duijsings, R. A. Notebaart, W. J. Melchers, and F. J. van Kuppeveld.** 2005. A proline-rich region in the coxsackievirus 3A protein is required for the protein to inhibit endoplasmic reticulum-to-golgi transport. J Virol **79:**5163-5173.

201. **Wessels, E., R. A. Notebaart, D. Duijsings, K. Lanke, B. Vergeer, W. J. Melchers, and F. J. van Kuppeveld.** 2006. Structure-function analysis of the coxsackievirus protein 3A: identification of residues important for dimerization, viral rna replication, and transport inhibition. J Biol Chem **281:**28232-28243.

202. **Why, H. J., B. T. Meany, P. J. Richardson, E. G. Olsen, N. E. Bowles, L. Cunningham, C. A. Freeke, and L. C. Archard.** 1994. Clinical and prognostic significance of detection of enteroviral RNA in the myocardium of patients with myocarditis or dilated cardiomyopathy. Circulation **89:**2582-2589.

203. **Wileman, T.** 2006. Aggresomes and autophagy generate sites for virus replication. Science **312:**875-878.

204. **Woodruff, J. F.** 1980. Viral myocarditis. A review. Am J Pathol **101:**425-484.

205. **Xiong, D., T. Yajima, B. K. Lim, A. Stenbit, A. Dublin, N. D. Dalton, D. Summers-Torres, J. D. Molkentin, H. Duplain, R. Wessely, J. Chen, and K. U. Knowlton.** 2007. Inducible cardiac-restricted expression of enteroviral protease 2A is sufficient to induce dilated cardiomyopathy. Circulation **115:**94-102.

206. **Yalamanchili, P., U. Datta, and A. Dasgupta.** 1997. Inhibition of host cell transcription by poliovirus: cleavage of transcription factor CREB by poliovirus-encoded protease 3Cpro. J Virol **71:**1220-1226.

207. **Yalamanchili, P., K. Weidman, and A. Dasgupta.** 1997. Cleavage of transcriptional activator Oct-1 by poliovirus encoded protease 3Cpro. Virology **239:**176-185.

208. **Yanagawa, B., O. B. Spiller, J. Choy, H. Luo, P. Cheung, H. M. Zhang, I. G. Goodfellow, D. J. Evans, A. Suarez, D. Yang, and B. M. McManus.** 2003. Coxsackievirus B3-associated myocardial pathology and viral load reduced by recombinant soluble human decay-accelerating factor in mice. Lab Invest **83:**75-85.

209. **Yuan, J., P. K. Cheung, H. Zhang, D. Chau, B. Yanagawa, C. Cheung, H. Luo, Y. Wang, A. Suarez, B. M. McManus, and D. Yang.** 2004. A phosphorothioate antisense oligodeoxynucleotide specifically inhibits coxsackievirus B3 replication in cardiomyocytes and mouse hearts. Lab Invest **84:**703-714.

210. **Zee-Cheng, C. S., C. C. Tsai, D. C. Palmer, J. E. Codd, D. G. Pennington, and G. A. Williams.** 1984. High incidence of myocarditis by endomyocardial biopsy in patients with idiopathic congestive cardiomyopathy. J Am Coll Cardiol **3:**63-70.

211. **Zeng, X., J. H. Overmeyer, and W. A. Maltese.** 2006. Functional specificity of the mammalian Beclin-Vps34 PI 3-kinase complex in macroautophagy versus endocytosis and lysosomal enzyme trafficking. J Cell Sci **119:**259-270.

212. **Zhang, X., G. Azhar, J. Chai, P. Sheridan, K. Nagano, T. Brown, J. Yang, K. Khrapko, A. M. Borras, J. Lawitts, R. P. Misra, and J. Y. Wei.** 2001. Cardiomyopathy in transgenic mice with cardiac-specific overexpression of serum response factor. Am J Physiol Heart Circ Physiol **280:**H1782-1792.

213. **Zhao, Y., J. F. Ransom, A. Li, V. Vedantham, M. von Drehle, A. N. Muth, T. Tsuchihashi, M. T. McManus, R. J. Schwartz, and D. Srivastava.** 2007. Dysregulation of cardiogenesis, cardiac conduction, and cell cycle in mice lacking miRNA-1-2. Cell **129:**303-317.

214. **Zhao, Z., L. B. Thackray, B. C. Miller, T. M. Lynn, M. M. Becker, E. Ward, N. N. Mizushima, M. R. Denison, and H. W. t. Virgin.** 2007. Coronavirus replication does not require the autophagy gene ATG5. Autophagy **3:**581-585.

215. **Zhou, B., N. Boudreau, C. Coulber, J. Hammarback, and M. Rabinovitch.** 1997. Microtubule-associated protein 1 light chain 3 is a fibronectin mRNA-binding protein linked to mRNA translation in lamb vascular smooth muscle cells. J Clin Invest **100:**3070-3082.

216. **Zhu, H., P. Tannous, J. L. Johnstone, Y. Kong, J. M. Shelton, J. A. Richardson, V. Le, B. Levine, B. A. Rothermel, and J. A. Hill.** 2007. Cardiac autophagy is a maladaptive response to hemodynamic stress. J Clin Invest **117:**1782-1793.